Dr-1761

200/
11-1. 75

CHEMICAL ENGINEERING DIVISION

WASTE MANAGEMENT PROGRAMS

QUARTERLY REPORT

January—March 1975

by

**M. J. Steindler, N. M. Levitz, W. J. Mecham,
W. B. Seefeldt, L. E. Trevorrow, I. O. Winsch,
T. F. Cannon, T. J. Gerding, B. J. Kullen,
D. S. Webster, and L. Burris**

MASTER

U of C-AUA-USERDA

ARGONNE NATIONAL LABORATORY, ARGONNE, ILLINOIS

Prepared for the U. S. ENERGY RESEARCH
AND DEVELOPMENT ADMINISTRATION
under Contract W-31-109-Eng-38

DISCLAIMER

This report was prepared as an account of work sponsored by an agency of the United States Government. Neither the United States Government nor any agency Thereof, nor any of their employees, makes any warranty, express or implied, or assumes any legal liability or responsibility for the accuracy, completeness, or usefulness of any information, apparatus, product, or process disclosed, or represents that its use would not infringe privately owned rights. Reference herein to any specific commercial product, process, or service by trade name, trademark, manufacturer, or otherwise does not necessarily constitute or imply its endorsement, recommendation, or favoring by the United States Government or any agency thereof. The views and opinions of authors expressed herein do not necessarily state or reflect those of the United States Government or any agency thereof.

DISCLAIMER

Portions of this document may be illegible in electronic image products. Images are produced from the best available original document.

The facilities of Argonne National Laboratory are owned by the United States Government. Under the terms of a contract (W-31-109-Eng-38) between the U. S. Energy Research and Development Administration, Argonne Universities Association and The University of Chicago, the University employs the staff and operates the Laboratory in accordance with policies and programs formulated, approved and reviewed by the Association.

ANL-75-43

ARGONNE NATIONAL LABORATORY
9700 South Cass Avenue
Argonne, Illinois 60439

CHEMICAL ENGINEERING DIVISION

WASTE MANAGEMENT PROGRAMS
QUARTERLY REPORT

January—March 1975

by

M. J. Steindler, N. M. Levitz, W. J. Mecham,
W. B. Seefeldt, L. E. Trevorrow, I. O. Winsch,
T. F. Cannon, T. J. Gerding, B. J. Kullen,
D. S. Webster, and L. Burris

June 1975

Previous reports in this series

ANL-8106   January-March 1974
ANL-8134   April-June 1974
ANL-8152   July-September 1974
ANL-75-23 October-December 1974

THIS PAGE

WAS INTENTIONALLY

LEFT BLANK

TABLE OF CONTENTS

iv

LIST OF FIGURES

LIST OF TABLES

CHEMICAL ENGINEERING DIVISION
WASTE MANAGEMENT PROGRAMS QUARTERLY REPORT

January - March 1975

by

M. J. Steindler, N. M. Levitz, W. J. Mecham,
W. B. Seefeldt, L. E. Trevorrow, I. O. Winsch,
T. F. Cannon, T. J. Gerding, B. J. Kullen,
D. S. Webster, and L. Burris

ABSTRACT

Development work on the study of consolidation techniques for
Zircaloy fuel-cladding hulls included scouting tests on volatility
schemes for separating the zirconium as the volatile tetrachloride
and ignition tests on several Zircaloy materials to further charac-
terize the pyrophoric behavior of Zircaloy. All tests were with
nonirradiated metal pending acquisition of irradiated samples. In
hydrochlorination runs with anhydrous HCl, analyses of the condensed
overhead products and reaction-boat residues tended to confirm the
expected behavior of the key elements, and indicate that a highly
decontaminated zirconium product and a consolidated plutonium-
containing fraction may be attainable. Studies on a pyrochemical
approach using molten zinc chloride to separate the zirconium as
the tetrachloride show that considerable flexibility exists in the
choice of salt-to-metal compositions.

Small-scale ignition tests using zirconium igniter powders
indicated that Zircaloy tubing, per se, does not exhibit pyrophoricity
in air, even at temperatures approaching the melting point of the
metal, whereas some types of fines can be ignited with a match.

Installation is nearly complete of a glovebox facility for
studies on the salvage of alpha-contaminated metals by pyrochemical
methods. Steel-melting experiments with noncontaminated metal are
in progress, using stand-in materials for plutonium. Compatibility
of slagging materials and crucible materials is being examined in
the initial studies.

Disposal of a major portion of fission product tritium formed
in light water reactor fuels by deep-well injection of the low-level
aqueous waste (LLAW) from plants reprocessing such fuels is being
evaluated. The question of siting is a very important factor in
determining the feasibility of this particular disposal option. The
influence of geologic and hydrologic considerations in the choice
of a disposal well site are reviewed. The various geophysical
parameters characterizing the ability of the receiving stratum to
hold and to transmit fluids are described. The acquisition of

information on these parameters by testing or from records is discussed. The use of geophysical parameters to predict the response of an aquifer to injection (*e.g.*, fluid movement and fracturing) is illustrated. A review is given of the status of information for U. S. sedimentary basins, the areas most likely to be generally suitable for siting of waste wells.

Work on the reliability of high-level-waste canisters included an examination of methods of relieving stresses induced in canisters due to differential contraction of canister and glass during cooling. These methods included: creep, shot-peening, and subcooling of the filler canister below storage temperatures. A method was investigated for relieving stresses in calcine-filled canisters.

Properties of fission product oxides were examined to elucidate possible adverse corrosive effects at the canister-waste interface.

SUMMARY

Consolidation Techniques for Fuel-Cladding Hulls

A study is in progress to develop a long-term management scheme for the contaminated, Zircaloy-based cladding waste stream that is generated by the chop-leach processing of spent LWR fuel. This program explores and evaluates chemical and mechanical process steps that will consolidate the waste and circumvent any pyrophoric hazard. Means of reducing the alpha-waste volume include exploratory studies for separating the zirconium from the long-lived alpha-emitters and other radionuclides. Initial work is with unirradiated Zircaloy tubing. Efforts to acquire irradiated hulls and tubing for later testing are continuing.

Two chemical methods selected for initial study provide separation of the zirconium as the volatile tetrachloride: (1) hydrochlorination with anhydrous HCl and (2) reaction with molten $ZnCl_2$. The laboratory-scale tube-furnace apparatus for Zircaloy hydrochlorination was completed during this period. A series of four scouting runs was made to establish the distribution of the minor alloy metal constituents between the volatile and nonvolatile fractions. This information is needed to evaluate the potential of hydrochlorination as a method for decontaminating and consolidating the waste. The runs were made, nominally, at 400°C. Mechanical difficulties, *e.g.*, insufficient line heating and inadequate $ZrCl_4$ trap design, resulted in early termination of the first run after 15 min, but after several modifications scheduled 2- and 4-hr runs were made successfully. Five-gram samples of Zircaloy-2 tubing were reacted to the extent of 60% and 97% in total run times of 1 hr and 6 hr. Analyses of the reaction-boat residues and condensed overhead products tend to confirm the expected behavior of the key elements, and suggest that a highly decontaminated zirconium product and a consolidated plutonium-containing fraction can be obtained. More quantitative information on the limits of detection for the analytical method, spark source mass spectrography, is being sought to complete the evaluation of the analytical results. Examination of the nonvolatile residue indicated that the oxide

coating on the metal did not impede the HCl-metal reaction, and that the coating itself was not attacked by the gaseous HCl.

In the investigation of zirconium separation by reaction with molten $ZnCl_2$, an experiment was made in which slightly less than the stoichiometric quantity of $ZnCl_2$ required to oxidize the Zircaloy charge was used to facilitate the removal of the $ZrCl_4$ by volatilization. The charge consisted of 104 g of tubing sections, 1/2 in. OD x 1/32 in. wall x 1 in. long, 300 g of $ZnCl_2$, 1 g of CeO_2 (as a stand-in for PuO_2), and 5 g of UO_2. The charge was placed in a tungsten crucible in an induction-heated tilt-pour furnace. The melt was held at 500°C for 6 hr under a 15-psig argon atmosphere. During the final 2 hr, the melt was stirred with a paddle at 400 rpm.

A small metal heel, consisting of zinc and unreacted Zircaloy, remained in the crucible but no salt remained, the $ZnCl_2$ having been completely reacted. The $ZrCl_4$ had volatilized during the run and had condensed on the wall regions downstream from the crucible since no condenser was provided. The technique of operating at or near stoichiometric $ZnCl_2/Zr$ ratios to separate the zirconium as $ZrCl_4$ appears attractive as a process option. Analytical results on the distribution of the CeO_2 and UO_2 are being obtained.

In exploring other pyrochemical options, an attempt was made to separate a zirconium phase from a 12 wt % Zr-Zn melt by cooling and precipitation of the zirconium. This was unsuccessful as a result of the formation of intermetallics such as $ZrZn_6$, $ZrZn_{14}$, and $ZrZn_{22}$, which have densities near that of zinc so that no distinct separation of phases was noted at either the top or the bottom of the final ingot.

Ignition tests were performed on several types of unirradiated Zircaloy materials. A series of nine tests with single short tubing sections and fine zirconium igniter powders at powder-to-tubing weight ratios up to 8 produced no sustained burning of the tubing. The powders ignited at 400°C and 430°C, and the burning system reached temperatures in the range 585 to 1600°C; for reference, the melting point of zirconium is about 1850°C. The tubing did glow, but only as long as the powders burned (25- to 80-sec periods) or when a torch was applied. An oxide coating was visible on the specimens after each test.

Qualitative ignition tests on several relatively high surface-to-volume Zircaloy materials gave the following results: (1) dry, clean turnings could not be ignited with a match, but did ignite with a gas-oxygen torch; (2) a small pellet made of saw fines could not be ignited with sparks or a match, but did ignite and burn quickly when heated with a gas-oxygen torch; (3) uncompacted saw fines could not be ignited with sparks but did ignite with a match. A zinc coating on Zircaloy tubing, intended to reduce the potential for pyrophoric behavior, showed no effects from a burning match, but did oxidize with no sustained burning when a gas-oxygen torch was applied. In general, the higher the surface-to-volume ratio, the more susceptible to ignition was the Zircaloy.

Oxidation tests on Zircaloy tubing sections were done in a muffle furnace to get comparative data. Tests were for 1 hr at 700, 800, and 900°C. With each 100°C increase in temperature, the oxidation rate increased about threefold.

However, the extent of oxidation was only 12% at the highest temperature, indicating a relative insensitivity of tubing to oxidation at this relatively high temperature range.

Fines obtained from the dry chopping of ordinary Zircaloy tubing were characterized as to size distribution and oxygen content, in the absence of data on chopped irradiated hulls.

Salvage of Alpha-Contaminated Metals

A program is in progress to identify and test methods for decontaminating metallic materials that have been used with plutonium, with the aim of salvaging the metal. The program is directed toward the decontamination of ERDA-owned equipment and facilities; decommissioned facilities are a major source of this material. Installation is nearly complete of a glovebox facility for the initial program of studies involving steel-melting and slagging techniques. The glove box will have an inert (helium) atmosphere for added flexibility. The key item of equipment is a tungsten-mesh resistance-heated furnace capable of temperatures near 3000°C. The major facility support systems, $e.g.$, helium purification and vacuum systems, have been installed and their mechanical testing is nearly complete. Preliminary heating tests on the furnace were satisfactory.

Supporting steel-melting experiments are in progress in which ordinary steel is used to examine the suitability of crucible materials, to test the effectiveness of slagging materials (using CeO_2 as a stand-in for PuO_2), and to test operating procedures. Steel melts with and without a slagging material have been completed, but their evaluation awaits analytical results. A MgO crucible was penetrated by cryolite ($3NaF-AlF_3$), used as a slagging material, indicating that materials selection is an important aspect of this program.

Storage and Disposal of Tritium

The suitability of a site for deep-well injection of waste-water can be assessed through consideration of a number of types of information. Recorded information on stratigraphy, structure, and lithology (composition and texture) of rock strata should be consulted. The properties of the natural subsurface water in the area should be considered ($e.g.$, chemical composition, viscosity, pressure, and compressibility). Data on the mechanical properties of the rock units, such as porosity, permeability, compressibility, temperature, and state of stress, should be considered. The hydrodynamics of the subsurface region ($i.e.$, the flow of natural water and its relevance to waste containment) can be deduced. The resources of the region and the possible effects of waste injection on their value should be taken into account.

Data describing the subsurface of a region may be obtained prior to drilling from records of state geologic surveys, oil and gas agencies, water-resources agencies, and private companies. As drilling on a particular well proceeds, data can be obtained from analysis of rock samples and formation fluids, by a large number of borehole geophysical logging techniques that have been developed, and from tests that involve pumping fluid into or out of the well at various stages of completion.

Predictions on the response of the aquifer to injection include effects on subsurface flow of natural fluids in the region of influence, effects of pressure, the rate and direction of flow of the waste, the possibility of hydraulic fracturing of the overburden, and the stimulation of earthquakes.

The areas most likely to have geologic properties suitable for deep-well injection are the sedimentary basins of the U. S. Recorded descriptions of the sedimentary basins of the eastern and middle sections of the U. S. are available in some detail, but the basins of the far western section of the country are less well explored and described. Recorded information on U. S. basins would serve only for preliminary assessments of the suitability of a region and would have to be followed by more detailed analysis of a particular site of interest.

Reliability of High-Level-Waste Containers

The reliability of containers for high-level wastes in the glass and calcine forms during (1) storage under water at a reprocessing plant, (2) transit to a Retrievable Surface Storage Facility (RSSF), and (3) storage at a RSSF is being examined. The several concepts of storage at an RSSF provide cooling by air or water. The metallurgical history of the containers, including operations involved in filling them with the waste, is also germane.

Stress corrosion cracking of stainless steels has been identified as one of the principal potential modes of failure of canisters. In the preceding report in this series (ANL-75-23), the differential contraction of the canister and glass following filling operations was found to introduce stress levels exceeding yield stresses.

In current work, stress relief by means of creep mechanisms was examined and was found to be ineffective. Subcooling of the filled canister below the final storage temperature was also examined as a stress relieving mechanism; this method has the potential of removing most stresses. A third method, shot peening of the filled canister, is capable of removing surface tensile stresses and can, in fact, put surface material in compression. Alternative methods for reducing susceptibility of stainless steel canisters to stress corrosion cracking were examined.

Internal pressurization of canisters due to decomposition of residual nitrates and volatilization of residual moisture in calcine was also identified as a source of stress. A method was examined in which the filled canister was treated at elevated temperatures to accomplish two objectives: the removal of residual stresses in the canister and the removal of residual nitrates and moisture from the calcine.

Reliability of canisters can also be affected by local corrosive effects between the canister and the waste. The properties of fission product oxides were examined to elucidate possible adverse effects. Most fission product oxides have high melting points. However, some, including noble metals, decompose at temperatures approaching 1000°C, yielding elements that are high melting and have low volatility. Ruthenium and technetium have fairly stable oxides; but in systems with high oxygen potential they can form higher oxides that are volatile. Alkali metal oxides have moderately high temperature

stability and are significantly volatile. Stability in the waste solid is strongly dependent on the matrix and the temperature. Eutectics are expected to form between oxides and between oxides and residual nitrates. This could lead to sintering and possibly melting.

Under the influence of temperature gradients present in the waste canister, volatile fission products and/or their compounds may be expected to migrate from high-temperature zones to low-temperature zones. Examples of such fission products are cesium, rubidium, and ruthenium. Migration is not expected to occur below temperatures near 600°C.

The system is sufficiently complex to preclude judgments about local corrosive effects without an experimental program.

Canister design parameters for temperature control were examined. At any given heating rate of the fission product oxides, the number of canisters required for calcine (no internal fins) is about four times greater than that for glass; the volume of each canister for glass is about twice that for calcine. The number of canisters required for calcine can be made equivalent to the number for glass if (1) the cooling time for calcine is four times that for glass, or (2) a sufficient number of internal fins is used in the canisters containing calcine.

I. CONSOLIDATION TECHNIQUES FOR FUEL-CLADDING HULLS
(N. M. Levitz, I. O. Winch, B. J. Kullen, T. F. Cannon)

A. Introduction

This program concerns the development of methods for the safe and economic long-term management of waste Zircaloy cladding* that is generated in the reprocessing of spent LWR fuel by the chop-leach process. The cladding is contaminated with long-lived alpha-emitters, fission products, and neutron-activation products. Current attention is being given to the potential of a pyrophoric hazard from Zircaloy, particularly from finely divided metal. Consolidation processes that transform the waste so that it can be classified and treated as a compact, nonpyrophoric, non-alpha-bearing waste (<10 nCi/g) are being identified, tested, and evaluated. The processes should also provide for the collection of the alpha-emitters in a compact form, amenable to storage, disposal, or further processing. Monitoring of the waste and the various process streams for plutonium content has been identified as a problem needing further development. Identification of methods for salvaging the Zircaloy for reuse remains a secondary goal. The plan of work includes review and evaluation of the literature to assess the state of knowledge and technology, an experimental phase, and a flow sheet and concept design phase that will identify process options. Resolution of the pyrophoricity question will be emphasized in the work this fiscal year.

Experimental work continues to stress methods that provide a separation of the zirconium as the volatile tetrachloride, namely, hydrochlorination with anhydrous HCl or reaction with molten $ZnCl_2$.[1,2] Efforts continued on the development of information related to the potential ignition of Zircaloy hulls; results of recent ignition tests with nonirradiated Zircaloy are presented.

Efforts to acquire some irradiated Zircaloy materials for characterization and test purposes continued. An on-site source of material has recently been found, and arrangements to acquire this material are in progress. Off-site sources have been virtually discounted, because of either cost or restrictions stemming from proprietary interests.

B. Hydrochlorination Studies

A tube-furnace apparatus[1] was completed this period to study the hydrochlorination of Zircaloy metal samples. The system was designed to investigate the reactions:

$$\text{Metals(solid) + HCl(gas)} \rightarrow \begin{array}{c} \text{Metal Chloride(gas)} \\ \text{or} \\ \text{Metal Chloride(solid)} \end{array} + H_2\text{(gas)}$$
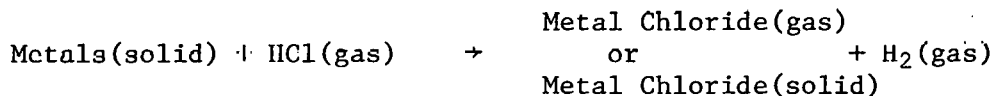
in terms of the distribution of the metal constituents (Sn, Fe, U, etc.) between the volatile and nonvolatile fractions. If it can be demonstrated

---

* Cladding in this context comprises the short Zircaloy tube segments referred to as hulls, as well as extraneous fuel element hardware such as Inconel grids and nozzles. Zircaloy is a zirconium-based alloy containing tin, iron, chromium, and sometimes nickel.

that the chlorides of actinides and other radioactive elements do not volatilize, hydrochlorination could become a process option not only for the consolidation of waste Zircaloy, but for the decontamination as well.

Two pairs of hydrochlorination runs were performed during the period, each pair of runs being associated with the reaction of a 1-in. section of Zircaloy-2 tubing with a 0.5-in. OD and a 0.03-in. wall thickness. The nominal reaction temperature was 400°C. Other conditions and results are listed in Table 1, and aspects peculiar to each run are described below.

The first hydrochlorination run (designated ZH-1) was terminated after only 15 min when the system pressure increased due to blockage with solids (condensed $ZrCl_4$) in the downstream portion of the apparatus. The run was characterized by a notable temperature rise at the reaction boat due to a faster-than-expected HCl-metal reaction and the appearance of entrained solids downstream from the main collection trap.

Of particular interest was the appearance of the partially reacted Zircaloy-2 tubing. The metal was dark and lustrous, in contrast to the original silvery appearance, and was covered with black pits randomly spaced 1 to 2 mm apart. Both the inner and outer surfaces were covered with a gray, cohesive film which, when peeled off, had the appearance of onion skin. It is thought that this film is the original Zircaloy oxide layer. If this is the case, then (1) oxided surface layers do not impede the metal-HCl reaction, and (2) oxided layers seem to be inert to HCl.

Since the $ZrCl_4$ had condensed in the outlet line of the furnace tube, additional line heating was provided. The system was modified to reach temperatures well above the sublimation temperature for $ZrCl_4$ (331°C). A modified cold trap for the collection of volatile chlorides was also installed.

Run ZH-1A was performed in an attempt to hydrochlorinate the Zircaloy-2 remaining from run ZH-1. After 45 min of hydrochlorination, line blockage was again experienced and HCl flow stopped. The run was terminated. Weighing of the metal residue in the reaction boat indicated that about 60% of the tubing had been reacted in the two runs.

Upon disassembly of the apparatus, it was found that the condensed chlorides essentially plugged the transfer line at the inlet to the product cold trap. Subsequently, a further modification of the product collection apparatus was made to relieve this problem.

In the next run, ZH-2, seven granules of ceramic UO_2 were placed in the reaction boat with the metal specimen. It was hoped that some indication of the behavior (or lack of behavior) of uranium dioxide would be seen. The run was conducted under somewhat more moderate conditions, a lower HCl gas flow rate and a lower initial temperature. HCl flow was maintained for 4 hr. At the end of the run, the UO_2 showed essentially no weight change. The collected chloride product was set aside as a sample (ZH-2-V), and the nonvolatile residue and UO_2 granules were replaced in the reaction boat for further hydrochlorination (run ZH-2A).

TABLE 1. Hydrochlorination of Zircaloy-2,
Conditions and Results.

		Gas Flow Rate, cc/min			System	Material Weight, g			
Run No.	Duration, min	N_2	HCl	Reaction Temp, °C	Pressure, mm Hg	Original Zr-2	Reacted Zr-2	Volatile Product	% Zr-2 Reacted
ZH-1	15	400-200	100-50	400	800-1000	4.60	2.77	4.65	60
ZH-1A	45	250	50	350-400	810-850				
ZH-2	240	250	50	260-350	810	5.11	4.96	3.87	97
ZH-2A	130	250-200	50-75	350-400	810-900			5.93	

HCl flow in run ZH-2A was maintained for about 2 hr. Weighing of the residue in the boat indicated that about 97% reaction of the Zircaloy-2 had been achieved in the combined run periods. The weight of the UO_2 granules remained essentially the same; visually, they appeared to be unreacted.

Samples of the overhead product and nonvolatile residues from runs ZH-1A, ZH-2, and ZH-2A were submitted for spark-source mass spectrographic analysis (performed by Battelle Memorial Institute, Columbus, Ohio). A specimen of the original Zircaloy-2 tubing (Z2A-2) was also submitted. Samples were all subjected to a total element scan at nominal precision.

Analyses for 73 elements reported in the six samples are listed in Table 2, and the calculated amounts and distribution of elements of interest are

TABLE 2. Mass Spectrographic Analysis of Zircaloy
and Reaction Products (ppmw)

		Sample Designation				
		Volatile Product			Nonvolatile Residue	
Element	Zircaloy Metal Z2A-2	ZH-1A	ZH-2	ZH-2A	ZH-1A	ZH-2A
Li	<0.003	0.005	<0.003	<0.003	0.1	2
Be	<0.003	<0.01	<0.005	<0.005	<0.003	<0.003
B	0.05	2	1	2	100	1000
F	<10a	20	5	5	20	100
Na	<30	<5	<3	<3	50	200
Mg	<30	<5	<1	<1	50	200
Al	50	20	20	10	500	5000
Si	30	20	<1	<1	200	3000
P	3	<0.3	<0.05	<0.05	20	50
S	20	<1	<0.5	<0.5	20	30
Cl	10	Major	Major	Major	High	High
K	0.1	1	10	3	20	200
Ca	<2	3	5	2	30	200
Sc	b	b	b	b	b	b
Ti	50	<30	<20	<20	50	300
V	<10c	<1	<0.5	<0.5	10	10

(Contd.)

TABLE 2. (Contd.)

| | | Sample Designation | | | | |
| | | Volatile Product | | | Nonvolatile Residue | |
Element	Zircaloy Metal Z2A-2	ZH-1A	ZH-2	ZH-2A	ZH-1A	ZH-2A
Cr	1000	<3	<2	<2	∿2%	∿2%
Mn	20	2	1	0.3	500	1000
Fe	2000	10	30	5	∿3%	∿3%
Co	<5	<0.3	<0.1	<0.3	5	20
Ni	30	100	<50	<20	2000	5000
Cu	10	100	500	300	∿5%	∿5%
Zn	<0.3	300	300	300	10	100
Ga	<0.2	<0.3	<0.5	<0.5	<0.3	<0.3
Ge	<0.1	<2	<3	<3	<2	<2
As	5	<0.2	<0.3	<0.3	50	100
Se	<1	<2	<2	<2	<1	<3
Br	<0.1	0.3	0.5	1	0.5	1
Rb	<0.03	<2	<2	<1	<0.5	<0.5
Sr	<0.1	<0.3	<0.5	<0.3	≤1	≤3
Y	<0.3	<0.3	<0.2	<0.2	1	1
Nb	3	<3	<20	<20	100	50
Mo	<0.5	≤3	<3	<3	<5	30
Ru	<0.3	<2	<1	<1	<2	<2
Rh	<2	<2	<1	<1	<2	<2
Pd	<5	<5	<5	<3	<10	<10
Ag	<3	<3	<5	<5	<3	<3
Cd	<3	<5	<10	<10	<30	<30
In	<10	<2	<3	<3	<100[d]	<100[d]
Sn	5000	100	2000	2000	∿5%	∿3%
Sb	1	<0.5	<0.3	<0.3	3	2
Te	<2	<5	<3	<3	<10	<10
I	<0.5	<2	<1	<1	<2	<2
Cs	<0.3	<3	<2	<2	<0.5	<0.5
Ba	<0.3	<2	<3	<3	10	20
La	<0.2	<2	<1	<1	<2	3
Ce	<0.1	<2	<1	<1	<2	<2
Pr	<0.3	<2	<3	<2	<2	<3
Nd	<0.2	<5	<3	<3	<3	<10
Sm	<0.2	<5	<3	<3	<3	<3
Eu	<0.1	<3	<2	<2	<3	<2
Gd	<0.2	<0.3	<1	<1	<0.5	<1
Tb	<0.05	<0.3	<0.5	<0.2	<1	<1
Dy	<0.2	<2	<1	<1	<2	<2
Ho	<0.05	<0.2	<0.2	<0.2	<0.5	<0.5
Er	<0.2	<0.5	<0.3	<0.3	<1	<1
Tm	<0.05	<0.2	<0.1	<0.1	<0.3	<0.3
Yb	<0.2	<0.5	<0.3	<0.3	<1	<1
Lu	<0.05	<0.2	<0.1	<0.1	<0.3	<0.3
Hf	20	<0.5	<0.3	<1	20	20
Ta	<10	<2	<0.3	<0.1	≤10	≤10

(Contd.)

TABLE 2. (Contd.)

Element	Zircaloy Metal Z2A-2	Sample Designation				
		Volatile Product			Nonvolatile Residue	
		ZH-1A	ZH-2	ZH-2A	ZH-1A	ZH-2A
W	<0.2	<0.2	<0.3	<0.3	≤1	3
Re	<0.3	<0.3	<0.2	<0.2	<1	<1
Os	<0.2	<0.5	<0.3	<0.3	<2	<2
Ir	<0.1	<0.1	<0.05	<0.05	<0.3	<0.3
Pt	<0.2	<0.2	<0.1	<0.3	<0.5	<0.5
Au	<2	<2	<2	<2	<0.2	<0.5
Hg	<0.2	<0.5	<0.3	<0.3	<0.3	<0.3
Tl	<0.1	<3	<2	<2	<0.3	<0.3
Pb	5	0.3	0.5	0.2	100	100
Bi	0.5	0.3	0.1	<0.1	2	3
Th	<0.2	<0.5	<0.3	<0.3	0.3	0.3
U	1	<0.5	<0.3	<0.3	5	10

[a] Possible contamination from HF etch.

[b] Zr interference.

[c] Memory from previous sample

[d] Sn interference.

given in Table 3. The indications are that the key elements previously expected (see ANL-8152)[1] to remain as nonvolatiles (*e.g.*, chromium, manganese, cobalt, nickel, and uranium) do so. Some of the elements predicted to volatilize as chlorides (iron and tin) did so in varying amounts. Antimony was not found in the volatile fraction, down to analytical limits of detection. The elements representing major activities that are induced by neutron capture and decay processes have been previously identified;[3] of these, chromium, nickel, cobalt, and niobium remained in the nonvolatile residue.

Major perturbations occurred in attempting a material balance (amounts of elements in reacted Zircaloy tubing compared to amounts found in the total of nonvolatile and volatile fractions). Amounts of nickel and zinc in the total of residual and volatilized material far outweigh the amounts calculated for the original Zircaloy reacted during the hydrochlorinations; this is believed due to the apparatus being constructed of commercial nickel tubing joined by silver solder that contains about 17 wt % zinc. Yet to be resolved is the fact that uranium, iron, antimony, cobalt, and hafnium analyses yield totals, in the reaction products, that are considerably less than the calculated amounts in the Zircaloy tubing reacted.

In general, hydrochlorination shows promise as a means of separating zirconium from the bulk of the elements in Zircaloys and providing a consolidated plutonium-containing fraction. Runs with irradiated Zircaloy-2 are being planned that should permit confirmation of this separation under more realistic process conditions.

Table 3. Calculated Amounts of Elements in
Samples from Hydrochlorination Runs
ZH-1, ZH-1A, ZH-2, and ZH-2A

Element	Element Weight Based on Reacted Zircaloy, μg	Total Element Weight in Volatile and Nonvolatile Fractions, μg	Element Distribution Based On Material Balance[b]	
			Fraction in Nonvolatiles	Fraction in Volatiles
Cr	7700	5100	High	L.D.
Mn	155	171	High	Low
Fe	15500	7900	High	Low
Co	37	2	High	L.D.
Ni	232	678[a]	High	L.D.
Zn	2	4300[a]	Moderate	High
Nb	23	23	High	L.D.
Sn	38700	31800	Moderate	High
Sb	8	1	High	L.D.
Ba	2	3	High	L.D.
Hf	155	5	High	L.D.
U	8	2	High	L.D.

[a] High values are attributed to these elements comprising the materials of construction; the tube furnace and reaction boat are nickel; zinc is a component of the silver solder.

[b] Not calculated because concentrations on many elements were below limits of detection (L.D.).

C. Pyrochemical Studies

A number of pyrochemical (molten metal/molten salt) process flow sheets appear to be applicable to the processing of Zircaloy hulls, with process selection being dependent on program objectives. Processes under initial consideration are intended (1) to transform the Zircaloy into a form that no longer represents a potential pyrophoric hazard, and (2) to effect a separation and concentration of the long-lived alpha-emitting radionuclides. It is also desired to maximize the recycle process reagents and thereby reduce the overall volume of alpha-bearing waste.

1. Oxidation of Zircaloy with ZnCl₂

Experimentation has continued on the use of $ZnCl_2$ as an oxidizing agent, the main reaction being $Zr + 2 ZnCl_2 \rightarrow ZrCl_4 + 2 Zn$. The intent is to separate $ZrCl_4$ by volatilization, leaving the actinides in the metal phase. The zinc would be rechlorinated and reused, effecting a net reduction in waste volume. In previous experiments, relatively high mole ratios (∿5) of salt to metal were used, leaving an excess of $ZnCl_2$. This almost totally suppressed the volatilization of the $ZrCl_4$ although the vapor pressure of pure

ZrCl$_4$ at 500°C, the current reaction temperature, is very much higher than that of ZnCl$_2$--9 x 10^4 mm Hg in contrast to 10 mm Hg. The extent of suppression may be gleaned from data on other salt systems (see Table 4)).[4] For example, the vapor pressure of ZrCl$_4$ from a mixture of 69.85 mol % ZrCl$_4$ and 30.15 mol % KCl is about 74% that of pure ZrCl$_4$. A modest 4 mol % increase in KCl concentration to 34.05 mol % lowers the ZrCl$_4$ vapor pressure drastically--to about 29% of that of the pure species.

Table 4. Suppression of ZrCl$_4$ Vapor Pressure in Binary Salt Systems[4]

Mixed Salt	Temperature, °C	Vapor Pressure of ZrCl$_4$ at Given Temperature, mm Hg	
		Pure Substance	Observed
62.28 mol % ZrCl$_4$ 37.72 mol % NaCl	381	3500	1159
69.85 mol % ZrCl$_4$ 30.15 mol % KCl	388.5	4100	3048
65.95 mol % ZrCl$_4$ 34.05 mol % KCl	387.5	4100	1208

In an effort to expedite the removal of ZrCl$_4$ in the present ZnCl$_2$ system, slightly less than the stoichiometric quantity of ZnCl$_2$ required to oxidize the Zircaloy charge was used in a recent experiment. The charge consisted of 104 g of Zircaloy tubing (22 sections, 1/2-in. OD x 1/32-in wall x 1 in. long), 300 g of ZnCl$_2$, 1 g of CeO$_2$ (a stand-in for PuO$_2$), and 5 g of UO$_2$. The charge was placed in a tungsten crucible in an induction-heated tilt-pour furnace. The melt was held at 500°C for a period of 6 hr under a 15-psig argon atmosphere. During the final two hours, the melt was mixed at a rate of 400 rpm.

At the end of the experiment, a small metal heel (consisting of zinc and unreacted Zircaloy) remained in the crucible, and vaporized salt (presumably ZrCl$_4$) covered the walls and graphite receiver in the sidearm of the tilt-pour furnace. Samples of the metal heel and vaporized salt are being analyzed, mainly to determine the distribution of the uranium and cerium. Since the ZnCl$_2$ was essentially all reacted during the reaction period, the ZrCl$_4$ was free to vaporize, thereby providing separation of the bulk constituent, zirconium, from the crucible residue.

An alternative approach is to use a slight excess of ZnCl$_2$. Volatilization of the ZrCl$_4$ would be somewhat suppressed during the reaction, but subsequent recovery of the ZrCl$_4$ from the mixed salt should be relatively easy. The use of binary or ternary chloride salts as the oxidant is also under consideration.

In an actual working system, the $ZrCl_4$ would be collected in condensers. If the $ZrCl_4$ is sufficiently free of alpha-emitting nuclides, possible subsequent process options include: (1) more conventional (nonretrievable) storage as a waste; the final form, chloride, oxide, or metal would depend on the flow sheet and (2) salvage. A known contaminant will be ^{93}Zr ($t_{1/2} = 9.5 \times 10^5$ yr), whose presence needs evaluation.

The process requires that the zinc be rechlorinated. The behavior of the radionuclides during this rechlorination needs to be examined. Limits in reuse of the zinc and final treatment of this metal phase also need study.

2. Miscellaneous Exploratory Pyrochemical Studies

An alternative pyrochemical concept suggested for separating the zirconium from the alpha-bearing waste stream would employ a zirconium precipitation step. Process steps include dissolution of the hulls in zinc, adjusting conditions such that the zirconium precipitates, and separation of the zirconium phase. An exploratory test of the precipitation step was made by preparing a 12 wt % zirconium-zinc solution at 850°C; materials included 360 g of Zircaloy-2 and 2640 g of zinc in a graphite crucible. A salt cover of $MgCl_2$-30 wt % NaCl-20 wt % KCl was used. Dissolution was completed in two hours. Slow cooling of the melt was expected to achieve some separation of the zirconium; however, analyses showed that only intermetallics formed, such as $ZrZn_6$, $ZrZn_{14}$, and $ZrZn_{22}$. Density differences between these materials and the zinc apparently were insufficient to effect any separation, and this approach is being abandoned.

D. Ignition and Other Miscellaneous Tests with Various Zircaloy Materials

A high interest exists in obtaining information on the possible pyrophoric behavior of Zircaloy hulls. In the absence of irradiated materials, ignition tests are being performed on unirradiated Zircaloy materials, including tubing, turnings, and fines from a sawing operation. To date, uncompacted saw fines appear rather susceptible to ignition.

1. Ignition Tests with Tubing

A series of nine small-scale burn tests on single Zircaloy tubing sections was carried out at Teledyne Wah Chang Albany (TWCA) through the cooperation of Dennis Tetz, Staff Engineer. TWCA is a large manufacturer of nuclear-grade Zircaloy metal and has an ongoing interest in this general area. The main intent in the TWCA experiments was to exaggerate the fines-to-metal ratio over that expected in the actual hulls case and to determine whether a Zircaloy tubing section could be ignited. Two types of zirconium igniter powders were used at powder-to-metal ratios in the range 0.25 to 8.0; the powders were designated as -300 mesh (<50 μm) Zr-2-Si dehydrided powder and 18-20 μm leached zirconium powder. Seven tests were made with Zircaloy sections, 0.312 in. long, cut from Zircaloy-4 scrap tubing stock, 0.578 in. dia, 0.031 in. wall thickness. One of these sections was autoclaved and hydrided until it contained 100 ppm hydrogen; the others were tested as is. Two tests were made with half-ring sections; these tests were the ones with the highest powder-to-metal weight ratio (8 to 1).

For each test, the powder was placed on a ceramic base, and the ring section (axis horizontal) was placed on the cone of powder. The materials,

initially at ambient conditions, were heated with a gas torch (or in one case, with an oxygen torch) until the powders ignited. The ignition temperature and burn time of the powder and the maximum temperature attained by the system were noted. Test conditions and results are shown in Table 5.

Ignition of the powder occurred at about 430°C and 400°C, the leached powder igniting at the lower temperature. Powder burn time ranged from 25 to 80 sec. Maximum observed temperatures during burning ranged from 585 to 1600°C.

The key result is that the tubing sections showed no sustained ignition (no pyrophoric behavior) after the powder burning ended. This was true at 1600°C, a temperature approaching the melting point of zirconium (∿1850°C), and even for the test in which an oxygen torch was used. Glowing of the tubing was observed, but only when the torch was directed at the tubing. An oxidized surface was noted on the tubing after each test, as expected.

2. Ignition Tests with Zircaloy Turnings

Zircaloy turnings used in ignition tests had a bright surface and were in the shape of small springs. They varied from 0.003-0.011 in. in thickness, 0.030 to 0.113 in. in width, and 0.25 in. to 3 in. in length. Not a single turning ignited with the flame of a match, but ignition did occur with the flame from a gas-oxygen torch.

3. Ignition Tests with Zircaloy Fines

Ignition tests were performed on Zircaloy fines obtained from a sawing operation. The saw fines were intermeshed spring-like pieces with a steel wool appearance. These were 0.001 in. x 0.001 in. in thickness and width and varied in length from 1/8 in. to 1 in.

A small portion of the saw fines was compacted to obtain a pellet weighing 0.2606 g and having a density of about 2.63 g/cc. Ignition of the pellet with sparks and matches was not possible. However, application of a flame from a gas-oxygen torch resulted in ignition; the pellet burned (oxidized quickly) with a bright glow.

A small pile of uncompacted saw fines did not ignite with a spark source but did ignite when the flame of a match was applied.

Although these tests on tubing and fines were not done with irradiated material, the results support the opinions of persons experienced in the field--that tubing would be difficult (perhaps impossible) to ignite and that fines can be ignited under some conditions. These results also confirm the experience reported in the literature, that relatively fine material with a relatively higher surface-to-volume ratio can be ignited with a low-energy ignition source, such as a match. Compacts require somewhat more energetic sources.

The quantity of fines in the actual chop-leach case is expected to be small (fines-to-metal weight ratio estimated at <0.01), adding to the likelihood that the hulls could not be ignited if they behave similarly to

Table 5. Ignition Tests Performed on Zircaloy Tubing Sections
(Courtesy of Teledyne Wah Chang Albany)

Tubing material: clean Zircaloy-4 in all tests, except test 7 which used an autoclaved, hydrided section containing 100 ppm hydrogen.

Tubing section dimensions: 0.312 in. length x 0.578 in. dia x 0.031 in. wall for all tests except tests 5 and 6 which each used a half-ring section; corresponding weights were 1.5 and 0.75 g.

Igniter powders: -300 mesh (<50 µm) Zr-2-Si dehydrided powder, tests 1-5; 18-20 µm leached Zr powder, tests 6-9.

Heat source: MAAP gas torch; in addition, an oxygen torch was used in test 9.

Initial conditions: materials at ambient conditions on a ceramic base.

	Igniter Powder		Test Piece			
Test No.	Mass, g	Powder-to-Test-Piece Weight Ratio	Ignition Temp, °C	Burn Time, sec	Maximum Temp Attained, °C	Remarks
1	0.375	0.25	430	30	822	Tubing did not ignite; all tubes had an oxidized surface at the end of the test.
2	1.5	1	430	80	585	
3	3.0	2	430	50	941	
4	6.0	4	430	70	894	
5	6.0	8	430	25	1150	
6	6.0	8	400	60	798	
7	6.0	4	400	50	1098	
8	6.0	4	400	65	1600	Burning powder plus torch used in attempt to ignite the tubing section. The tubing only glowed and only while the torch flame was applied.
9	6.0	4	400	70	1600	

16

nonirradiated tubing. Similar tests with irradiated Zircaloy tubing will be conducted when material becomes available.

The collaboration of TWCA in providing these tests and materials for our own tests is gratefully acknowledged.

4. Ignition Tests on Zinc-Coated Tubing

A technique considered for reducing the potential for pyrophoric behavior of Zircaloy hull compacts is to coat the material with an inert substance such as zinc. The effectiveness of such a coating is being explored in simple coating and heating tests. Initial tests were made on sections of compacted Zircaloy tubing which had been coated by being dipped in molten zinc at 575°C for 10 to 15 min. Heat from a match showed no effect on the zinc coating; the application of a gas-oxygen torch resulted in oxidation of the zinc coating, but produced no self-sustaining flame. Future tests will be made on zinc-coated scrap Zircaloy turnings and saw fines.

5. Oxidation of Zircaloy Tubing in Air

Earlier tests showed that ignition of Zircaloy tubing sections with a gas-oxygen torch was not possible and resulted only in oxidation of the tubing. An experiment was conducted to determine the extent to which Zircaloy-2 tubing sections would oxidize in air in a 1-hr period. Heating was done in a muffle furnace at temperatures of 700, 800, and 900°C. The results of the test are shown in Table 6. The results indicate that each 100°C increase in temperature, the oxidation rate increases by about a factor of three. The extent of oxidation of the tubing sections was only about 13%, even at the highest temperature tested. No signs of ignition of the Zircaloy, even at 900°C, were noted. Oxide formed on the surface of Zircaloy tube sections may act as a protective coating in preventing burning or ignition.

Table 6. Oxidation of Zircaloy Tubing in Air

Specimen	Temp, °C	Wt gain, g	Oxidation, wt %
1	700	0.0198	1.22
2	700	0.0249	1.49
3	800	0.0731	4.45
4	800	0.0774	4.6
5	900	0.2135	13.1
6	900	0.2079	12.1

6. Analysis of Fines Produced by Chopping Zircaloy Tubing

Since the concern over pyrophoric behavior of Zircaloy seems to stem mainly from experience with finely divided material, information on the quantities and size distribution of the fines produced by chopping Zircaloy-clad fuel is of particular interest. Unfortunately, virtually no information has been found in the literature on this subject, but, for a first approximation, fines obtained from the dry chopping of ordinary Zircaloy tubing at

Teledyne Wah Chang Albany were characterized by sieve analysis and determination of their oxygen content (see Table 7). No specific values were obtained for the quantities of fines produced per batch of tubing, but the weight ratio of fines-to-tubing was estimated to be much less than 0.01.

Table 7. Sieve Analysis and Oxygen Content
of Fines Resulting from Chopping
of Zircaloy Tubing

Particle Size			Oxygen Content,
Mesh No.	˙μm	wt %	wt %
+ 8	+ 2380	66.3	0.11
+ 10	+ 2000	5.8	0.14
+ 12	+ 1680	1.5	NA
+ 14	+ 1410	2.9	NA
+ 25	+ 710	13.5	0.46
+ 45	+ 350	7.3	NA
- 45	< 350	2.7	3.32

The chopper fines varied from micron-sized particles to chunks and slivers 0.100 in. (2.54 mm) thick x 3/8 in. (9.52 mm) wide x 3/4 in. (19.0 mm) long. The surfaces of the metal were bright, with some silver-gray, scale-like particles.

About 2/3 of the particles were larger than 8 mesh; these had the lowest oxygen content, 0.108%. The particles smaller than 45 mesh, which represented 2.7% of this particular sample, had an oxygen content of 3.32%. Higher oxygen contents were expected for the smaller particles, since oxygen content is generally a function of surface-to-volume ratios.

For comparison, an oxygen analysis of fines produced in the sawing of massive Zircaloy showed an oxygen content of 0.30%, while Zircaloy turnings had an oxygen content of 0.24%. It is surprising that the saw fines had such a low oxygen content, but this may be related to a liquid coolant having been used during these machining operations, which may have inhibited surface oxidation.

Since irradiated Zircaloy is expected to be more brittle than the tubing used in this work, a larger fraction of fines can be expected. Further information in this area awaits actual chopping of high-burnup fuel.

II. SALVAGE OF ALPHA-CONTAMINATED METALS
(T. J. Gerding, I. O. Winsch, T. Cannon, N. Levitz)

Development work is in progress on decontamination methods for waste metal contaminated with alpha-active elements, particularly plutonium. This waste is accumulating at ERDA facilities as a result of upgrading and/or

replacement of equipment and the decommissioning of entire alpha facilities. Current regulations require that wastes containing long-lived alpha activity at levels above 10 nCi/g of waste, when stored, be retrievable. This type of storage is expensive. This provides incentive for reducing the volume of waste needing specialized care. The analytical uncertainty associated with sampling irregularly shaped materials (*e.g.*, equipment items) after chemical/mechanical surface cleaning suggested that the material be reduced to standard forms (ingots, slabs).[5] Melting/slagging techniques were selected to achieve program objectives.[6]

A glovebox facility is being set up for work with plutonium-contaminated metal. Setup of this facility was delayed several months when the glovebox initially intended for this work was diverted to satisfy other Divisional commitments, and another glovebox had to be located and made suitable. Supporting studies are being made with steel containing no plutonium to test steel-melting procedures, to help select crucible materials (particularly for use with slagging materials, which can be corrosive), and to otherwise characterize candidate systems. Recent support work is described.

A. Glovebox Facilities

A 1 1/2-by 3-module CHENHAM[*] glovebox with support systems is being completed for steel-melting experiments associated with the program on salvage of plutonium-contaminated metals. The glovebox will have a helium atmosphere for added flexibility.

The key item of equipment in the glovebox is a Brew, Model 1064-C resistance-heated furnace modified to facilitate glovebox operation and maintenance. The unit is capable of temperatures approaching 3000°C. This unit has tungsten mesh elements and can be operated at high current inputs, up to 1000 amperes, at about 35 V. Preliminary heating tests on the furnace were satisfactory. The heated zone will accommodate metal samples weighing up to 1.0 kg. It is also proposed to install in the glovebox a small laboratory-type arc melter with a sample capacity of about 50 g before the glovebox is closed up for "hot" operation.

The major support systems include a helium purification system, the furnace coolant recirculation system, a vacuum system, and safety interlocks. These have all been installed and are undergoing mechanical testing. Remaining work before startup of work with plutonium includes window installation and cold testing of the furnace.

B. Supporting Studies

Supporting studies in progress consist of steel-melting experiments with noncontaminated steel, using CeO_2 as a stand-in for PuO_2. The object is to determine the feasibility of drossing or slagging the CeO_2; several slagging materials will be tested. Some slagging materials common to the steel industry are being acquired; others are being made *in situ*, during melting of the steel.

---

[*] CENHAM refers to Chemical Engineering Division High Alpha Module.

Four scouting steel-melting experiments have been completed on noncontaminated steel scrap in an induction-heated furnace. In each of the initial three experiments, about 450 g of mild steel and 0.5 g of CeO_2 were charged to slip-cast magnesia crucibles (2.5-in. OD x 2.25-in. ID x 5.275 in. high). The charges were heated under an argon atmosphere to about 1500°C and were liquated at this temperature for two hours. The melts were allowed to cool in the crucible, and the ingots were then removed for sampling. Turnings were machined from the top and bottom of the ingots; after sectioning drillings were taken as samples from interior portions of the ingots. Analyses are pending.

The fourth experiment was performed similarly to the above-described experiments except that cryolite, $3NaF-AlF_3$, was added as a slagging material. The ingot from this melt was sampled as above.

The MgO crucibles used in the first three experiments were observed to be slightly undercut (evidence of corrosive attack); the crucibles adhered to the ingots in some areas. In the fourth experiment, the cryolite reacted with the crucible at the molten steel-salt interface and completely penetrated the crucible wall. More resistant crucible materials will be sought for future steel-melting experiments.

The furnace is being fitted with a quartz sight glass to permit use of a pyrometer to monitor temperature, since thermocouple lifetimes have been shortened due to the corrosive nature of the system.

C.   Slag Preparation

Numerous slagging materials used in the steel industry may be suitable for separating PuO_2 from molten steel; a partial listing is shown below:

1. $CaO \cdot SiO_2$
2. $CaO \cdot MgO \cdot SiO_2$
3. $CaO \cdot CaF_2 \cdot SiO_2$
4. $CaO \cdot Al_2O_3 \cdot SiO_2$
5. $SiO_2 \cdot B_2O_3$
6. $CaO \cdot Fe_2O_3$

A problem exists in the selection of materials to evaluate. Experience of Fullam[7] in working with alpha- and beta-gamma-contaminated stainless steel may be of some help. A compilation by Shaw[8] on experience with uranium-contaminated steel is currently under review. In view of a lack of technical bases, empirical testing of individual slagging materials appears to be necessary and represents the present direction of effort.

III. STORAGE AND DISPOSAL OF TRITIUM
(L. E. Trevorrow)

A. Introduction

The general, long-range objective of this project is to evaluate alter-
natives in the management of tritium in waste arising from the production of
power by nuclear reactors. In the near term, electric power will be produced
predominantly by light-water reactors. Unless tritium is removed from the
fuel (e.g., by the Voloxidation process) before dissolution in aqueous acid
(an early step in Purex reprocessing flow sheets), a major portion of the
tritium formed by ternary fission in light water reactors is expected to
appear in the low-level aqueous waste (LLAW) stream of the plants for repro-
cessing spent fuel from LWRs.

Presently accepted schemes for managing this waste stream include dis-
persal as a vapor to the atmosphere or as a liquid to surface streams; this
waste stream is diluted with air or water to concentrations lower than those
specified by radiation concentration guidelines. Such dispersal schemes,
however, have met some objection by groups and agencies who believe that
the radiological risks associated with these schemes are excessive. In pre-
paration for the possibility that these objections might ultimately result
in more restrictive regulations on disposal, alternative disposal techniques
have been proposed by several organizations involved in nuclear energy develop-
ment. The evaluation of such proposals constitutes the main effort in this
project.

Proposals for retention of the tritium contained in LLAW have generally
fallen into two categories: those that do and those that do not involve con-
centration (i.e., isotope separation). The disposal option currently being
evaluated (i.e., deep-well injection of LLAW) is one that does not involve
concentration. Past efforts in the evaluation of this option have included
a preliminary survey of literature[6] and a selection of factors (based on
that survey and on communications with representatives of the U.S. Geological
Survey and with a consulting geological engineer) to be considered in an
evaluation.

The choice of a site for deep-well injection is one of the most important
factors bearing on the question of feasibility of disposal of tritium by
deep-well injection of LLAW. It includes such considerations as: the geologi-
cal properties necessary for containing and transmitting fluids; prospecting
and analysis for these properties; predictions, based on the geological
characteristics, of the behavior of contained fluids; and existing information
on the geographic location of suitable geology in the U.S. The remainder of
Section III of this report is a discussion of siting considerations contri-
buted by the consulting geological engineer participating in the project,
Professor D. L. Warner (U. of Missouri-Rolla).

B. General Considerations

Selection of a site for a wastewater injection well begins at the regional
level, then is narrowed to the vicinity of the site, and finally focuses upon
the immediate well location. Outlined in Table 8 are factors to be considered
in site evaluation at the regional and local levels.

Table 8. Factors to be Considered for Geologic and
          Hydrologic Evaluation of Site for
          Subsurface Waste Injection

Regional geologic and hydrologic framework

Physiography and general geology; structural geology;
stratigraphy; groundwater; mineral resources; seismicity;
hydrodynamics.

Local geology and geohydrology

A. Structural geology
B. Geologic description of subsurface rock units

1. General rock types and characteristics.
2. Injection horizons and confining beds

Lithology; thickness and vertical and lateral
distribution; areal distribution; porosity
(type and distribution, as well as amount);
permeability (same as areal distribution);
reservoir temperature and pressure; chemical
characteristics of reservoir fluids; forma-
tion breakdown or fracture pressure; hydro-
dynamics.

3. Groundwater aquifers at the site and in the
    vicinity

Depth; thickness; general character; amount
of use and potential for use.

4. Mineral resources and their occurrence at the well
    site and in the immediate area.

Oil and gas (including past, present, and
possible future development); coal; brines;
other.

Experience has shown that nearly all types of rocks can, under favorable
circumstances, have sufficient porosity and permeability to yield or accept
large quantities of fluids. Sedimentary rocks, especially those deposited
in a marine environment, are most likely to have the geologic characteristics
suitable for waste-injection wells. These characteristics are (1) an injection
zone with sufficient permeability, porosity, thickness, and areal extent to act
as a liquid-storage reservoir at safe injection pressures; and (2) an injection
zone that is vertically below the level of fresh-water circulation and is
confined vertically by rocks that are, for practical purposes, impermeable
to waste liquids.

Vertical confinement of injected wastes is important not only for the
protection of usable water resources, but also for the protection of developed
and undeveloped deposits of hydrocarbons and other minerals. The effect of
lateral movement of waste on such natural resources also must be considered.

The minimum depth of burial, the necessary thickness of confining strata, and the minimum salinity of water in the injection zone have not been established quantitatively, and it may be possible to specify these constraints only for individual cases, as has been done in the past.

The minimum depth of burial can be considered to be the depth at which a confined saline-water-bearing zone is present; it may be between a few hundred feet and several thousand feet.

Regulatory agencies will specify allowable salinity of water in an injection zone to be used for storage. The level specified will be that considered necessary to protect usable groundwater resources. Other chemical and physical properties of subsurface water must be known in order to compute fluid flow rates and directions and in order to anticipate the possibility of chemical reactions between aquifer fluids and injected wastewater. The lithology of the aquifers and aquicludes must also be evaluated to anticipate possible chemical reactions with injected wastewater.

The thickness and permeability necessary to allow fluid injection at the desired injection rate can be estimated from equations developed by petroleum engineers and groundwater hydrologists. The geometry of the injection zone also determines its suitability for waste injection. A thick lens of highly permeable sandstone might not be satisfactory for injection if it is small and surrounded by impermeable beds, because pressure buildup in the lens would be rapid, in comparison with that in a "blanket" sandstone.

It may be desirable in some cases to inject wastes into a known geologic structural feature. Under favorable conditions, this practice would help to ensure the confinement of the waste within a specified area and also might allow its recovery at a later date if, for example, recovery of the dissolved solids should become economically feasible. Wastes of relatively high specific gravity stored in closed synclines would not tend to leak upward into fresh-water-bearing strata and would not move laterally into hydrocarbon-bearing anticlinal features under hydrostatic conditions.

In addition to stratigraphy, structure, and rock properties, which are factors routinely considered in subsurface studies, aquifer hydrodynamics may be significant in the evaluation of waste-injection well sites. The presence of a natural hydrodynamic gradient in the injection zone will cause the injected waste to be distributed asymmetrically about the well bore and to be transported through the aquifer even after injection has ceased. The entrapment of fluids is modified under hydrodynamic conditions.

Hydrodynamic dispersion--the mixing of displacing and displaced fluids during movement through porous media--may cause much wider distribution of waste in the injection zone than would otherwise be anticipated. Dispersion is known to occur in essentially homogeneous isotropic sandstone, and it could lead to particularly rapid lateral distribution of waste in heterogeneous sandstone and fractured, or cavernous strata. Sorption of waste constituents by aquifer minerals retards the spread of waste from the injection site.

The mathematical models now available are satisfactory for accurately predicting the movement of waste in most natural aquifers only under restrictive, simplified physical circumstances. Even if knowledge of the physics of

fluid movement in natural aquifers were considerably more advanced, the determination of the physical parameters that characterize an injection zone still would be difficult if few subsurface data were available. These restrictions do not, however, preclude quantitative estimation of the rate and direction of movement of injected waste.

The maximum pressure at which liquids can be injected without causing hydraulic fracturing may be the factor limiting the intake rate and operating life of an injection well. The injection pressure at which hydraulic fracturing will occur is related directly to the magnitude of regional rock stress and the natural strength of the injection zone.

Other considerations in the determination of site suitability are:

(1) the presence of abnormally high natural fluid pressure and temperature in the potential injection zone that may make injection difficult or uneconomical;

(2) the local incidence of earthquakes that can cause movement along faults and damage to the subsurface well facilities;

(3) the presence of abandoned, improperly plugged wells that penetrate the injection zone and provide a means for escape of injected waste to groundwater aquifers or to the surface; and

(4) the potential of the area for earthquake activity that could be triggered by wastewater injection.

C.   Factors in Site Evaluation

1.   Stratigraphic Geology

Sandstone, limestone, and dolomite strata are commonly porous and permeable enough in the unfractured state to be suitable injection zones. Naturally fractured limestone, dolomite, shale, and other rocks also may be satisfactory. Rocks with solution or fracture porosity may be preferable to rocks with intergranular porosity because commonly, solution and fracture flow channels are relatively large in comparison with intergranular pores and are not, therefore, as likely to be plugged by suspended solids in the injected liquids. Waste injection into limestone and dolomite has proved particularly successful in some places because the permeability of these rocks can be improved greatly by acid treatment.

Unfractured shale, clay, slate, anhydrite, gypsum, marl, and bentonite have been found to provide good seals against the upward flow of fluids. Limestone and dolomite may be satisfactory confining strata, but these rocks commonly contain fractures or solution channels, and their adequacy must be determined carefully in each case.

Regional stratigraphy is determined by use of outcrop and borehole data that have been interpreted and are generally presented in the form of columnar sections, isopach maps, facies maps, and cross sections.

The basic data unit used in studies of stratigraphic geology is the columnar section, which is a graphic representation of the sequence, thickness,

lithology, and relationship of the rock units at a location. A generalized columnar section may be prepared, which shows these parameters for a region. Figure 1 is a generalized columnar section for northeastern Illinois. Columnar sections are prepared by use of cores, cuttings, and geophysical logs from boreholes and from outcrops when they are present. Some possible injection horizons in Figure 1 are indicated by the fact that they are being used for natural gas storage. Of these possible injection units, the Mt. Simon Formation is the deepest and is overlain by the Eau Claire Formation, which may contain confining shale beds. On the other hand, the St. Peter Formation is the shallowest and is overlain by limestones and dolomites which are less dependable as aquitards; therefore, the St. Peter Formation has a lesser potential for wastewater injection.

Isopachous maps indicate, by contour lines, the varying thickness of a stratigraphic unit. Figure 2 is an isopachous map of the Mt. Simon Formation in Illinois, showing that this sandstone unit varies in thickness from 0 to over 2,000 feet within that state. Other factors being equal, locations where the Mt. Simon Formation is thickest have the greatest potential for wastewater injection.

The facies of a stratigraphic unit are its laterally varying aspects, such as lithology, fossil content, and so forth. For example, the Eau Claire Formation, which overlies the Mt. Simon Formation, consists of a mixture of siltstone, shale, dolomite, and sandstone in northeastern Illinois (Figure 1), but eastward, it passes by facies change into sandstone, shale, or dolomite at various locations in the east-west cross section as shown in Figure 3.

Types of facies maps include ratio maps, percentage maps, and isolith maps. These facies maps are different ways of showing the relative amounts of the various lithologies in a rock unit or units. The ratio and percentage maps show contours of the ratios or percentages of the aggregate thicknesses of lithologic classes.

Figure 4 is a lithologic ratio map, showing the relative ratios of sandstone, shale, and dolomite in post-Mt. Simon pre-Knox rocks in Ohio. This figure generally shows that this group of rocks changes from a sandy facies in western Ohio to a dolomite facies in eastern Ohio. The rocks depicted in Figure 4 are equivalent to the Eau Claire Formation in Figures 1 and 3. In the absence of further information, Figure 4 shows that the Eau Claire Formation becomes less promising as a confining unit as it is traced from west to east across Ohio.

Local stratigraphy is first projected for the well location from regional data (such as that discussed above) before a well is drilled, then is determined in detail for the well as it is drilled. As previously mentioned, the means of displaying the stratigraphy of a well is the columnar section.

2.   Structural Geology

Structural geology means the folding, faulting, and fracturing of rocks and the geographic distribution of these features. One means of showing regional structural geologic features is a map that includes areas or lines of major features. Figure 5 is such a map for the Ohio River basin. Major

SYS-TEM	SER-IES	STAGE	MEGA-GROUP	GROUP	FORMATION	GRAPHIC COLUMN	THICK-NESS (FEET)	LITHOLOGY
ORDOVICIAN	CINCINNATIAN	RICH.		MAQUOKETA	Neda		0-15	Shale, red, hematitic, oolitic
		MA.			Brainard		0-100	Shale, dolomitic, greenish gray
		ED.			Ft. Atkinson		5-50	Dolomite and limestone, coarse-grained; shale, green
					Scales		90-100	Shale, dolomitic, brownish gray
	CHAMPLAINIAN	TRENTONIAN	OTTAWA	GALENA	Wise Lake - Dunleith		170-210	Dolomite, buff, medium-grained
					Guttenberg		0-15	Dolomite, buff, red speckled
				PLATTEVILLE	Nachusa		0-50	Dolomite and limestone, buff
					Grand Detour		20-40	Dolomite and limestone, gray mottling
		BLACKRIVERAN			Mifflin		20-50	Dolomite and limestone, orange speckled
					Pecatonica		20-50	Dolomite, brown, fine-grained
				ANCELL	Glenwood		0-80	Sandstone and dolomite
					St Peter		100-600	Sandstone, fine grained, rubble at base (Kress Member)
	CANADIAN		KNOX	PRAIRIE DU CHIEN	Shakopee		0-67	Dolomite, sandy
					New Richmond		0-35	Sandstone, dolomitic
					Oneota		190-250	Dolomite, slightly sandy; oolitic chert
					Gunter		0-15	Sandstone, dolomitic
CAMBRIAN	CROIXAN	TREMPEALEAUAN			Eminence		50-150	Dolomite, sandy, oolitic chert
					Potosi		90-220	Dolomite, slightly sandy at top and base, light gray to light brown, drusy quartz
		FRANCONIAN			Franconia / Davis Mbr.		50-200	Sandstone, dolomite and shale; glauconitic
					Ironton		80-130	Sandstone, medium-grained; dolomitic in part
					Galesville		10-100	Sandstone, fine-grained
		DRESBACHIAN	POTS-DAM		Proviso Mbr. / Eau Claire / Lombard Mbr. / Elmhurst Mbr.		370-575	Siltstone, shale, dolomite, sandstone, glauconite
					Mt Simon		1200-2900	Sandstone, fine- to coarse-grained

Fig. 1. Generalized Columnar Section of Cambrian and Ordovician Strata in Northeastern Illinois[9] Black Dots Indicate Gas Storage Zones. Abbreviations: Ed. - Edonian; Ma. - Maysvillian; Rich. - Richmondian.
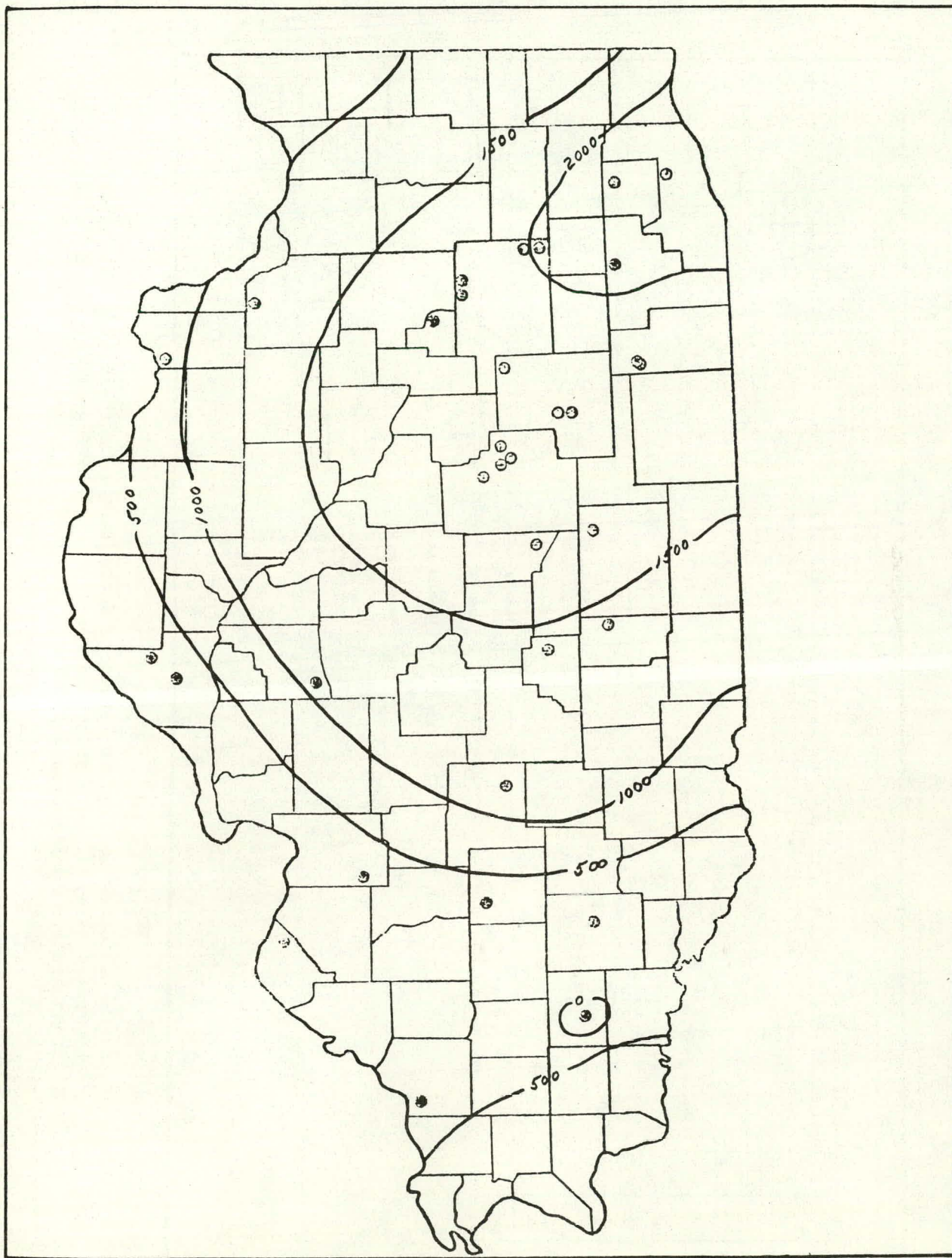
Fig. 2.   Isopachous Map of the Mt. Simon
Formation in Illinois

Fig. 3.   East-West Cross Section of Paleozoic Rocks in the Northern Ohio River Valley[10]
(Modified after cross sections in American Association of Petroleum Geologists
cross section Publication 4, 1966.)
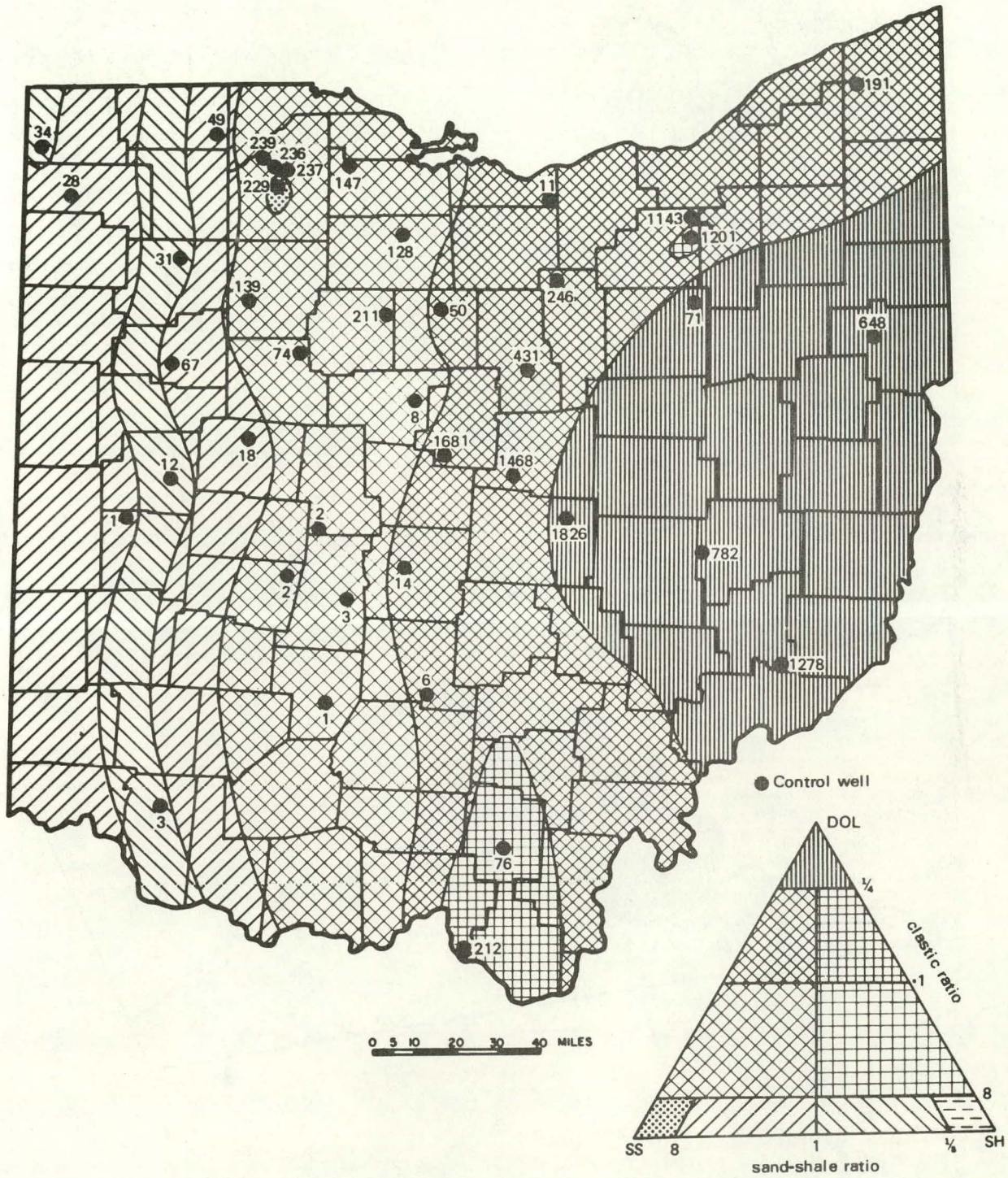
Fig. 4. Lithologic Ratio Map of Post—Mt. Simon
Pre—Knox Rocks[11]

Fig. 5.

Map of the Ohio River
Basin and Vicinity
Showing Some Major
Geologic Features. Data
Modified from Published
Maps.

EXPLANATION

OHIO RIVER BASIN BOUNDARY

NAMES AND APPROXIMATE OUTLINES
OF MAJOR SYNCLINAL BASINS

AXIS OF MAJOR ANTICLINAL FOLD

AXIS OF MAJOR SYNCLINAL FOLD

METAMORPHIC AND IGNEOUS CRYSTALLINE ROCKS,
PRIMARILY OF PRECAMBRIAN AGE

AREAS OF COMPLEX FAULTING OR COMPLEX
FAULTING AND FOLDING

AREAS OF COMPLEX FOLDING
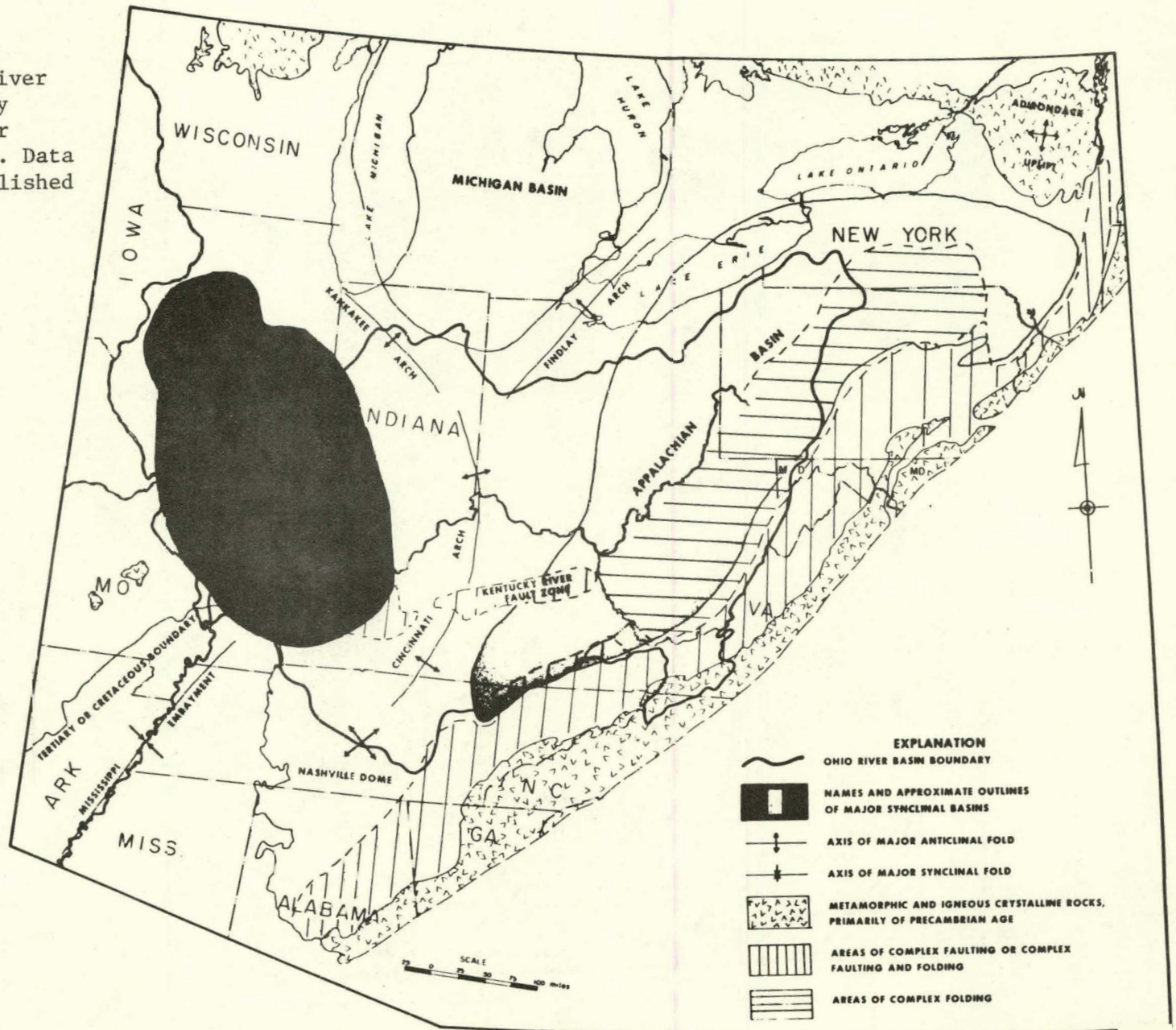
synclinal basins or downwarps of the crust shown in Fig. 5 are the Appalachian basin, the Illinois basin, and portions of the Michigan basin and the Mississippi embayment. The Cincinnati arch and its continuations, the Kankakee and Findlay arches to the north and the Nashville dome to the south are major uplifts separating the basins. The outcrop of crystalline rocks that forms the core of the Applachian Mountain ranges represents a major anticlinal fold that bounds the Appalachian basin on the southeast. Each of the major folds has many smaller ones superimposed upon it. The southeastern portion of the Appalachian basin is, in particular, complexly deformed by many smaller folds as indicated in the figure. Also, a zone of very intense and complex folding, faulting, and fracturing ranging in width from a few miles up to about 80 miles borders the northeast-southwest trending crystalline core of the Appalachian Mountains from the Alabama-Georgia border north into Canada. Other areas of relatively intense rock deformation are the faulted and fractured Rough Creek, Kentucky River, and associated fault zones.

Another type of map is the structural contour map. Figure 6 is a structural contour map of the top of the Mt. Simon Formation in Illinois. Such a map allows estimation of the approximate depth to the mapped unit and shows the location of known faults and folds that may influence decisions concerning the location and monitoring of an injection well. It would be immediately apparent from Fig. 6 that the Mt. Simon Formation is not a promising injection zone in southeastern Illinois and southwestern Indiana because it is at great depth and because that area is a highly faulted area. A still-more-detailed structural map will often be prepared for the immediate vicinity of the injection well.

3. Lithology

Lithology refers to the composition and texture of a rock. The generalized columnar section in Fig. 1 contains brief, highly generalized lithologic descriptions of rock units in northeastern Illinois. The descriptions prepared for individual wells are very detailed. An example of a description of a core from the top of the Mt. Simon Formation in one well is shown in Table 9.[13]

Such detailed descriptions are prepared from cores, cuttings, and geophysical logs and are necessary for determining the rock-unit characteristics in a test well. From such descriptions and other data, injection intervals, confining beds, and casing points are selected and other engineering decisions are made.

4. Subsurface Water

a. Chemistry

Judgment as to whether injection of wastewater into a rock unit is permitted depends, in part, on the chemistry of the aquifer water. The chemistry of aquifer water is also important because of the possibility of reactivity with injected wastewater.

Policy concerning the minimum salinity of water in aquifers approved for wastewater injection varies by state. Groundwaters containing less than 1,000 mg/l of dissolved solids will be protected except under
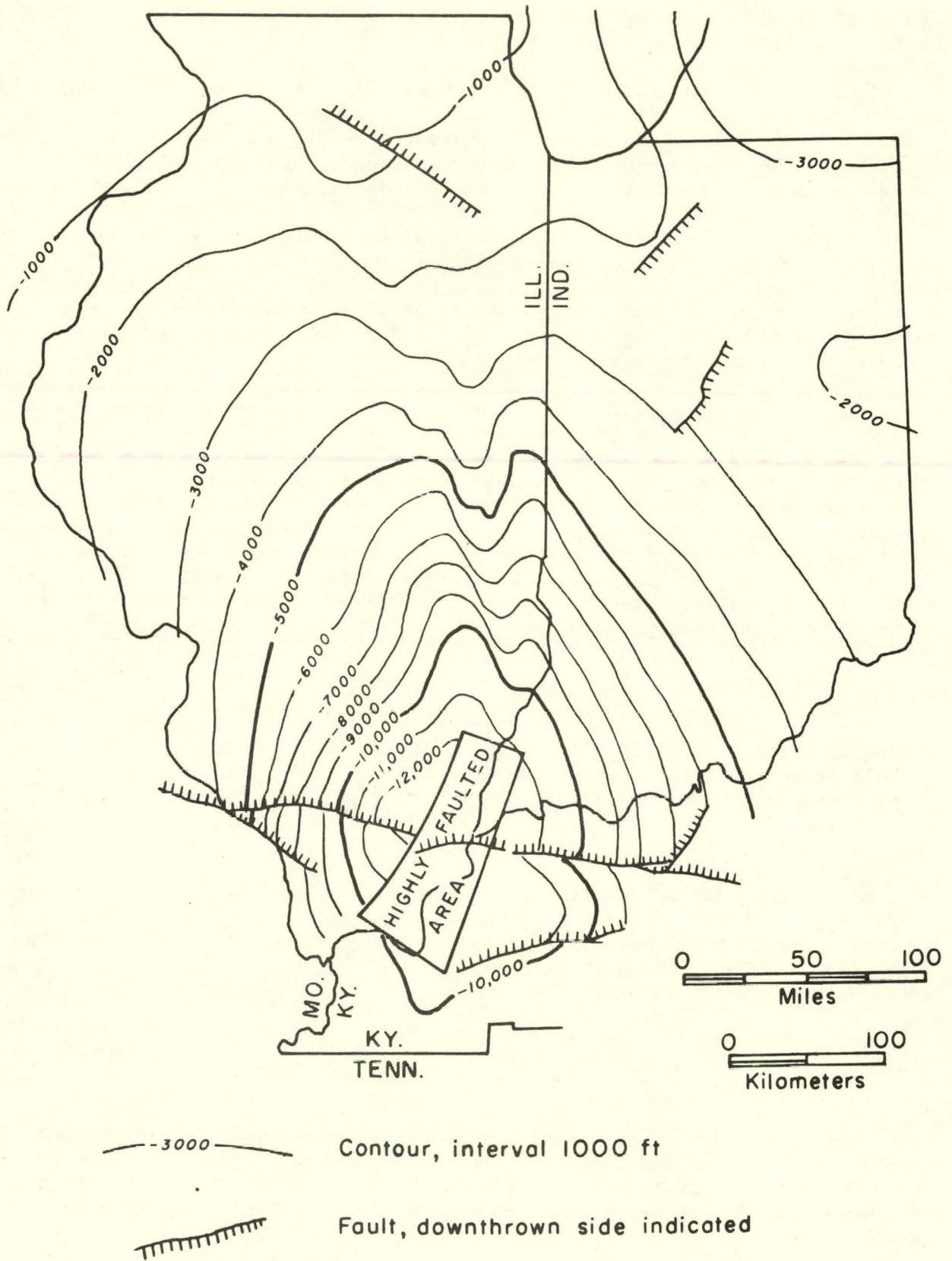
Fig. 6. Structural Contour Map of the Top of
the Mt. Simon Formation (Bond, 1972).[11]

Table 9. Detailed Description of a Core Taken from the
Top of the Mt. Simon Formation from a Well in
Illinois

Footage	Description
3019.4 - 3020.5	Sandstone; grayish-white; medium to very coarse grained; grains are broken, pitted, and chipped; very cohesive and hard; very tight; semi-quartzitic.
3020.5 - 3021.8	Sandstone; as above; very poor sorting; medium to very coarse, rounded grains, with abundant fine-grained matrix; glassy; slightly pyritic; cohesive and hard; not as tight as above zone; limited mud invasion.
3021.8 - 3023.8	Sandstone; good sorting; very fine to fine, subangular grains; slightly pyritic; cohesive and firm; limited mud invasion; very few shale laminations.

unusual circumstances. Water containing less than 500 mg/l is presently considered to be acceptable for potable water to be used by interstate carriers;[14] formerly,[15] if such water was not available, water containing 1,000 ppm of dissolved solids was considered acceptable. The minimum salinity may be set at a level higher than 1,000 mg/l of dissolved solids to provide a margin of safety. Water with several times this dissolved solids content is now used in some geographic areas and may be more widely used in the future.

Illinois agencies have determined that groundwater containing less than 10,000 mg/l should be protected. Groundwaters in New York have been classified, based on quality. According to the New York classification, water having a total dissolved solids content of 1,000 mg/l or less is considered to be fresh. Waste injection is prohibited in aquifers containing water with dissolved solids content of 2,000 mg/l or less. In Florida, the limiting value is 1,500 mg/l. Figure 7 shows the approximate depth to aquifers containing greater than 1,000 mg/l of dissolved solids in the Ohio Valley and adjacent areas. This map gives a very broad indication of the depth range to which surface casing must extend in order to close off aquifers containing potable water. It also shows that there are no saline water-bearing aquifers to be used for disposal in portions of the eastern Ohio Valley.

In Illinois, the Mt. Simon Formation has been found to contain water ranging in dissolved solids content from less than 1,000 mg/l in the northern part of the state to over 300,000 mg/l in the southern part. Such information can be displayed in the form of an isocon map (Fig. 8). Most of the dissolved solids is sodium chloride, but significant amounts of calcium, magnesium, and sulfate are also present (Table 10).

Samples of formation water for detailed analysis are obtained during well construction by drill-stem tests and, after construction, by

Fig. 7.

Map of the Ohio River Basin and Vicinity Showing Depth Below the Land Surface to the Shallowest Aquifers that Contain Water with Dissolved Solids Content Greater than 1,000 Parts Per Million.[10] (Data modified from Fath. 1965.)

EXPLANATION

LESS THAN 500 FT.

500 TO 1,000 FT.

MORE THAN 1,000 FT.

NO AQUIFERS WITH WATER CONTAINING MORE THAN 1,000 PPM. DISSOLVED SOLIDS.

METAMORPHIC AND IGNEOUS CRYSTALLINE ROCKS PRIMARILY OF PRECAMBRIAN AGE.

SCALE

34
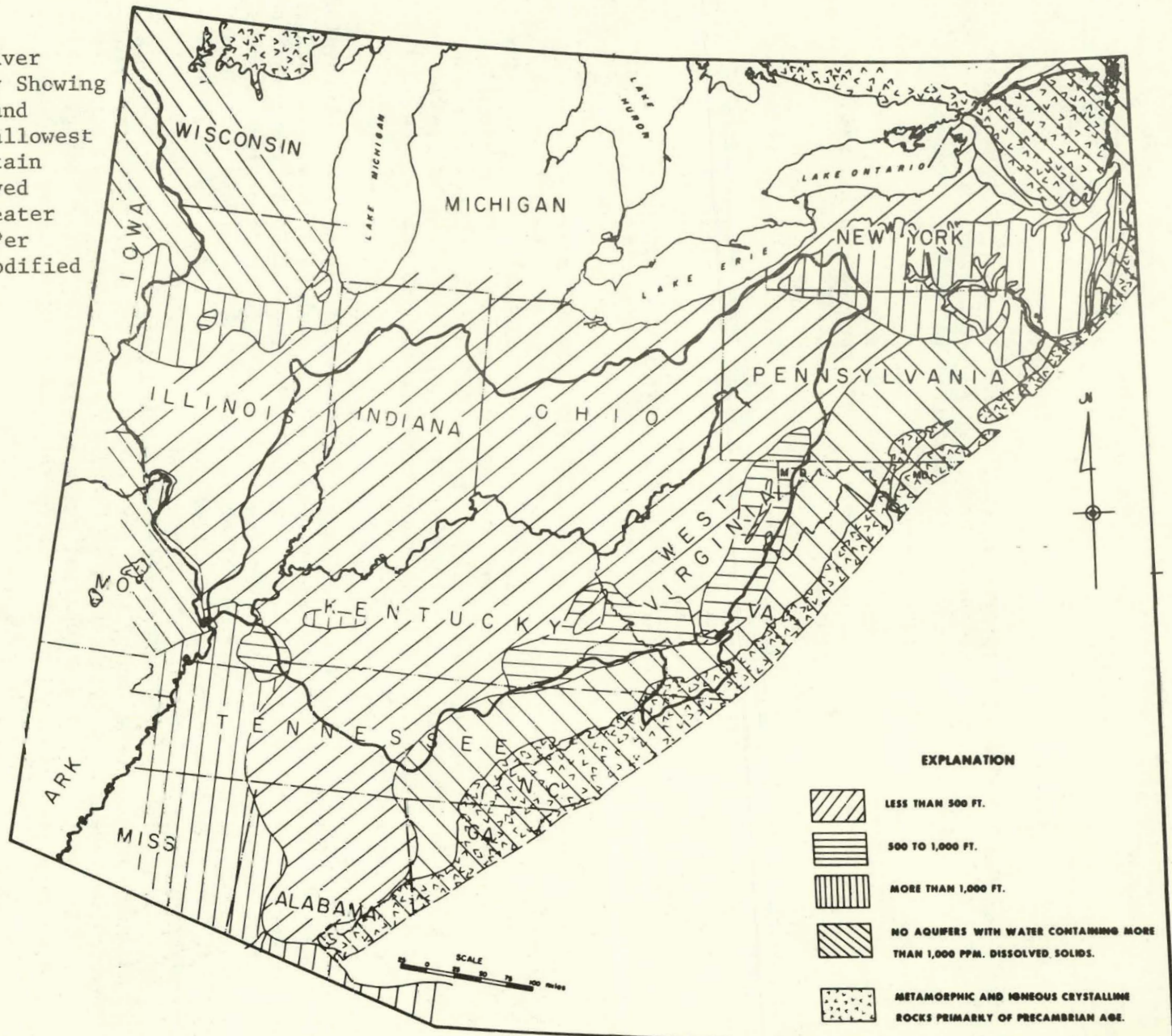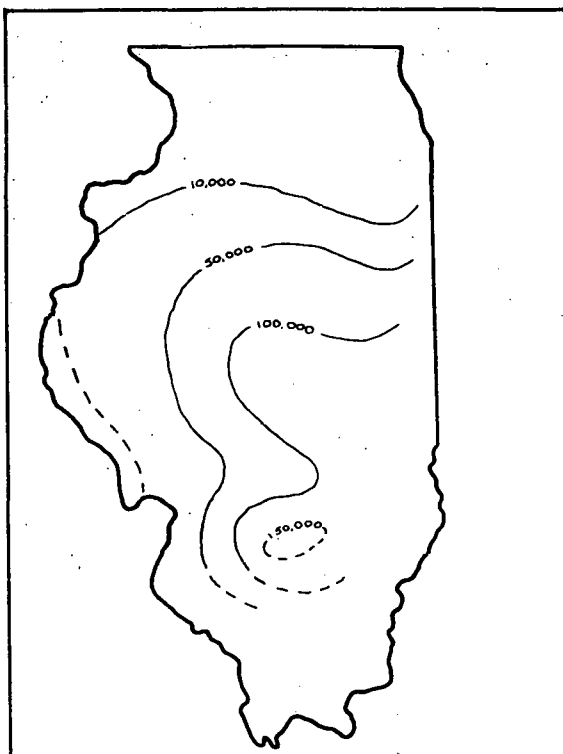
Fig. 8. Isocon Map Showing the Dissolved Solids Content in Parts
per Million Parts of Water in the Upper 100 Feet of the
Mt. Simon Formation in Illinois

pumping tests. Geophysical logs are also useful for estimating the dissolved
solids content of aquifer water in intervals that are not sampled, as will be
discussed later in Section c.

Table 10. Analysis of Water from the Mt. Simon
Formation in the Vicinity of Bloomington
Illinois.

<u>Analysis</u>

Specific gravity	1.050	
pH	6.6	
Hydrogen sulfide	0.0	mg/ℓ
Carbonate alkalinity	0.0	mg/ℓ
Bicarbonate alkalinity	68	mg/ℓ
Chlorides	39,250	mg/ℓ
Total hardness	17,900	mg/ℓ
Calcium	5,200	mg/ℓ
Magnesium	1,190	mg/ℓ
Sulfates	1,700	mg/ℓ
Manganese	1.3	mg/ℓ
Total iron	27.0	mg/ℓ
Total dissolved solids (calculated)	65,460	mg/ℓ

b.   Viscosity

Viscosity is the tendency of a fluid to resist flow, and the unit used is the centipoise. In most areas, both the temperature and dissolved solids content of subsurface waters increase with depth. Figure 9 shows the combined effects of these two variables on viscosity. The figure shows that the effects tend to be offsetting. In a typical example of a 3,000-foot-deep well with a bottom-hole temperature of 38°C (100°F) and formation water with a total dissolved solids content of 120,000 ppm, the viscosity of the water would be about 0.85 centipoise as compared with a viscosity of 1.0 centipoise for fresh water at 20°C (68°F). If it were not for the increased salinity, the viscosity of the water at 38°C (100°F) would be much lower, about 0.7 centipoise for fresh water.
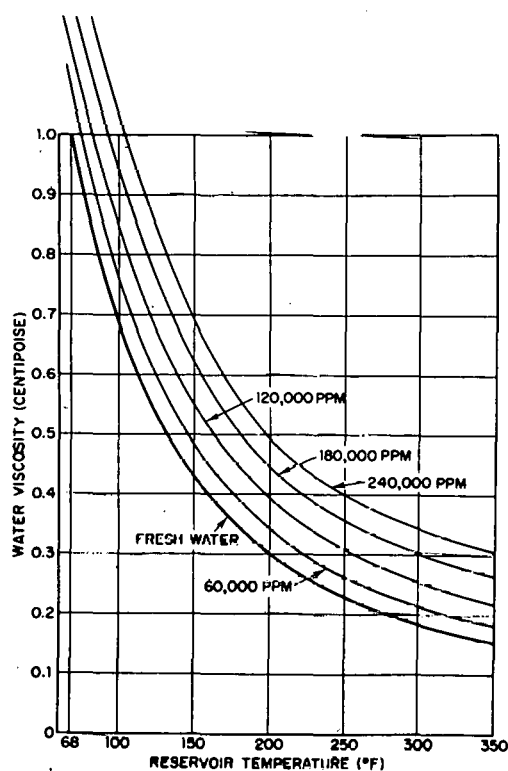
Fig. 9.   Viscosity of Subsurface Water as a Function
          of Reservoir Temperature and Total Dissolved
          Solids Content

c.   Density

The density of subsurface water must be taken into account in the equations for subsurface fluid flow, since gravity is the driving force for regional flow and the greater the density of a column of water, the greater the pressure (force) it can exert. Also, reservoir fluid density is a consideration in predicting wastewater movement. Within the range of

temperature and pressure encountered in wastewater injection, these two
variables have a small effect on fluid density. For example, at a reservoir
temperature of 93°C (200°F), which might be encountered at a depth of 10,000
feet, the density of fresh water would be 0.965 as compared with 1.0 at 16°C
(60°F). Pressure has a similar effect, but in the opposite direction, so that
the two variables are nearly offsetting in normal circumstances in subsurface
reservoirs. A potentially more important influence on the density of water
in subsurface reservoirs is the total dissolved solids content. Figure 10
shows the relationship between dissolved solids content and relative density
in deep aquifers in the Illinois basin. From the graph, it can be seen that
density increases as large as 15 percent have been observed in very saline
formation waters.
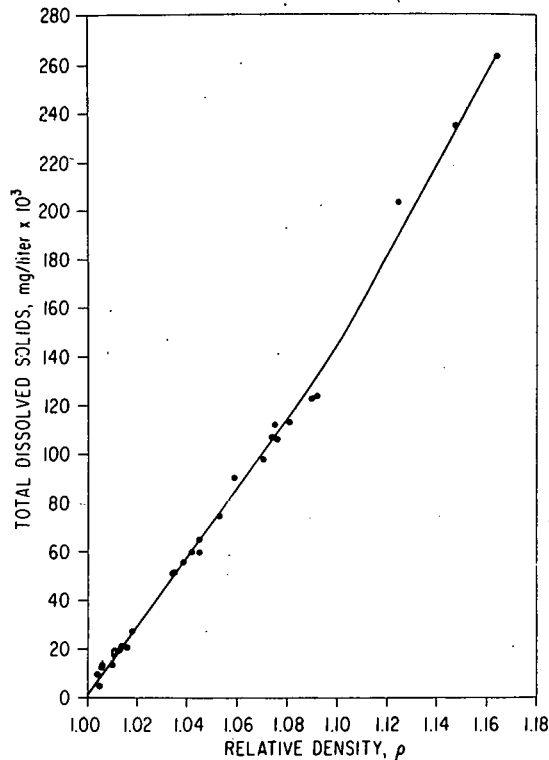
Fig. 10. Relative Density and Dissolved
          Solids Content of Brines in Deep
          Aquifers of the Illinois Basin[12]

d.   Pressure

        The total fluid pressure in the subsurface reservoir during
injection is the sum of the natural reservoir pressure plus that which must
be added in order to emplace the desired amount of wastewater. Since the
total pressure may be the constraining limit on the injection rate, the
original reservoir pressure must be known.

Fluid pressure can be measured directly in the borehole at the depth of the injection horizon, usually by performing a drill-stem test, described below. Fluid pressure at the injection horizon can also be measured indirectly by determining the static water level in the borehole, then computing the pressure of the fluid column at the depth of interest.

Figure 11 shows how fluid pressure increases with depth in strata beneath the water table or in a well bore filled with fresh water with a specific gravity[*] of 1.0. When the average specific gravity of the water is other than 1.0, the rate of pressure increase varies accordingly. For example, if a well bore is filled with formation water having a dissolved solids content of 65,000 mg/l and a specific gravity of 1.05, then fluid pressure increases at a rate of 0.455 psi/ft and would be 455 psi at the bottom of a 1,000-foot-deep water-filled well.
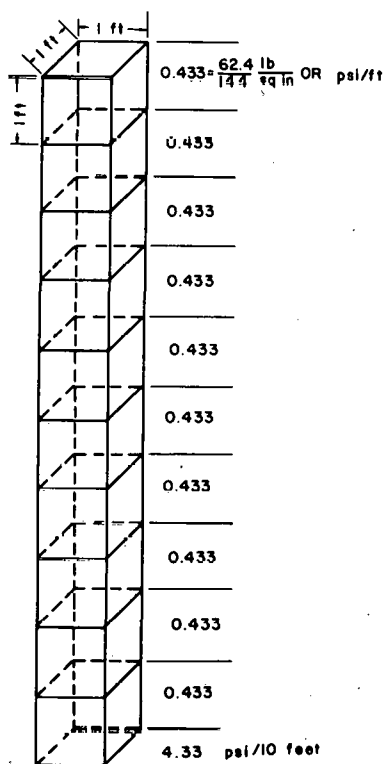
Fig. 11. Hydrostatic Pressure Gradient in a Column of Fresh Water[17]

Although instances of truly anomalous formation pressure are likely to be relatively rare at sites selected for wastewater injection, the existence of unusually high or low pressures and the possible reasons for

_____

[*] Specific gravity is the ratio of the mass of a body to that of an equal volume of pure water: for practical purposes, the numerical values of density and specific gravity are equal. Specific gravity, however, is dimensionless.

their existence should be recognized. Some causes of anomalous pressure are:

(1) Compaction of sediments
(2) Tectonic forces
(3) Osmotic effects
(4) Massive extraction or injection of fluids

Abnormally high pressures can result from causes 1, 2, and 3 and from massive injection of fluids. Abnormally low pressures can result from osmotic effects and extraction of fluids. Abnormally high pressures resulting from compaction of sediments are common in deep wells of the Gulf Coast.[18] Berry[19] has concluded that abnormally high pressures in the California Coast Ranges are a result of tectonic forces. Hanshaw[20] discusses natural osmotic effects and their relation to subsurface wastewater injection.

e. Fluid Compressibility

The compressibility of an elastic medium is defined as:

$$\beta = \frac{-\partial V}{V \partial p} \quad \text{Dimensions} - [F/L^2]^{-1} \tag{1}$$

where β = compressibility of medium; units are pressure^{-1}

V = volume

p = pressure

The compressibility of water varies with both temperature and pressure, as is shown in Fig. 12. For problems in wastewater injection, β will generally be within the range of 2.8 to 3.3×10^{-6} psi^{-1} and 3.0×10^{-6} psi^{-1} is a reasonable value to assume in most cases.

5. Mechanical Properties of Injection and Confining Units

a. Porosity

Total porosity is defined as:

$$\phi = \frac{V_v}{V_t} \quad \text{[dimensionless]} \tag{2}$$

where ϕ = porosity, expressed as a decimal fraction

V_v = volume of voids

V_t = total volume of rock sample

Porosity is also commonly expressed as a percentage. In comparison with total porosity, effective porosity is based on the total volume of _interconnected_ voids. Effective porosity better defines the hydraulic properties of a rock unit, since only interconnected porosity is available to fluids flowing through a rock.
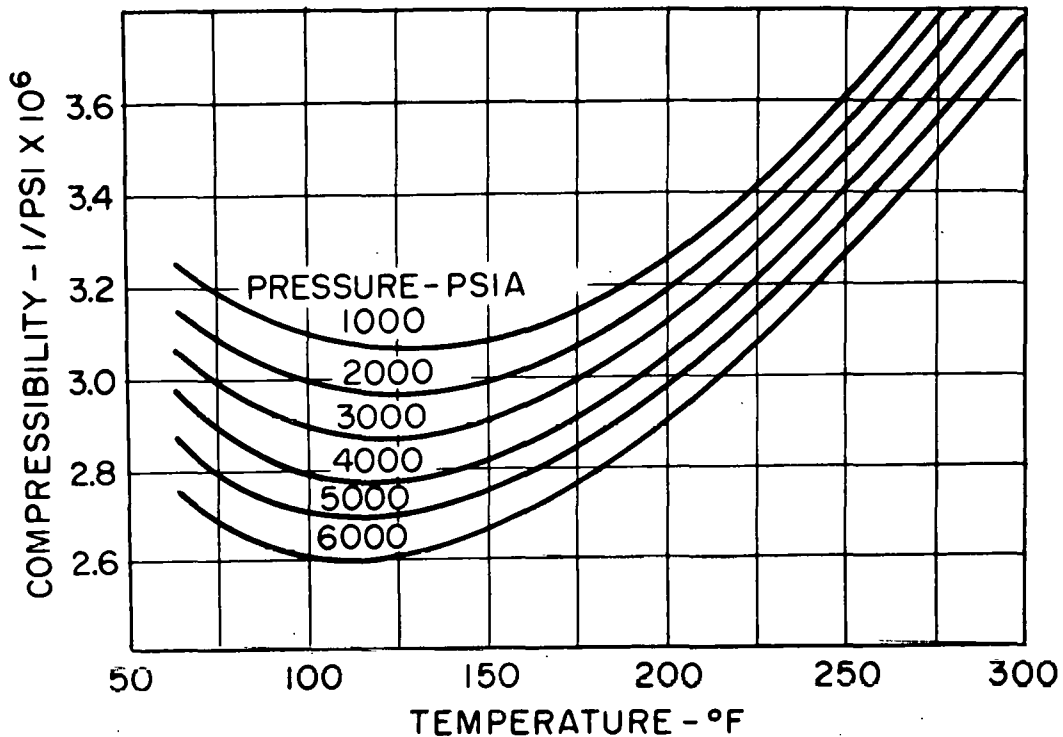
Fig. 12. Variation in the Compressibility of
Water with Temperature and Pressure[17]

Porosity may also be classified as primary or secondary.
Primary porosity includes original intergranular or intercrystalline pores
and the porosity associated with fossils, bedding planes, and so forth.
Secondary porosity results from fractures, solution channels, and from
recrystallization and dolomitization. Intergranular porosity occurs princi-
pally in unconsolidated sands and in sandstones and can be measured reasonably
well in the laboratory using core samples taken from wells. Porosity contri-
buted by fractures and solution channels is difficult to measure in the
laboratory. Various borehole geophysical methods that are discussed below
can be used to determine the porosity of strata in place. Effective porosity
values in reservoir formations range from a maximum of about 0.40 in uncon-
solidated sands to as little as 0.02 in dense limestones. The average porosity
of the Mt. Simon Formation in Illinois ranges from about 2 percent to 16 per-
cent, as shown in Figure 13

b. Permeability

Permeability is the capacity of a rock to transmit fluid; it
is related to but not equivalent to effective porosity. Permeability is
quantified by the coefficient of permeability or hydraulic conductivity. When
the properties of both the fluid and the porous medium are considered, the
coefficient of permeability $\overline{K}$ is defined by Darcy's law as:

$$\overline{K} = \frac{Q\mu}{A\rho g}\frac{dL}{dh} \text{ Dimensions--}[L^2] \tag{3}$$

where Q = flow rate through porous medium

    A = cross-sectional area through which flow occurs

    μ = fluid viscosity

    ρ = fluid density

    L = length of porous medium through which flow occurs

    h = fluid head loss along L

    g = acceleration of gravity
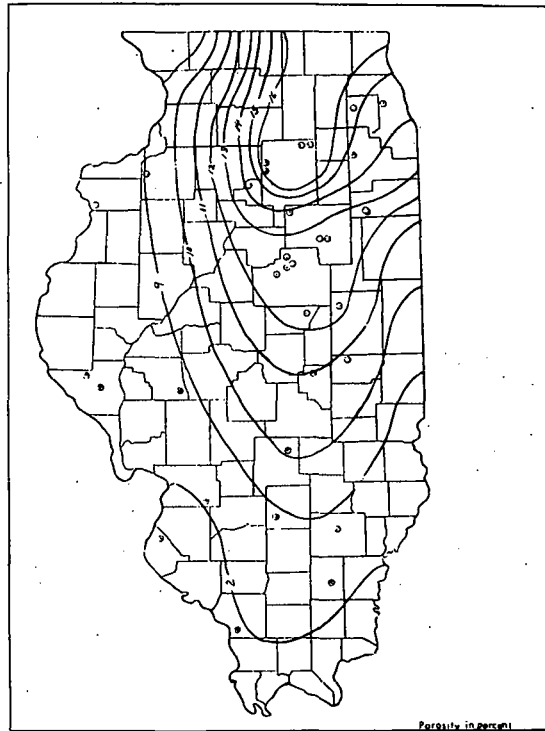
Fig. 13. Distribution of Average Porosity of
the Mt. Simon Formation in Illinois

If cgs units are used, the coefficient of permeability from Equation 3 is expressed in cm^2. The unit of permeability used in oil field work is the darcy, which is defined by:

$$\overline{K} = \frac{Q\mu}{A} \frac{dL}{dp} \quad \text{Dimensions--}[L^2] \tag{4}$$

where $p = \rho gh$ = pressure

$$1 \text{ darcy} = \frac{1 \text{ cm}^3/\text{sec} \times 1 \text{ centipoise} \times 1 \text{ cm}}{1 \text{ cm}^2 \times 1 \text{ atmosphere}}$$

A still simpler form of Darcy's law is used in groundwater studies, where the density and viscosity of water do not vary greatly.

$$K = \frac{Q}{A} \frac{dL}{dh} \quad \text{Dimensions--}[L/T] \tag{5}$$

The constant K is referred to as hydraulic conductivity and is usually expressed in cm/sec or in U.S. Geological Survey units, which are gallons/day x ft^2 (meinzers). A table for conversion of permeability units is given below (Table 11).

<p style="text-align:center">Table 11. Equivalency of Permeability
Values in Various Units[21]</p>

1 darcy	$= 9.87 \times 10^{-9}$ cm^2 $= 1.062 \times 10^{-11}$ ft^2
10^{-10} cm^2	$= 1.012 \times 10^{-2}$ darcys
0.1 cm/day	$= 1.15 \times 10^{-6}$ cm/sec $= 1.18 \times 10^{-11}$ cm^2 for water at 20°C
1.0 cm/sec	$= 1.02 \times 10^{-5}$ cm^2 for water at 20°C
1 darcy	$= 18.2$ meinzer units for water at 16°C (60°F)
1 meinzer	$= 0.134$ ft/day $= 4.72 \times 10^{-5}$ cm/sec $= 5.5 \times 10^{-2}$ darcys for water at 16°C (60°F)

Permeability values for the formations used for wastewater injection range generally from several darcies to less than a millidarcy (one millidarcy = 10^{-3} darcy). Average permeability values for the Mt. Simon Formation in Illinois range from more than 100 millidarcies in the north to less than 1 millidarcy in the south. The permeability of shale beds in the Eau Claire Formation, overlying the Mt. Simon Formation, is consistently less than 0.001 millidarcy.

A useful constant in hydrogeologic work is the coefficient of transmissivity (transmissibility), which is the permeability or hydraulic conductivity multiplied by the thickness of the aquifer. When the unit of permeability is the darcy, transmissivity is in darcy-feet/centipoise.

c. Aquifer Compressibility

The compressibility of an aquifer includes the compressibility of the aquifer skeleton and that of the contained fluids. Thus, the total compressibility of an aquifer is

$$C = \phi\beta + \alpha, \quad [F/L^2]^{-1} \tag{6}$$

where C = compressibility of aquifer, in units of pressure^{-1}

ϕ = porosity

β = compressibility of water

α = compressibility of aquifer skeleton

The compressibility of water has previously been discussed. The compressibility of aquifer skeletons varies greatly, from as little as 1×10^{-8} psi^{-1} in consolidated rocks to as much as 1×10^{-5} psi^{-1} in unconsolidated materials.

The coefficient used in analysis of reservoir response to injection or pumping is the storage coefficient, S, (storativity), which is defined by:

$$S = \phi\gamma b \ (\beta + \frac{\alpha}{\phi}) \ \text{[dimensionless]} \qquad (7)$$

where ϕ, β, and α are as previously defined, and

S = storage coefficient

γ = ρg = specific weight of water per unit area

b = aquifer thickness

The storage coefficient is the volume of water an aquifer releases or takes into storage per unit surface area per unit change in hydraulic head. The storage coefficient may be estimated from the equation above, or it may be determined from aquifer tests. Values of S are reported to range from 5×10^{-5} to 5×10^{-3} for confined aquifers. As an estimate of the value of S for the Mt. Simon Formation in northern Illinois, assume that ϕ = 11%, b = 1,700 ft, γ = 0.45 psi/ft, β = 3.0×10^{-6} psi^{-1}, and α = 6.7×10^{-6} psi^{-1}.* Then, from the equation above, S = 5.4×10^{-3}. This is a high value, but the aquifer is very thick. If the compression of the water alone were considered, S would be 2.5×10^{-4}. The Illinois State Water Survey estimated an average storage coefficient of 1×10^{-4} for the Mt. Simon Formation in northern Illinois, which is probably too low if the entire thickness of the formation is considered.

d. Temperature

The temperature of the aquifer and its contained fluids is important because of the effect that temperature has on fluid properties. The temperature of shallow groundwater is generally about 1 to 1 1/2°C (2 to 3°F) higher than the mean annual air temperature. In Illinois, this ranges from about 16°C (60°F) in the south to 10°C (50°F) in the north. Below 30 to 60 feet, the temperature increases approximately 1/2 to 1°C (1 to 2°F) per 100 feet of depth. Figure 14 is a geothermal gradient map of

---

* Testing of the Mt. Simon Formation (in a gas storage field in northern Illinois) yielded a value of compressibility of the formation and its contained water of about 7×10^{-6} psi^{-1}. Since the water occupies only 11% of the rock, the rock skeleton compressibility at that location is 6.7×10^{-6} psi^{-1}.
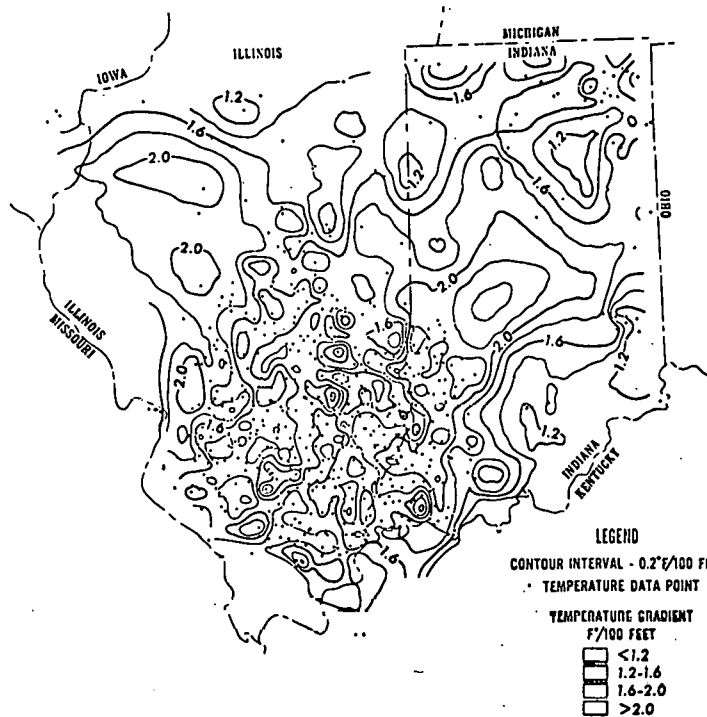
Fig. 14. Geothermal Gradient Map[23] of Illinois and Indiana,
          Modified Portfolio Map No. 10, from the American
          Association of Petroleum Geologists Geothermal
          Survey of North America

Illinois and Indiana. At a depth of 3,000 feet, in northern Illinois, the
calculated temperature is about 30°C (86°F). The measured temperature at
3,000 feet near Pontiac, Illinois, was 90°F. Geothermal gradient maps for
the United States have been prepared by the American Association of Petroleum
Geologists, Tulsa, Oklahoma[23] and can be obtained from that organization.
Figure 14 is a modification of an AAPG map.

e. State of Stress

In order to predict the pressure at which hydraulic fracturing
or fault movement would be expected to occur, it is necessary to estimate
the state of stress at the depth of the injection horizon. On the other hand,
determination of the actual fracture pressure allows computation of the state
of stress.[24]

The general equation for total normal stress across a plane in
a porous medium is:

$$S_t = P_o + \sigma_i \quad \text{Dimensions--}[F/L^2] \tag{8}$$

where S_t = total stress

P_o = fluid pressure

σ_i = effective or intergranular normal stress

Effective stress, as defined by Equation 8, is the stress available to resist hydraulic fracturing or the stress across a fault plane that acts to prevent movement on that fault. The equation shows that if total stress remains constant, an increase in fluid pressure reduces the effective stress and a decrease in fluid pressure increases effective stress. When the effective stress is reduced to zero by fluid injection, hydraulic fracturing occurs. Fault movement occurs before normal stresses across the fault plane are reduced to zero, since there must be some shear stress acting on the fault blocks to cause them to move.

In a sedimentary rock sequence, the total normal vertical stress increases with depth of burial, under increasing thicknesses of rock and fluid. It is commonly assumed (and the validity of the assumption can easily be verified) that the normal vertical stress increases at an average rate of about 1 psi/ft of depth. The lateral stresses may be greater or less than the vertical stress, depending on geologic conditions. In areas where crustal rocks are being actively compressed, lateral stresses may exceed vertical ones. In areas where crustal rocks are not in active compression, lateral stresses should be less than the vertical stress. The basis of estimating lateral stress prior to drilling of a well is hydraulic fracturing data from nearby wells and/or knowledge of the tectonic state of the region in which the well is located. The tectonic state of various regions is only now being determined. For example, Kehle[24] concluded, as a result of hydraulic fracturing data from four wells, that the stresses at the well locations in Oklahoma and Texas were representative of an area that was tectonically in a relaxed state. In contrast, Sbar and Sykes[25] characterized much of the eastern and north-central United States as being in a state of active tectonic compression. Further discussion concerning the state of stress and hydraulic fracturing is presented below in the section on hydraulic fracturing.

6. Hydrodynamics

Hydrodynamics, as the term has been adopted for use in subsurface hydrology, refers to the state of potential for flow of subsurface fluids, particularly in deep sedimentary basins. As examples of its application, recent publications by Bond[12] and Clifford[26] discuss the flow potential in deep aquifers of Illinois, Indiana, and Ohio as determined from pressure, water level, and water density measurements made in deep wells.

The potential for flow in deep aquifers that are used for wastewater injection is important, because it can be used to estimate natural groundwater flow rates and directions. Figure 15 is a map showing the potentiometric surface of the Mt. Simon Formation in Ohio and Indiana. The arrows indicate the directions of regional groundwater flow in the Mt. Simon Formation as indicated by the potentiometric contours. Bond[12,27] discusses some of the difficulties in interpretation and application of potentiometric data.

7. Subsurface Resources

The occurrence of oil, gas, coal, mineralized brines, and occasionally other less abundant minerals requires consideration when evaluating an injection well site. Of the mineral resources, oil and gas most frequently require consideration because of their wide geographic distribution and because rock

units that contain them are often physically well suited for waste injection. Also, units suitable for waste injection are favorable for natural gas storage, which is extensively practiced in the north-central states.
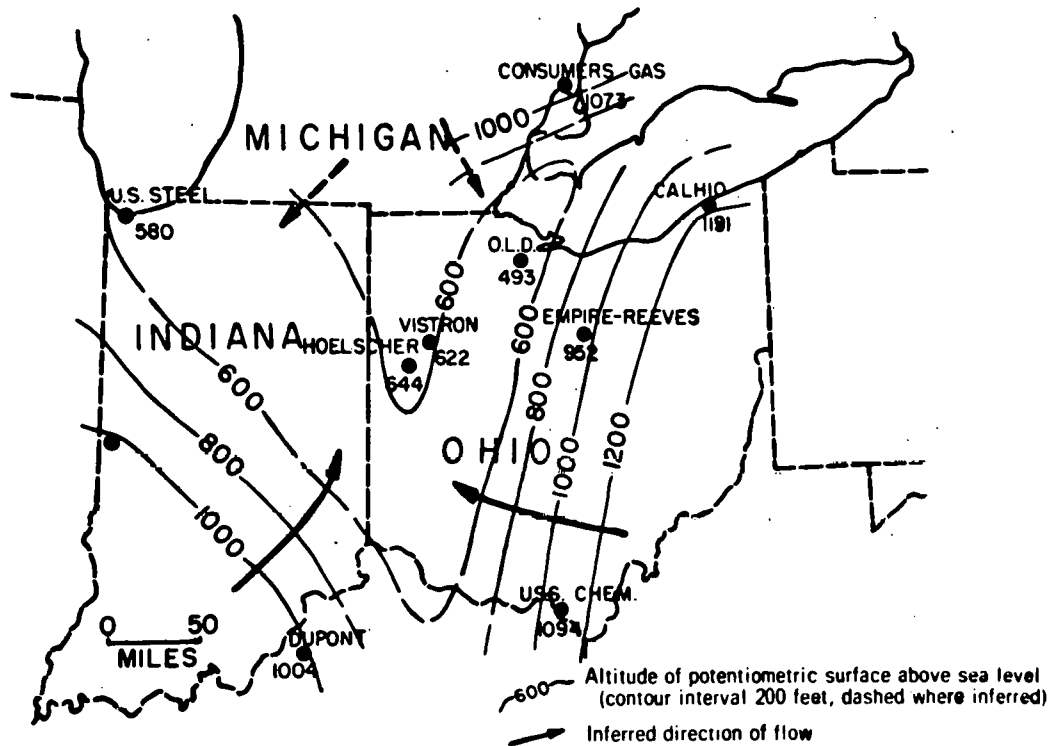
Fig. 15. Potentiometric Surface Map of the
Mt. Simon Formation in Ohio and Vicinity[26]

The presence of oil and gas resources in the immediate vicinity of an injection well site does not necessarily preclude wastewater injection, but may limit it. The possible limitations include the desire to protect the developed or undeveloped resources and the added difficulty of assuring confinement because each well provides an additional possible pathway for escape of wastewater or saline formation water.

In reviewing the occurrence of subsurface resources, the locations, construction, use, and ownership of all wells, both shallow and deep, within the area of influence of the injection well should be determined. The plugging record for all abandoned deep wells should be obtained to verify the adequacy of such plugging. In states where oil has been produced for many years, there are often areas where wells are known to have been drilled, but for which no records are available: there are also wells whose locations are known but for which plugging records are not available or for which plugging is known to have been inadequate. Documenting the status of deep wells near

the injection well may be the most important step in monitoring injection wells in areas that are or have been active oil or gas provinces because these wells provide the greatest hazard for escape of wastewater or formation water from otherwise well-confined aquifers.

D.   Acquisition of Subsurface Data

1.   Prior to Drilling

In order to estimate the performance of injection wells and to evaluate the subsurface environment prior to construction, the types of information described in the section on the subsurface environment are estimated from sources such as the types of figures and tables in that section. The information in such figures and tables is obtained, of course, from previously drilled wells; if it has not been compiled and formed into maps, cross sections, and tables, this may be necessary before it can be used. Basic information for previously drilled wells is available in most states from state geological surveys, oil and gas agencies, and water resources agencies. In addition, private companies acquire and sell well logs and other subsurface data. In some cases, it may be necessary to go to individual oil companies or consultants for subsurface data not publicly available. Companies and individuals are usually cooperative in releasing information that is not considered confidential.

2.   During Well Construction and Testing

a.   Rock Samples

Most deep wells drilled today are drilled by rotary drilling rigs. Rotary drilling rigs use two basic types of drilling bits--rock bits and core bits. Rock bits grind the stone into small chips that are carried from the hole by a viscous drilling mud. The chips are periodically collected, usually after each five or ten feet of new drilling, washed, and examined with a low-power binocular microscope. The methods for collection, examination, and description of such samples are presented in a reference edited by Haun and LeRoy.[28] Drilling of soft, unconsolidated clays will not yield chips-- the clay will break down into mud; unconsolidated or soft sandstones will break down into individual grains. Samples are of only limited value in such areas.

Cores taken with rotary core bits and barrels give a much more accurate picture of the subsurface formations than cuttings, but core samples are very expensive (costing more than $50/ft) in deep wells and can usually be afforded only in limited numbers. In deep wells, core samples are commonly about four inches in diameter. Cores and cuttings are described similarly, but since a continuous sample of the formation is available from cores, a detailed foot by foot description can be prepared. Whole-core samples can be analyzed for porosity and permeability in the laboratory, or small cores can be taken from a large core and analyzed. The latter procedure is the most common.

b.   Formation Fluids

Before drilling of deep wells is completed, samples of water from subsurface formations can be obtained from cores by formation testing devices and by swabbing.

When cores are taken (as previously described), the water in the cores can be carefully extracted and its chemistry analyzed. Contamination is a serious problem, since cores are exposed to infiltration by drilling mud and mud filtrate.

Drill-stem testing is a technique whereby a zone in an open bore hole can be isolated by an expandable packer or packers, allowing fluid from the formation to flow through a valve into the drill pipe. The technology of drill-stem testing is well described by Pirson.[16]

Swabbing is a method of producing fluid that is similar to pumping a well. In swabbing, fluid is lifted from the bore hole through the drill pipe, casing, or tubing by a swab that falls freely downward through the pipe and its contained fluid, but that seats against the pipe walls on the upstroke, drawing a volume of fluid above it as it is raised. Swabbing may be used in conjunction with drill-stem testing to increase the volume of fluid obtained. The advantage of swabbing is that it can be repeated until all drilling mud has been removed from the pipe and the formation; the chemistry of the water obtained then reaches a steady state. This procedure helps to ensure that a representative sample of formation water is obtained.

c. Borehole Geophysical Logs

After a well has been drilled, a variety of borehole logging tools are available that can be used for recording the nature of the formations penetrated and their contained fluids. In borehole logging, a probe is lowered into a well at the end of a wire cable; selected geophysical properties are measured as a function of depth and are recorded at the surface.

Currently used methods of well logging are too numerous to discuss in detail here. A broad classification of the more commonly used methods is shown in Table 12,[29] together with their main applications. Because the variety of available logging methods is so great, the suite used in logging a well must be carefully selected to provide the desired information at an acceptable cost. Local practice in the particular geographic area is a valuable guide, since it represents the cumulative experience obtained from logging many wells. Some objectives in logging of injection wells will generally be to determine lithology; bed thickness; amount, location, and type of porosity; and salinity of formation water. In order to achieve these objectives, a commonly chosen suite of logs will include a gamma ray log, a focused resistivity log, and one or more porosity measuring logs selected from among the various radiation and elastic wave logs. Some other frequently used logs include the spontaneous and potential (SP) and nonfocused electric logs, the caliper log, and the temperature log. Keys and Brown[30] provide a rather extensive review of the application of borehole geophysical logs to wastewater injection.

d. Testing of Injection Units and Confining Beds

Examination of the records of many of the wastewater injection wells that have been constructed up to the present time shows that, with few exceptions, a maximum amount of usable geologic and engineering information has not been obtained during the testing of wastewater injection wells. This

Table 12. Well Logging Methods and their Applications
(modified after Jennings and Timur)[29]

Method	Property	Application
Electrical		
Spontaneous Potential (SP)	Electrochemical and electrokinetic potentials	Formation water resistivity (R_w) Shales and nonshales Bed thickness Shaliness
Nonfocused Electric Log	Resistivity	(a) Water and gas/oil saturation (b) Porosity of water zones (c) R_w in zones of known porosity (d) True resistivity of formation (R_t) (e) Resistivity of invaded zone
Focused Conductivity Log	Resistivity	(a), (b), (c), (d) Very good for estimating R_t in either fresh water or oil-base mud
Focused Resistivity Logs	Resistivity	(a), (b), (c), (d) Especially good for determining R_t of thin beds Depth of invasion
Focused and Nonfocused Microresistivity Logs	Resistivity	Resistivity of the flushed zone (R_{xo}) for calculating porosity Bed thickness
Elastic Wave Propagation		
Transmission	Compressional and shear wave velocities	Porosity Lithology Elastic properties, bulk and pore compressibilities
	Compressional and shear wave attenuations	Location of fractures Cement bond quality
Reflection	Amplitude of reflected waves	Location of vugs, fractures Orientation of fractures and bed boundaries Casing inspection

(Contd.)

Table 12.   (Contd.)

Method	Property	Application
	Radiation	
Gamma Ray	Natural radioactivity	Shales and nonshales Shaliness
Spectral Gamma Ray	Natural radioactivity	Lithologic identification
Gamma-Gamma	Bulk density	Porosity, Lithology
Neutron-Gamma	Hydrogen content	Porosity
Neutron-Thermal Neutron	Hydrogen content	Porosity Gas from liquid
Neutron-Epithermal Neutron	Hydrogen content	Porosity Gas from liquid
Pulsed Neutron Capture	Decay rate of thermal neutrons	Water and gas/oil saturations Reevaluation of old wells
Spectral Neutron	Induced gamma ray spectra	Location of hydrocarbons Lithology
	Other	
Caliper	Borehole diameter	Calculation of cement volume Location of mud cake
Dipmeter	Azimuth and incli- ation of bedding planes	Dip and strike of beds
Deviation Log	Azimuth and incli- nation of borehole	Borehole position
Gravity meter	Density	Formation density
Ultra-Long Spaced Electric Log	Resistivity	Salt flank location
Nuclear Magnetism	Amount of free hydro- gen. Relaxation rate of hydrogen	Effective porosity and permeability of sands Porosity for carbonates
Production or injectivity	Temperature, flow rate, fluid specific gravity, pressure	Downhole production or injection
Temperature Log	Temperature	Formation temperature

is regrettable because such tests provide the best basis for analyzing reservoir conditions prior to injection, for predicting the long-term behavior of the well and the reservoir, for detecting and understanding changes in well performance that may occur during operation, and for analyzing the history of a well from its records.

A well can be tested by pumping from it or injecting into it. Measurements of reservoir pressure or water level can be made (1) during pumping or injection or (2) after pumping or injection has ceased and the reservoir is adjusting to its original condition. Furthermore, reservoir pressure or water level can be measured in the principal well or in adjacent observation wells. Any one of these approaches will yield much the same information.

e. Drill Stem Testing

In the case of the usual deep and rather expensive wastewater injection well, there will be no observation well and testing will be in the well itself. In the sequence of well construction and testing, the first type of formation test likely to be made is the drill stem test (DST). As has previously been mentioned, this test is analogous to a pumping test of limited duration. Quantitative analysis is usually done using data obtained during the period of pressure buildup following the period in which the fluid in the reservoir is allowed to flow.

If a test is successful, pressure buildup data from the test are taken from the DST chart and tabulated. These data are then plotted and a series of calculations of formation properties is made. The important properties that are routinely calculated are:

1. Static bottom hole pressure

2. Transmissivity

3. Average effective permeability

4. Damage ratio

5. Approximate radius of investigation

The static bottom hole pressure as determined from a successful test is assumed to closely represent the formation pressure at the elevation of the pressure-recording device. Transmissivity is average permeability multiplied by the thickness of the test interval. The damage ratio is an indication of the amount of plugging of pores in the formation during drilling of the well. In addition to this routine information, drill stem tests may indicate the presence of and distance to nearby faults or facies changes that act as barriers to flow or channels for rapid flow.

For detailed presentations of drill stem test analysis, the reader is referred to Gatlin,[31] Lynch,[32] Matthews and Russell,[33] and Pirson.[16]

f. Injectivity Tests

After an injection well has been drilled and possible injection intervals have been identified by coring, by geophysical logging, and by drill

stem testing, injection tests will usually be run. For initial injection testing, truck-mounted pumps are often rented, and treated water is used for injection rather than wastewater. Frequently, more than one possible injection interval is present and tests are performed on the intervals individually or on more than one at a time. The common practice when performing an injection test is to begin injection at a fraction of the final estimated rate, to inject at this rate for at least several hours, then to repeat this process at increasingly greater rates until a limiting injection rate or pressure is reached. Injection is then stopped and the reservoir is allowed to return to its original pressure state. Pressures may or may not be recorded during this falloff period.

Regardless of the sequence in which a test is performed, if pressure, time, and flow data are accurately recorded and the test is run long enough, it is theoretically possible to analyze the test. However, the simpler the test, the simpler and probably the more reliable the interpretation. Tests performed on more than one interval at a time are particularly difficult to interpret and should be avoided if possible; alternatively, both single and multiple zone tests may be performed.

If early time data are available, a form of analysis that involves curve matching can be employed. Figure 16 is such a plot of recovery
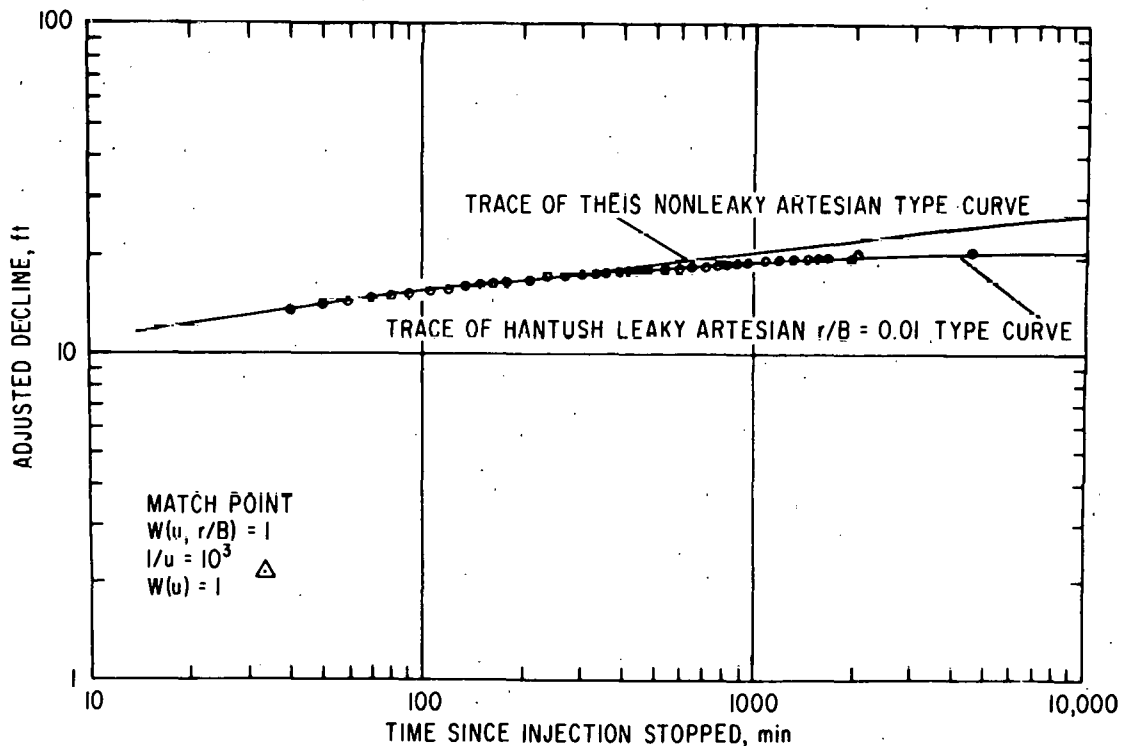
Fig. 16. Recovery Data and Matching-Type-Curves for an Injection Well at Mulberry, Florida[34]

data for an injection well at Mulberry, Florida. The details of the analysis of this test are given by Wilson et al.[34] The most interesting aspect of this example is that the test data indicate an observable amount of leakage through the confining beds. Witherspoon and Neumann[35] discuss in some detail the theory and procedure for analysis of leaky confining beds and give two field examples from gas storage projects.

Readers wishing to pursue the subject of aquifer testing further are referred to the same references previously given for drill stem test analysis, particularly to the Society of Petroleum Engineers Monograph prepared by Matthews and Russell.[33] Additionally, publications in the ground-water field by Lohman[36] and Kruseman and De Ridder[37] are excellent recent summaries of this subject, as is the reference by Witherspoon et al.,[38] which was prepared for the underground gas storage industry.

E. Prediction of Aquifer Response

1. Regional Flow

The basic equation used to describe the flow of fluids in porous media is Darcy's law, alternative forms of which are given by Equations 3, 4, and 5. Darcy's law alone can be used for calculations of steady flow. Steady flow occurs when fluid is entering and leaving an aquifer at the same rate, so that no change in the volume of the aquifer or its contained fluid is occurring with time.

When flow is unsteady or, as stated in oil field terminology, when formation pressures are transient, Darcy's law must be combined with the continuity equation so that time and the compressibility of the aquifer and aquifer fluids may be taken into account. The appropriate differential equation and its derivation may be found in most modern texts on hydrogeology and petroleum reservoir engineering, along with numerous solutions.

As examples of the application of Darcy's law for steady flow to analysis of regional flow, the velocity of natural flow in the Mt. Simon Formation in Ohio and the lower Floridian aquifer in Florida will be considered.

From Fig. 15, it can be seen that, at the location of the Empire-Reeves injection well, the hydraulic gradient is 8 feet per mile toward the northwest. At this location, the Mt. Simon Formation has a permeability of 24 millidarcies (from a drill-stem test) and a porosity of 10.4 percent.[26]

Rearranging Darcy's law:

$$\bar{v} = \frac{Q}{A} = K \frac{dh}{dL} \quad \text{Dimensions--[L/T]}$$

where $\bar{v}$ = apparent velocity through entire area A.

Then

$$v = \frac{\bar{v}}{\phi} = \frac{Q}{A\phi} = \frac{K}{\phi} \frac{dh}{dL}$$

where: v = average velocity of·flow through pores

ϕ = porosity

From the data given above, converted to consistent units and entered into the Darcy equation

$$v = \frac{21.3639 \text{ ft/yr}}{0.104} \times \frac{8 \text{ ft/mile}}{5{,}280 \text{ ft/mile}}$$

$$= 0.31 \text{ ft/yr}$$

This evaluation shows that water in the Mt. Simon Formation in north-central Ohio is moving northwest at a rate of 0.31 ft/yr. The source of the hydraulic gradient and the fate of the moving water are not understood. Furthermore, there are complications in the analysis itself, as pointed out by Bond.[27] However, in spite of such uncertainties, it can be indisputably concluded that water in the Mt. Simon Formation is moving at a negligible rate, if at all, at this location.

As a further example, Fig. 17[39] shows the potentiometric surface for the lower Floridan aquifer in northwest Florida. There the hydraulic gradient was estimated to be about 1.33 ft/mile toward the southwest in the vicinity of the Monsanto Company injection well prior to its operation. The permeability is about one darcy and the porosity is estimated to be 10 percent.[39,40] The velocity of natural flow in the lower Floridan aquifer is then estimated to be

$$v = \frac{890 \text{ ft/yr}}{0.10} \times \frac{1.33 \text{ ft/mile}}{5{,}280 \text{ ft/mile}} = 2.24 \text{ ft/yr}$$

This analysis is more easily interpreted than the previous one for Ohio, because it is well known that the source of hydraulic head lies to the north of the injection well site and that the discharge area lies to the south beneath the Gulf of Mexico. The velocity of flow is again very low; it appears that more than 200,000 years would be required for injected waste to reach the estimated subsea discharge point about 100 miles to the south.

2. Pressure Effects of Injection

Wastewater injected into deep aquifers does not move into empty voids; rather, it displaces existing fluids, primarily saline water. The displacement process requires exertion of some pressure, in excess of the natural formation pressure. The pressure increase is greatest at the injection well and decreases in approximately a logarithmic manner at increasing distances from the well. The amount of excess pressure required and the distance to which it extends depend on the properties of the formation and the fluids, the amount of fluid being injected, and the length of time injection has been going on. The pressure or head changes resulting from injection are added to the original regional hydraulic gradients to obtain a new potentiometric surface map that depicts the combined effects of regional flow and the local disturbances.

By use of the theory that has been described, potentiometric surface maps can be produced to show the anticipated situation at any time in the
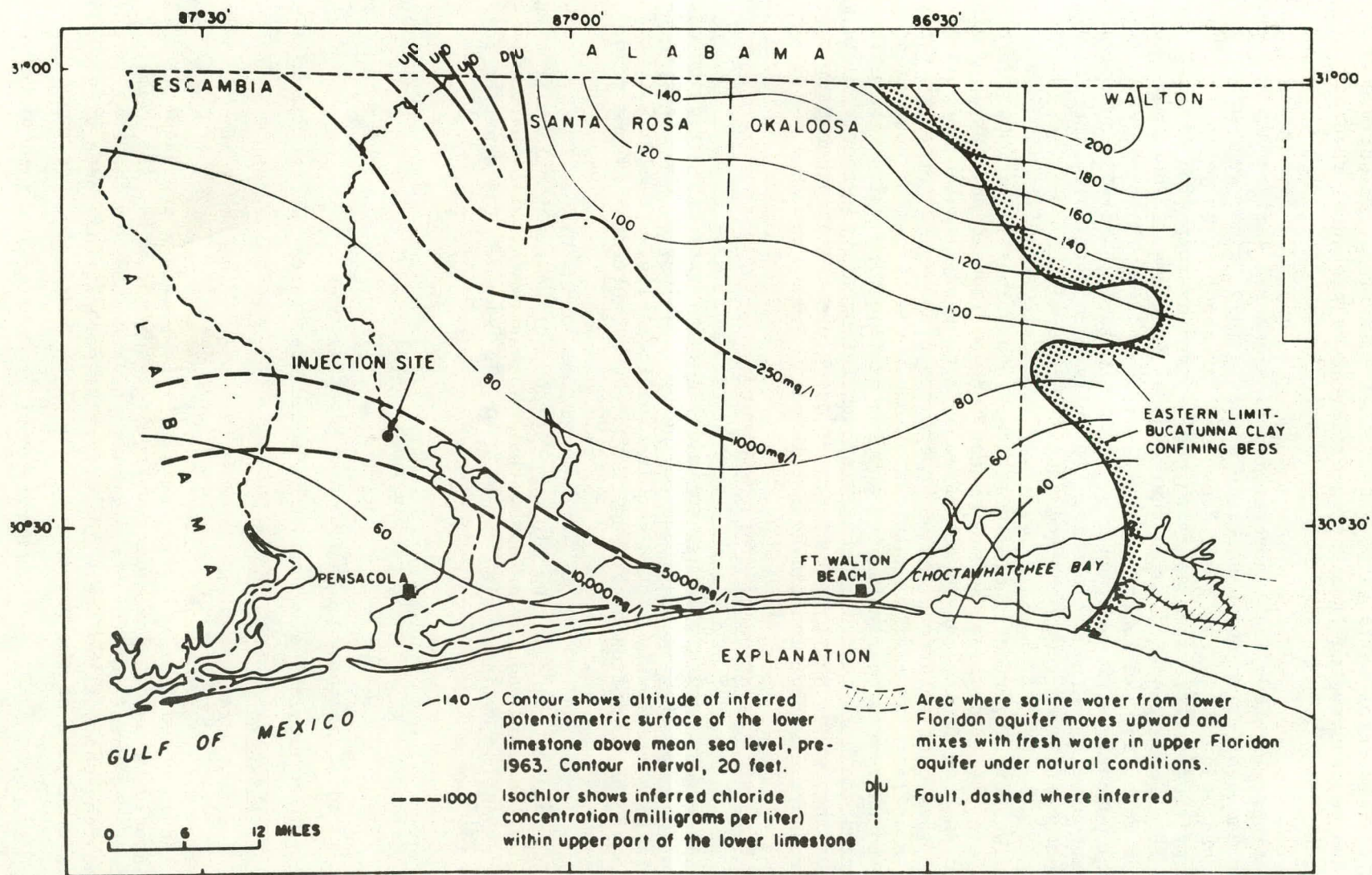
Fig. 17. Hydrogeology of the Lower Floridan Aquifer in Northwest Florida[39]

future. If observation wells exist, the actual potentiometric surface at any time can be constructed from the water levels or pressures recorded in the wells.

Figure 18 shows the theoretical potentiometric surface map for the lower Floridan aquifer in northwestern Florida in 1971, after wastewater injection had been in progress near Pensacola for about eight years.[39] The estimated pressure effects of injection can be seen by comparing Fig. 17 with Fig. 18. Comparison indicates that changes in hydraulic head may extend 30 miles or more from the injection site. Although Fig. 18 is titled a theoretical potentiometric surface map, it is, in fact, partially substantiated by observation wells. If more observation wells were available, the map would be constructed entirely from observed data.

Two very important characteristics of solutions to groundwater flow equations are that individual solutions can be superimposed and that hydrologic boundaries such as faults can be simulated by a properly located imaginary well. The fact that solutions can be superimposed allows the pressure effects of multiple wells to be easily analyzed. Because the effect of boundaries is analogous to that of properly located pumping or injection wells, the existence of boundaries can be detected by observing aquifer pressure response to injection or pumping; conversely, the effects of known or suspected boundaries on aquifer pressure distribution can be estimated.

3. Rate and Direction of Fluid Movement

As with pressure response to injection, the rate and direction of movement of the injected fluid depend on the hydrogeology of the site; therefore, the same factors previously listed require consideration. In addition, the properties of the formation water and the injected wastewater assume major importance.

A good estimate of the <u>minimum</u> distance of wastewater flow from an injection well can be made by assuming that the wastewater will uniformly occupy an expanding cylinder with the well at the center. The equation for this case is:

$$r = \sqrt{\frac{V}{\pi b \phi}} \quad \text{Dimensions--[L]} \tag{9}$$

where: r = radial distance of wastewater front from well

$V = Qt$ = cumulative volume of injected wastewater, where t is time

b = <u>effective</u> aquifer thickness

ϕ = average <u>effective</u> porosity

It is noted that effective aquifer thickness and average effective porosity should be used. The effective aquifer thickness is, for example, that part of the total aquifer that consists of sandstone in the case of a mixed sandstone-shale lithology. The effective porosity has been previously defined as that part of the porosity in which the pores are interconnected.

Fig. 18. Theoretical Potentiometric Surface of Lower Limestone
of Floridan Aquifer in Late 1971 (Goolsby, 1972).[39]

In most situations, the minimum radial distance of travel will be exceeded, because of dispersion, density segregation, and channeling through high-permeability zones. Flow may also be in a preferred direction, rather than radial, because of hydrologic discontinuities (*e.g.*, faults), selectively oriented permeability paths, or natural flow gradients.

An estimate of the influence of dispersion can be made with the following equation:

$$r' = r + 2.3\sqrt{Dr} \quad \text{Dimensions--[L]} \quad (10)$$

where: r' = radial distance of travel with dispersion

D = dispersion coefficient; 3 ft for sandstone aquifers and 65 ft for limestone or dolomite aquifers

Equation 10 is obtained by solving equation (10.6.65) of Bear[41] for the radial distance at which the injection front has a chemical concentration of 0.2% of the injected fluid.

The detailed development of dispersion theory is presented by Bear (1972).[39] The dispersion coefficients given are high values for sandstone and limestone aquifers obtained from the literature. No actual dispersion coefficients are known to have been obtained for any existing injection well.

Calculations of the distance of wastewater travel for 148 wastewater injection wells in the United States were made by Warner using Equations 9 and 10 and were summarized by the Environmental Protection Agency,[42] as shown in Table 13. The calculations revealed that, even with dispersion, in 96 percent of the cases and after 50 years of operation, the wastewater will have traveled less than 6,000 feet from the injection well. Thus, in most cases, the distance of travel will not be of concern if actual conditions comply even generally with the assumptions made; even if such calculations are in error by several hundred percent, there would still be no cause for concern in most cases because of the distance from the injection zone to the nearest other well penetration or known resource.

To proceed beyond the calculations that have been shown may not be necessary and in many cases, may not be meaningful. However, possibly some of the additional complications that are mentioned may be accounted for. For example, Bear and Jacobs[43] in one of a series of reports considered the flow of water from a groundwater recharge well in an aquifer of uniform flow, when the densities and viscosities of the injected and interstitial fluids are the same. Gelhar and others[44] developed analytical techniques for describing the mixing of injected and interstitial waters of different densities.

So far, the travel of the injected wastewater has been treated as though it was an inert fluid and would not react with the aquifer water or minerals, would not be affected by bacterial action, and would not decompose or radioactively decay. If the wastewater is not inert, changes in chemical composition with time and distance may also need to be considered. Bredehoeft and Pinder[45] discuss the methodology for a unified approach to this type of problem, and Robertson and Barraclough[46] presented an example of a case in

Table 13. Calculated Distance of Wastewater Travel for
148 Injection Wells after 10 and 50 Years of
Operation Using Equations 4-9 and 4-10[42]

Without Dispersion	10 Years		50 Years	
0-1000 FT	89		34	
1001-2000	44	97.2%	45	
2001-3000	11		27	97.2%
3001-4000	2		15	
4001-5000	0		13	
5001-6000	2		7	
6001-7000	0		0	
7001-8000	0		2	
8001-15,000	0		2	
With Dispersion				
0-1000 FT	69		23	
1001-2000	58	96%	44	
2001-3000	15		32	96%
3001-4000	2		17	
4001-5000	1		11	
5001-6000	0		10	
6001-7000	2		1	
7001-8000	0		2	
8001-15,000	0		3	

which radioactive decay, dispersion, and reversible sorption were considered.
However, no procedure exists at this time for simultaneously considering the
full range of practical possibilities that may be involved in wastewater
movement.

In spite of the degree of sophistication used in the development of
theories for rate and direction of travel of injected fluid from an injection
well, nonuniform distribution of porosity and permeability will preclude
making accurate estimates in many cases. In general, wastewater flow in
unfractured sand or sandstone aquifers would be expected to agree more closely
with theory than would flow in fractured reservoirs or in carbonate aquifers
with solution permeability. However, even in sand aquifers, flow can be
expected to be nonideal, as shown by tests reported by Brown and Silvey.[47]
Particularly large deviations from predictions may occur in limestone or
dolomite aquifers.

4. Hydraulic Fracturing

Hydraulic fracturing may be deliberately accomplished to increase
formation permeability, or it may occur during injection testing or waste-
water injection if the fracture initiation pressure is exceeded. Regulatory

policy may or may not permit short-term hydraulic fracturing operations
for well stimulation, but continuous injection at pressures above the fracture
point is prohibited by most if not all agencies. This is because of the
danger of damage to well facilities and because of the uncertainty about the
direction of fracturing and injected fluid flow as fractures continue to be
extended.

Figure 19 is a schematic diagram of bottom-hole pressure versus
time during hydraulic fracturing. Before injection begins, the pressure is
that of the formation fluid (p_o) and the column of fluid in the well bore.
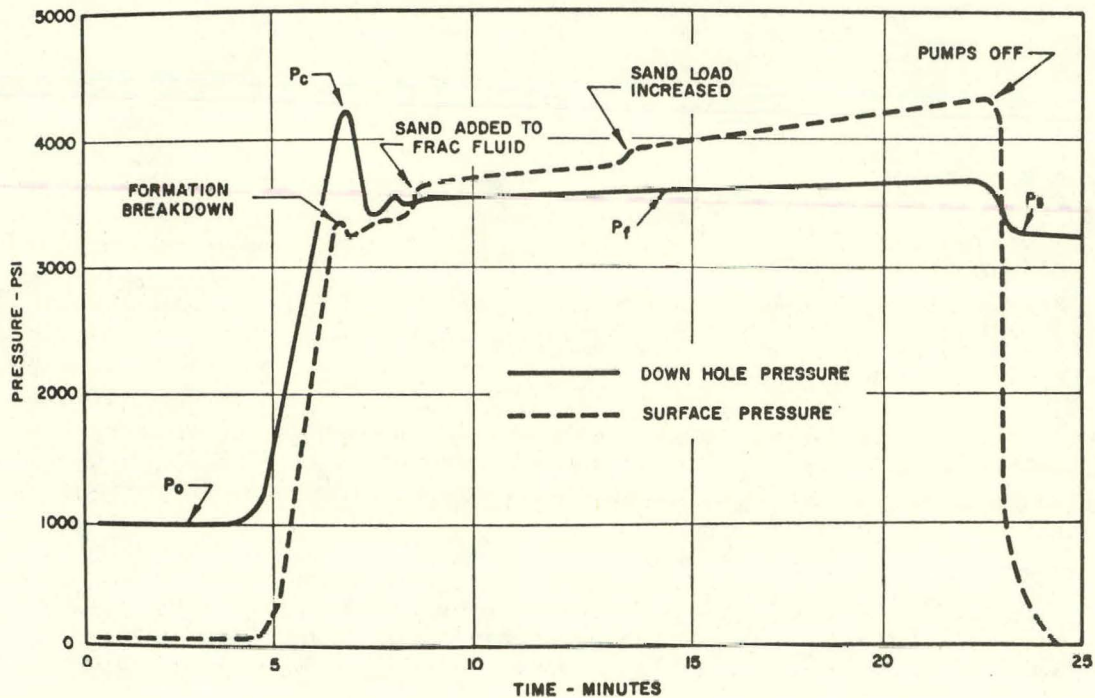
Fig. 19. Schematic Diagram of Pressure *vs.* Time
During Hydraulic Fracturing[24]

Pressure is increased until fracturing occurs; then, as fluid continues to
be pumped into the well, the pressure stabilizes at p_f, the flowing pressure,
and the fractures continue to be extended. When injection is stopped, and
the well is shut-in, the pressure quickly stabilizes to a constant value,
the instantaneous shut-in pressure. This pressure is considered to be equal
to the least principal earth stress in the vicinity of the well.

In estimating the fluid pressure at which hydraulic fracturing will
occur, one of two conditions is usually assumed:

(1)   That the least principal stress is less than the vertical
         lithostatic stress caused by the rock column. In this case,
         fractures are assumed to be vertical.

(2) That the vertical lithostatic stress is the least principal
stress. In this case, fractures will be horizontal.

In the first case, the minimum bottom-hole pressure required to
initiate a hydraulic fracture can be estimated from Hubbert:[48]

$$p_i = \frac{S_z + 2p_o}{3} \text{ Dimensions--}[F/L^2] \tag{11}$$

where: p_i = fracture initiation pressure

S_z = total lithostatic stress

p_o = formation fluid pressure

The fracture gradient, that is, the injection pressure required
per foot of depth, can be estimated by entering representative unit values
into Equation 11. Typical values for S_z and p_o are, respectively, 1.0 and
0.46 psi/ft. This yields a p_i gradient of 0.64 psi/ft as a minimum value
for initiation of hydraulic fractures. This situation implies a minimum
lateral earth stress. As the lateral stresses increase, the bottom-hole
fracture initiation pressure also increases up to a limiting value of 1.0
psi/ft. Actually, fracture pressures may exceed 1.0 psi/ft when the rocks
have significant tensile strength and no inherent fractures that pass through
the well bore. In any particular case, injection tests can be run to deter-
mine what the actual fracture pressure is; then, operating injection pressures
can be held below the instantaneous shut-in pressure. In the absence of any
specific data, arbitrary limitations of from 0.5 to 1.0 psi per foot of depth
have been imposed on operating injection wells. Regional experience should
be used as a criterion in establishing an arbitrary limit, since regional
tectonic conditions and fluid pressure gradients dictate what a safe limit
will be.

5. Generation of Earthquakes

As a matter of background, it is widely but not universally accepted
that a series of earthquakes that began in the Denver area in 1962 was ini-
tiated by injection of wastewater into a well at the Rocky Mountain Arsenal.
Since the time of association of seismic activity with wastewater injection
at Denver, apparently similar situations have been observed at Rangely,
Colorado, and Dale, New York, the former related to water injection for
secondary recovery of oil and the latter to disposal of brine from solution
mining of salt. On the other hand, there are presently about 160 operating
industrial wastewater injection wells and tens of thousands of oil field
brine disposal wells that have apparently never caused any noticeable seismic
disturbance, and so these three examples would have to be considered very
rare.

It has been erroneously stated by many that the seismic events have
been stimulated by "lubrication" of a fault zone by injected fluids. What
has happened, if injection has been involved, is that the water pressure on
a fault plane has been increased, thus decreasing the friction on that plane
and allowing movement and consequent release of stored seismic energy.

Based on this interpretation of the mechanism of earthquake triggering by fluid injection, some of the conditions that would have to exist in order to have such earthquakes would be:

(1) A fault with forces acting to cause movement of the blocks on either side of the fault plane, but with movement being successfully resisted by frictional forces.

(2) An injection well that is constructed close enough, vertically and horizontally, to the fault so that the fluid pressure changes caused by injection will be transmitted to the fault plane.

(3) Injection at a sufficiently great rate and for a sufficiently long time to increase fluid pressure on the fault plane to the point that frictional forces resisting movement become less than the forces tending to cause movement. At this time, movement will occur and stored seismic energy will be released. That is, an earthquake will occur.

As has been discussed earlier in the section on state of stress, relatively little is known about stress distribution in the earth's crust and even less is known about stress distribution along fault systems. In the absence of this information, only qualitative estimates of the probability of earthquake stimulation can be made. In the great majority of cases, the potential for earthquake stimulation will be nonexistent or negligible because only very limited areas in this country are susceptible to earthquake occurrence. The susceptible areas are delineated by records of earthquakes that have occurred in the past and by tectonic maps showing geologic features that are associated with belts of actual or potential earthquake activity.

In a case where subsurface stresses are known or are determined by hydraulic fracturing or other means, and where the location and orientation of the fault plane are known, a quantitative estimate of the pressure required to cause fault movement can be made. Raleigh[49] provides an example of such a calculation from the Rangely, Colorado, oil field.

F.   Characteristics of Sedimentary Basins in the United States

Synclinal sedimentary basins and the Atlantic and Gulf coastal plains (Fig. 20)[50] are particularly favorable sites for deep waste-injection wells because they contain relatively thick sequences of salt-water-bearing sedimentary rocks and because the subsurface geology of these basins commonly is relatively well known. Galley[51] discussed general aspects of geologic basin studies as related to deep-well disposal of radioactive waste.

During the early 1960s, a series of reports concerning the suitability of selected basins for radioactive waste disposal was prepared for the Atomic Energy Commission by the U.S. Geological Survey (USGS). These reports included ones by Repenning[52] on the Central Valley of California, Sandberg[53] on the Williston basin, Beikman[54] on the Powder River basin, MacLachlan[55] on the Anadarko basin, and LeGrand[56] on the Atlantic and Gulf coastal plains. Love and Hoover[57] briefly summarized the geology of many sedimentary basins in the United States.

AREA OF VOLCANIC PLATEAUS

WILLISTON

SNAKE RIVER VOLCANIC

BIG HORN

POWDER RIVER

WIND R.

GREEN R.

WASHAKIE

LARAMIE

MICHIGAN

BASIN AND RANGE PROVINCE

GREAT CENTRAL VALLEY

SIERRA NEVADA BATHOLITH

DENVER

SALINA

FOREST CITY

UINTA

PICEANCE

ILLINOIS

APPALACHIAN

BLACK MESA

RATON

OZARK UPLIFT

SAN JUAN

DALHART

ANADARKO

PALO DURO

ARKOMA

ARBUCKLE MTS.

WICHITA MTS. UPLIFT

FT. WORTH

MID-LAND

COASTAL PLAIN

COASTAL PLAIN

DELAWARE

LLANO UPLIFT

COASTAL PLAIN

LEGEND

EXTENSIVE AREAS WHERE RELATIVELY IMPERMEABLE IGNEOUS-INTRUSIVE AND METAMORPHIC ROCKS ARE EXPOSED AT SURFACE

EXTENSIVE AREAS WHERE VOLCANIC SEQUENCES ARE EXPOSED AT SURFACE

BOUNDARIES OF GEOLOGIC FEATURES

(DENVER) APPROXIMATE BASIN OUTLINES

● INDUSTRIAL WASTE INJECTION SYSTEMS (FEBRUARY, 1966)
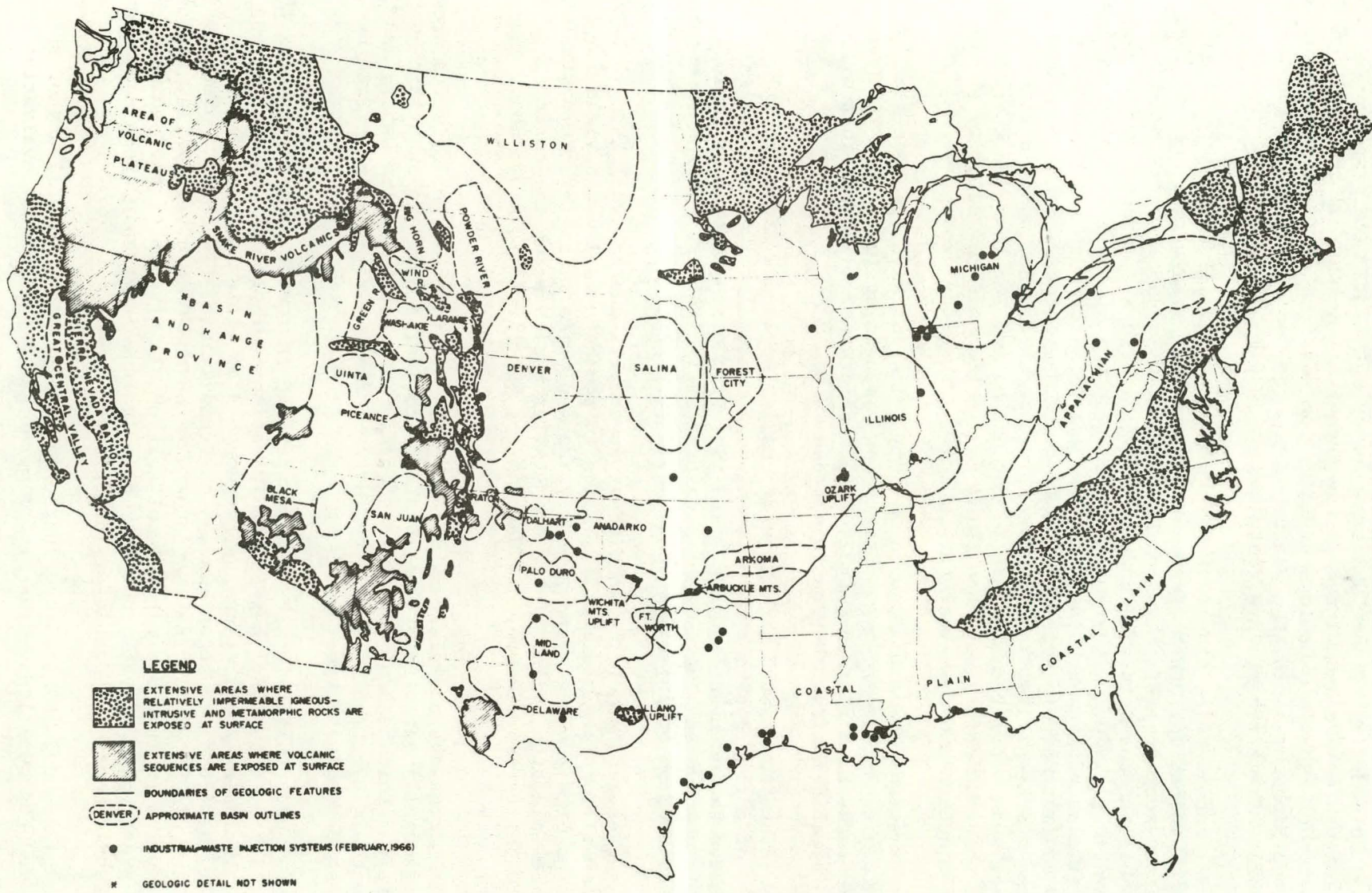
× GEOLOGIC DETAIL NOT SHOWN

Fig. 20. Geologic Features Significant in Waste-Injection Well-Site Evaluation and Locations of Some Industrial Wastewater Injection Systems[50]

In addition to the USGS basin reports, reports were prepared for the AEC by members of a subcommittee of the Research Committee of the American Association of Petroleum Geologists (AAPG) on portions of the Appalachian basin, the Michigan basin, the Salina basin, the Denver basin, and the San Juan basin. These reports are contained in AAPG Memoir 10.[51]

Just as major synclinal basins are geologically favorable sites for wastewater injection, other areas may be generally unfavorable because the sedimentary-rock cover is thin or absent. Extensive areas where relatively impermeable igneous-intrusive and metamorphic rocks are exposed at the surface are shown in Fig. 20. With the possible exception of small parts, these areas can be eliminated from consideration for waste injection. The exposure of igneous and metamorphic rocks in the Arbuckle Mountains, Wichita Mountains, Llano and Ozark uplifts, the exposures just south of the Canadian shield, and other such exposures are perhaps not extensive, but they are significant because the sedimentary sequence thins toward them and the salinity of the formation waters decreases near the outcrops around the exposures.

Regions shown in Fig. 20 where a thick volcanic sequence lies at the surface generally are not suitable for waste-injection wells. Although volcanic rocks have fissures, fractures, and interbedded gravel that will accept injected fluids, they contain fresh water.

The immense and geologically complex Basin and Range province is a series of narrow basins and intervening, structurally positive ranges. Some of the basins might provide waste-injection sites, but their geology is mostly unknown and the cost of obtaining sufficient information to ensure safe construction of injection wells would be very great.

The geology of the West Coast is complex and not well known. Relatively small Tertiary sedimentary basins in southern California yield large quantities of oil and gas and probably are geologically satisfactory sites for waste-injection wells. There are similar basins along the coast of northern California, Oregon, and Washington, but little is known about their geology.

Areas not underlain by major basins or prominent geologic features may be generally satisfactory for waste injection if they are underlain by a sufficient thickness of sedimentary rocks that contain saline water, and if potential injection zones are sealed from fresh-water-bearing strata by impermeable confining beds.

Some publications have been prepared in recent years describing the feasibility of industrial wastewater injection in individual states and one region, including publications by Bergstron[58] on Illinois, Kreidler[59] on New York, Newton[60] on Oregon, Rudd[61] on Pennsylvania, Clifford[62] on Ohio, Tucker and Kidd[63] on Alabama, and ORSANCO[10] on the Ohio Rivery Valley region. These reports include descriptions of part or all of some of the sedimentary basins previously analyzed, but they also include interbasin areas and discuss state requirements and regulatory experience.

It should be realized that only rarely, if ever, will any of the listed reports constitute a basis for more than a preliminary evaluation of

the suitability of a specific site, unless the site is in a totally unacceptable location (in which case no further evaluation is needed). If a site is located in a generally acceptable area, a detailed examination of the local geology and subsurface hydrology must be performed prior to construction of a test well, and a reevaluation must be made after the well has been constructed and tested.

Often, much of the information available for local site evaluation will be in the hands of the geological survey of the state in which the site is located. Additional possible information sources are other state agencies (*e.g.*, divisions of oil and gas, water surveys, bureaus of mines, and environmental protection agencies), federal agencies (particularly the U.S. Geological Survey and the Environmental Protection Agency) and oil and perhaps mining companies operating in the area. In oil- and gas-producing areas, it is common to find companies that collect and provide well logs and other subsurface information for very reasonable charges in comparison with what it costs to locate and duplicate the information independently. Unfortunately, the ways in which geologic and subsurface engineering information is used are so varied that thus far these data have not been collected and filed in such a way that they can be automatically retrieved and applied to evaluation of an injection well site. Hidalgo and Woodfork[64] describe a project in which data from well logs and hydraulic fracturing records for a 1,785-square-mile area in West Virginia were transferred to computer cards; these data were then used to prepare computer-drawn maps for preliminary injection-well site evaluation. This was, however, an experimental effort, and such a capability is not generally available.

IV. RELIABILITY OF HIGH-LEVEL-WASTE CONTAINERS
(W. Seefeldt and W. Mecham)

A. Purpose and Scope

The purpose of the container reliability studies is to identify as quantitatively as possible the reliability against failure and leakage of the canisters used to contain high-level wastes in a glass or calcine form.

Container degradation due to internal metallurgical characteristics, thermal and mechanical events occurring during transport and handling (but not major events such as earthquakes and tornadoes), and interactions with internal and external environments are being considered.

Environments included are interim storage of solidified wastes at a reprocessing plant, transport from a reprocessing plant to a Retrievable Surface Storage Facility (RSSF), interim storage at the RSSF, and transport to the ultimate disposal site.

The study requires the establishment of reference systems prior to the determination of canister reliability. Three storage concepts have been developed by Atlantic Richfield Hanford Company (ARHCO) for application to an RSSF. These concepts will be part of the reference system. In addition, waste compositions, canister material and fabrication methods, coolant compositions, and mechanical and thermal events should be selected for the reference system.

The three concepts of interim storage at the RSSF are:

(1) the Water Basin Concept, in which canisters are stored bare in a water pool,

(2) the Air-Cooled Basin Concept, in which canisters are overpacked in mild steel and stored and cooled in air moving by thermal convection, and

(3) the Sealed Storage Cask Concept, in which canisters are overpacked in mild steel, encased in a freestanding concrete shield placed outdoors on a concrete pad, and cooled by thermal convection.

The sequence of events to be considered for reference was 10 years of interim storage under water at a reprocessing plant, followed by 100 years of interim storage at an RSSF, together with transfer from both facilities. In addition, 40 years of interim storage under water at the reprocessing plant followed by shipment to the ultimate disposal site is considered.

Initially, the two waste forms to be considered for incorporation into the reference systems were calcine and glass, but no specific compositions were established for reference purposes. Through discussions with Division of Waste Management and Transportation (DWMT), two modes of heat transfer for the calcine form were established: with and without internal fins. This was later reduced to one mode: with fins.

B. **Methods for Removal of Stresses in a Stainless Steel Canister Containing Solidified Waste**

1. **Background**

   a. **Introduction**

   In the previous quarterly report, stress levels associated with the cooling of molten glass in stainless steel canisters were reported. The stresses arise from the fact that the coefficient of expansion (contraction) of stainless steel is significantly greater than that of borosilicate glass. Stress-relieving mechanisms during cooling were not considered. Assuming elastic strain only, the incremental stress ΔS (psi) for incremental cooling ΔT (°F) was estimated to be 214 psi/°F using the following equation:

$$\frac{\Delta S}{\Delta T} = \frac{E_s \left(C_s - C_g \right)}{\left(\dfrac{E_s}{E_g} \right) \left(\dfrac{w}{r} \right) \left(1 - \mu \right) + 1}$$

where: E_s = modulus of elasticity of stainless steel = 28 x 10^6 psi

E_g = modulus of elasticity of glass = 9.5 x 10^6 psi

w = thickness of stainless steel = 0.375 in.

r = inside radius of canister = 6.0 in.

μ = Poisson's ratio for glass

C_s = coefficient of thermal expansion for stainless steel
   = 10.4×10^{-6} °F^{-1}

C_g = coefficient of thermal expansion for glass = 1.8×10^{-6} °F^{-1}

Thus, 56°C (100°F) of cooling can impart substantial stress levels to the stainless steel. The total cooling range extends from the softening point of glass (1500°F or 816°C) to the canister temperature in water storage (140°F or 60°C).

Methods of removing such stresses are examined in the following sections. The methods include: (1) creep strain (2) yield strain, and (3) shot-peening.

Before stress-removing methods are discussed, (1) the thermal expansion coefficients of various glasses as related to the value used in the calculation and (2) the relationship of the viscosity of glasses to stress relieving are considered.

b.   Thermal Expansion of Glasses

For the purpose of our preliminary analysis, we have assumed for glass the well-established properties of commercial Pyrex (Corning 7740). Coefficients of thermal expansion of glasses and glass-ceramics vary widely. A presentation of thermal expansions of typical materials of interest is shown in Fig. 21. Included in the figure is a recent measurement at PNL of the expansion of a simulated waste glass.
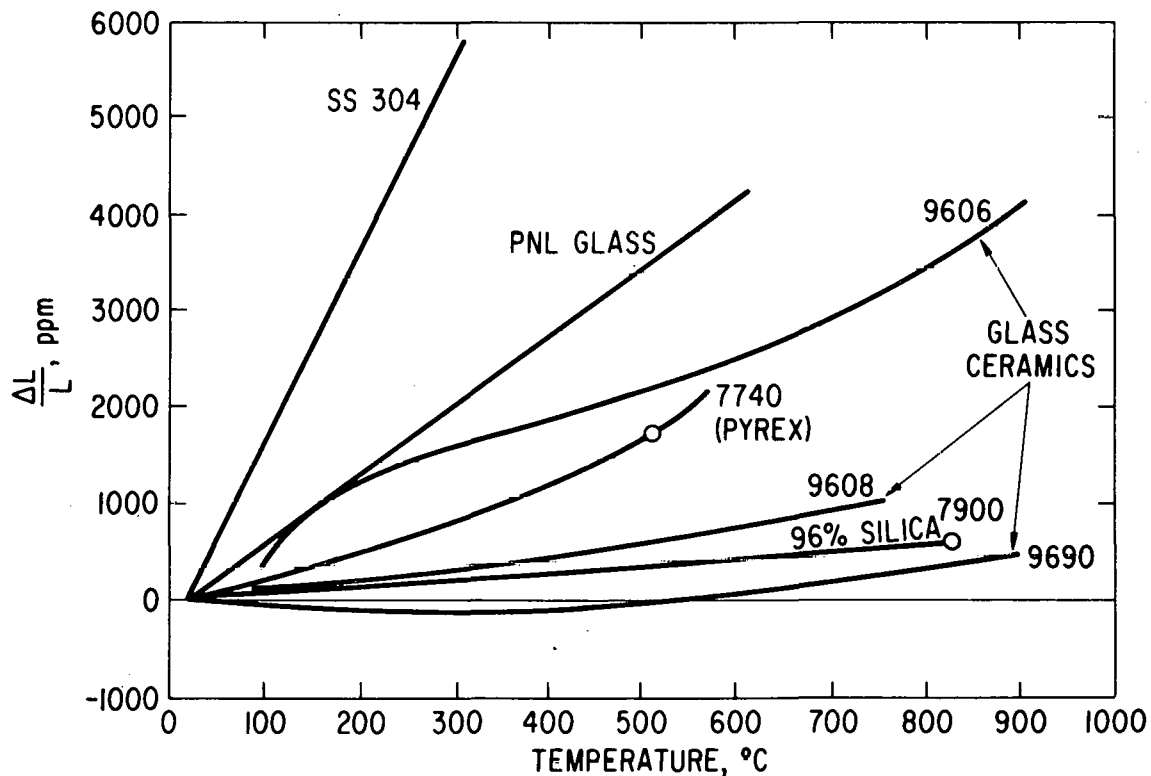

Fig. 21.   Expansion Characteristics of Selected Glasses, Glass Ceramics, and Stainless Steel [Note added lines for SS 304 (smooth) and a simulated glass (73-109) by PNL][65]

c. Viscosity of Glasses

The rigidity of glass at elevated temperature requires special consideration, since glass does not have a definite melting point. At room temperature, commercial glasses are very hard and brittle. Viscosities at various stages of melting for representative glasses--a borosilicate glass (Pyrex), a nearly pure silica glass (96% silica, quartz-like), and an alumino-silicate glass manufactured by Corning--are given in Table 14. The Practical Property column lists the lowest viscosity (highest fluidity) condition at the top; viscosity increases as one proceeds downward.

Table 14. Viscosity of Representative Commercial Glasses[66]

Practical Property	Viscosity, poises	Temperature, °C		
		Pyrex[a]	96% Silica[b]	Alumino-Silicate[c]
Melting Range	50 to 500	–	–	–
"Melting Point"	100	–	–	–
Pressing Range	500 to 7000	>1300	–	>1200
"Working Point"	10,000	1245	–	1190
Blowing and Drawing Range	1×10^4 to 1×10^5	>900	>1600	>1100
"Flow Point"	1×10^5	>900	>1600	>1000
Softening Range	3×10^7 to 1.5×10^8	>820	>1500	>915
"Softening Point"	3×10^7	820	1500	915
"Annealing Point"	1×10^{13}	565	910	715
"Strain Point"	3.2×10^{14}	515	820	670
"Upper Use Temperature" "Extreme"	$\sim 10^{15}$	490	1100	650
"Normal"	$>10^{16}$	230	800	200

[a] Corning type 7740[1]

[b] Corning type 7900[1]

[c] Corning type 1/20[1]

A practical characterization of the viscosity is provided in the table by using some descriptive terms used in glass manufacture. The "strain point" is the lowest temperature at which there is practical stress relief in short periods (hours). The "upper use temperature" is the temperature above which slow distortion is possible due to load stresses and is also the temperature above which the glass is vulnerable to thermal shock. The higher the melting and softening points of the glass, the higher is the temperature at which long-term creep can reduce stresses; these properties

depend on composition and the state of vitrification. A glass-ceramic[66] (Corning "Pyroceram" radomes for ballistic missiles) has a softening point of 1350°C.

In contrast to glass, granular calcine waste is not monolithic and does not impose comparable stress on the canister.

2. Methods of Stress Relief

Removal of the stresses imposed by cooling could be by creep strain (*i.e.*, time-dependent strain under stress), by yield strain (*i.e.*, essentially instantaneous plastic deformation at sufficiently high stress), or by shot-peening.

a. Stress Relief by Creep

Creep rates for both stainless steel and glass are highly temperature dependent. At temperatures below about 750°F (400°C), creep rates of steel and glass are so low that this method is not practical to effect major stress relief. Therefore, since creep is not effective for stress relief for the final cooling in the range of 400 to 65°C (750 to 150°F), very high residual stresses, well in excess of the yield stress, would remain.

b. Stress Relief by Yield

As the filled canister is cooled to 750°F and lower, stresses in the stainless steel will rapidly increase to and exceed the yield point (about 39,000 psi), at which point yield strain will occur and stress will no longer increase as calculated for elastic strain.

However, the magnitude of stress required to reach the yield point increases in 304L with continuing deformation; this phenomenon is termed work hardening. The extent of work hardening is related to the total amount of plastic deformation or strain. The maximum possible strain of stainless steel required for this application is associated with differential thermal contraction during cooling—about 1.5%. This amount of deformation is well below the elongation for rupture, which for fully annealed metal is more than 50%, and for cold-worked metal is not less than 9%. For 1.5% strain, the yield stress will not rise above about 40,000 psi.

Reference Properties of Stainless Steel. Reference properties of stainless steel used in this discussion are summarized in Table 15. Nominal tensile properties are summarized in Table 16. Creep and rupture data are given in Table 17. Elevated-temperature strength as a function of temperature is shown in Fig. 22 and the effect of cold work on the yield strength is shown in Fig. 23. It should be noted that the nominal properties shown above allow individual production lots of SS 304L to vary considerably, and some variation may also be expected within a lot. Yield strengths for 304L vary from 20,000 psi to 50,000 psi.[68]

Description of Subcooling Method. It is possible to remove the elastic tensile load stress that remains on the canister after cooling of the solidified glass by continuing the cooling below the reference waste storage temperature (∿60°C or 140°F). The additional cooling will cause

the stainless steel to yield further. If this additional yield strain is as large as the elastic strain at the yield stress, then, when the temperature is raised to the storage temperature, the elastic load stress will be completely removed, and this source of stress will not be present to produce stress corrosion cracking in subsequent exposure of the canister to the storage environment. The operations involved in subcooling are shown in the diagram in Fig. 24.

The amount of subcooling below 60°C (140°F) depends on the properties of the materials, the subcooled temperature T_{sc}, and the storage temperature T_s as follows:

$$\left(T_s - T_{sc}\right)(\Delta C) = \frac{S_y}{E_s}$$

or

$$T_{sc} = T_s - \frac{S_y}{E_s(\Delta C)}$$

where: T_s = storage temperature, °F

T_{sc} = minimum cooling temperature, °F

ΔC = differential thermal expansion for SS 304 and Pyrex, approximately 8.6 x 10^{-6}/°F

S_y = yield stress in stainless steel at T_c, including the effect of work hardening, approximately 40,000 psi

E_s = modulus of elasticity in stainless steel at T_c, approximately 29 x 10^6 psi

Table 15. Properties of Stainless Steel Types 304 and 304L

Melting Range, °F	2550-2650
Specific Heat (32-212°F), Btu/(lb)(°F)	0.12
Thermal Conductivity (212°F), Btu/(hr)(ft²)(°F/ft)	9.4
Coefficient of Thermal Expansion (32-1200°F), per °F	10.4 x 10^{-6}
Modulus of Elasticity, 10^6 psi	28
Modulus of Rigidity, 10^6 psi	12.5
Density, lb/in.³	0.29

Table 16. Nominal Tensile Properties of
Stainless Steel 304 and 304L[67]

Form and Condition	Yield Strength (0.2% offset), 10 psi	Tensile Strength, 10 psi	Elongation (2 in.), %	Reduction of area, %	Rockwell Hardness
Type 304					
Sheet and strip					
Annealed	42	84	55	–	B80
Bars					
Annealed	35	85	60	70	–
Cold drawn	60-95	100-125	60-25	–	–
Wire					
Annealed	35	90-105	60[a]	65	B83
Soft temper	60-90	100-125	45[a]	65	B95
Hard temper	105-125	140-160	25[a]	55	C33
Type 304L					
Sheet and strip					
Annealed	39	81	55	–	B79

[a] Gage length 4 x diameter.

For the values indicated,

$$T_s - T_{sc} = 160°F.$$

If

$$T_s = 140°F, \; T_{sc} = -20°F \; (-29°C)$$

The reduction of circumferential tensile stress to zero by
this method will require close control and accurate knowledge of the properties
used above. Stainless steel 304L has generally good properties at subzero
temperatures; the tensile strength increases markedly at low temperature and
this will affect the stress-strain relationship.

Table 17. Creep and Stress-Rupture Properties of Annealed
Wrought Stainless Steel Type 304[67]

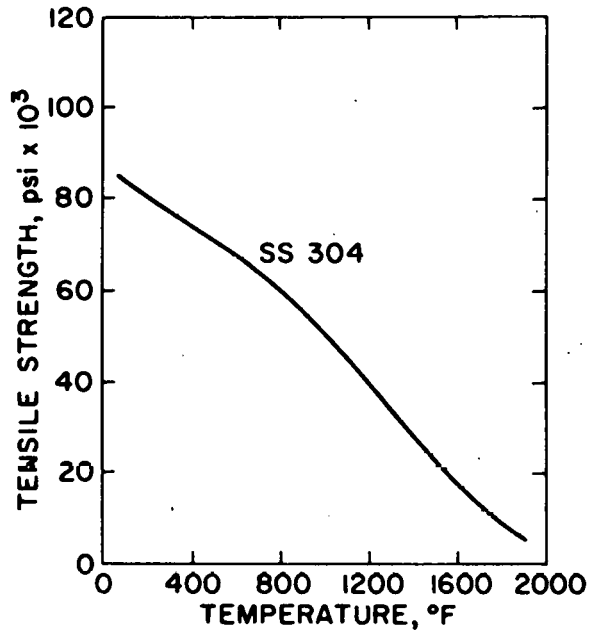| AISI Type	Test Temperature, °F	Stress, ksi, for creep rate of		Stress, ksi, for rupture in 100 hr
		0.00001%/hr	0.0001%/hr	
304	1000	12	20	47
	1200	4	8	23
	1500	1	2	7

Fig. 22. Short-time Elevated-Temperature Tensile
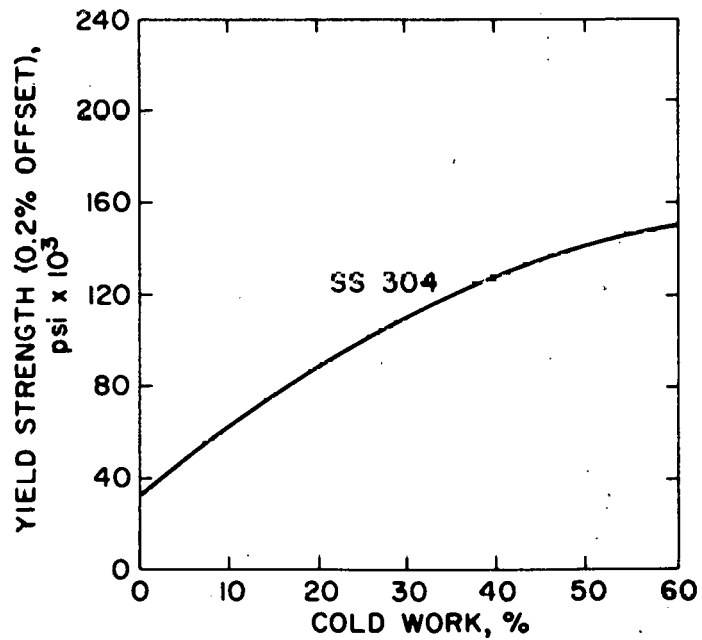Strength of Stainless Steel 304[67]

Fig. 23. Effect of Cold Work on the Yield
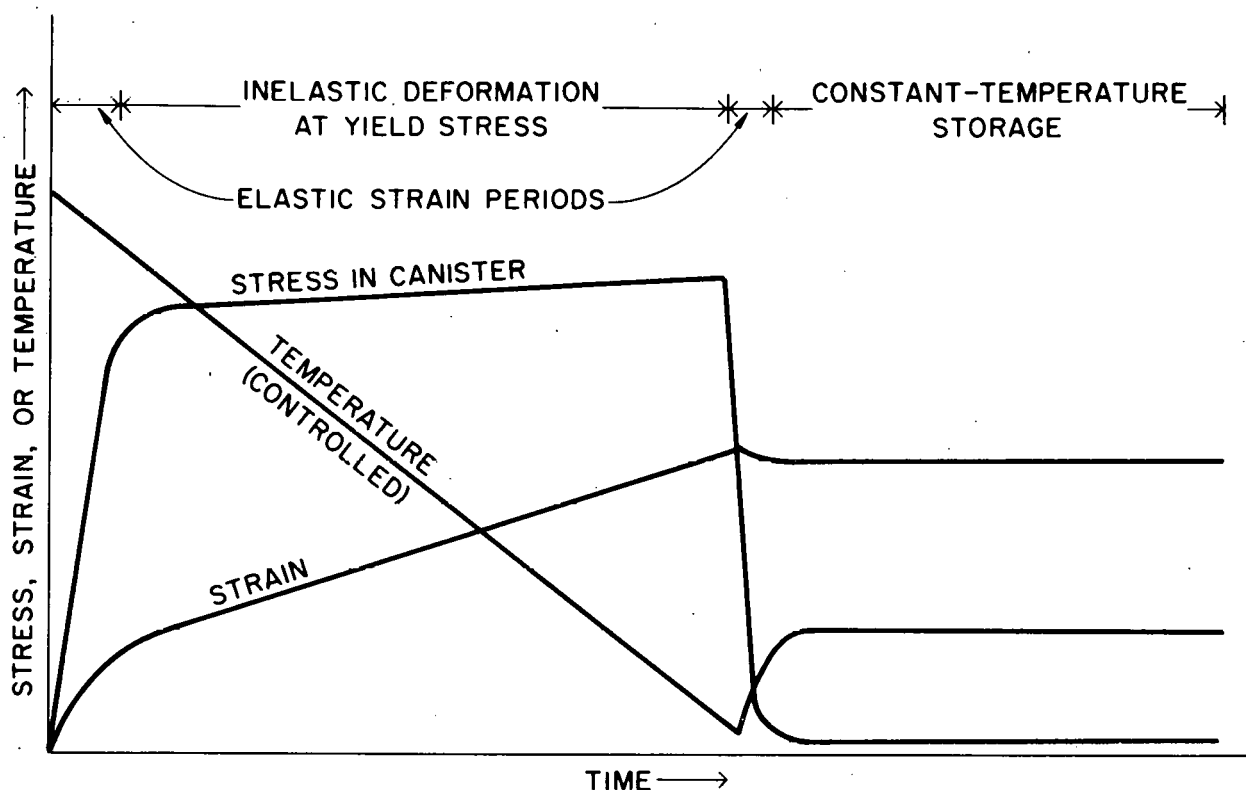Strength of Stainless Steel[67]

Fig. 24. Stress-Strain History for Controlled Cooling of Canister
Containing Glass to Achieve Near-Zero Final Stress

The practical utility of the subcooling method for removing
elastic load stress is, however, limited, since (1) it involves special low-
temperature cooling, which has practical difficulties, (2) it calls for
additional deformation that may damage the canister, and (3) it does not
remove the residual internal stresses in the steel or "heal" surface defects
as does stress relief by high-temperature treatment.

c. Residual Stresses

"Residual stresses" are defined as those remaining in a
material in the absence of external loads or changes in temperature; they
range from microscopic stresses from misfitting solute atoms and individual
dislocations of the crystal lattice, to macroscopic stresses over parts of a
material that have undergone uneven plastic deformation, as in bending and
welding. Microscopic stresses on a scale somewhat larger than atomic are
involved in dislocation pile-ups and other diffusionless shear transformations
accompanying plastic strain. Residual stresses play fundamental roles in
initiation and in propagation of cracks in stress corrosion cracking, fatigue
failures, and brittle fracture.[69]

The effects of localized residual stresses are the same as the
effects of load stress or any other stress. Residual stresses can be removed
with relatively small amounts of plastic flow in the absence of load stresses.
Therefore, relief of residual stress is commonly achieved by increasing the

temperature to allow creep strain to take place to offset the elastic strain that gives rise to the residual stress[69]

The subcooling method of stress relief (see above) is capable of removing the bulk load stresses induced in the canister, but residual stresses will probably remain. A heat treatment for removal of the residual stresses would be effective if (1) the adhesion of the glass to the canister was so low that an air gap develops as a result of the differential coefficients of expansion, and (2) the glass does not flow to fill the gap, thus re-creating the conditions that produced the bulk load stress initially. If these conditions cannot be met, alternative methods of relieving residual stresses would be required.

d. A Mechanical Method of Stress Relief: Shot-Peening

Since it is surface tensile stress that is determinative of stress corrosion cracking, any mechanical treatment of the surface that tends to apply compressive stresses (or to reduce tensile stresses) will have a favorable effect in reducing susceptibility to cracking. One of the most important commercial methods for removing residual surface stresses is shot-peening, a process in which steel shot at high velocity is propelled against the surface by a jet of compressed air.[66] An illustration of the effect of shot-peening on stress distribution is given in Fig. 25. Note that surface stress (at depths near zero) is removed by shot-peening.

The reference canister and cooling method does not entail any of the forms of macro processes that would leave severe residual stresses, *e.g.*, sharp bending or welding. The deformations are quite even and symmetrical for the cylindrical configuration and of a moderate degree, *i.e.*, about 1.5% plastic deformation (cold-working) in a material (304L) that has a room temperature rupture elongation of more than 50%. The microimperfections of greatest importance for our reference case are those associated with sensitization of stainless steel, namely, the precipitation of carbides in grain boundaries at 425 to 980°C (800 to 1800°F). This phenomenon is to be avoided by selecting a canister material with low carbon content by temperature control. As a practical matter, the short time required for the operation of filling the canister with glass and cooling down to the storage temperature would probably not result in direct failures. If major stresses imposed by cooling were removed and possibly a surface shot-peening were given after cooldown, the final and residual stresses present in the long storage period could be so low that stress corrosion cracking (SCC) would be minimal. Details of the reference system and further evaluation of SCC for low stresses are required.

3. Alternative Methods for Reducing Susceptibility of a Stainless Steel Canister to Stress Corrosion Cracking

If methods of stress relief such as those discussed above are not effective for stress relief, and if stress corrosion cracking proves a serious problem in canister storage, alternatives in the operational design could be used; for example:

(1) precasting of glass and "cold" insertion of the casting into the canister,
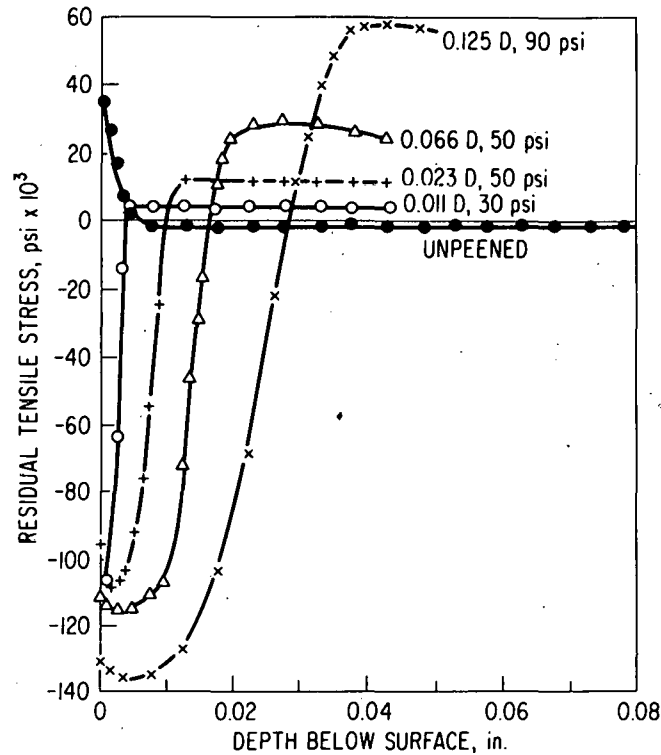
Fig. 25. Illustration of Shot-Peening.[69] Effect of
shot diameter and air pressure on stress
distribution for steel of hardness R_c12.
(Lessells and Broderick, 1956. Courtesy
of Institution of Mechanical Engineers.)

(2) use of an internal, stress-absorbing liner for the canister,

(3) use of an outer, secondary container for contact with water,

(4) use of air cooling rather than water cooling for storage and
shipping,

(5) use of a surface coating immune to stress corrosion cracking,

(6) use of another alloy for the canister (*i.e.*, an alloy rela-
tively more immune to SCC).

Since it is the surface of the canister that is of prime importance
in SCC, a method of surface treatment that would reduce susceptibility to
SCC would be relevant. One such treatment is that reported in a review
article by Latahisian and Staehle.[70] A diffused nickel surface on 18-8
stainless steel was found by some investigators to be the surface treatment
that conferred the greatest resistance to cracking. A layer of nickel about
0.12 mm thick was deposited by electroplating and then diffused by heating
to 1010°C for 100 hours.[70]

The above change of the surface alloy composition by depositing
a layer of nickel is consistent with a compilation of the cracking suscep-
tibilities of alloy steels as a function of nickel composition. In the words

of the report, "The ferritic stainless steels (*e.g.*, type 430) with no nickel do not crack, nor does Inconel 600."[70] It would appear that SS 304, with 8% nickel, is the most vulnerable composition from this particular standpoint.

However, all alloys and surface treatments have some damage susceptibility, and careful evaluation for the full range of conditions would be required for their consideration by the designers of the reference canister and RSSF.

C. Stabilizing Waste Calcine for Canister Storage

1. Background

The major requirements or design criteria applied to packages of solid waste in retrievable canisters are strength, inertness, and impenetrability of the package. The above general criteria are intended to cover the overall aspects of stability and leachability of the package as a whole, as well as individual components of the composite waste package, including interactive effects and features of the environment that affect package integrity.

In this section, we address the inertness or stability of the solid waste form itself, and its compatability with the canister. Leachability (*per se*) of the solid waste form will not be considered, because the canister, if it remains intact, is capable of preventing leaching of the solid waste. Specifically, we address here a possible method of treating solid waste prepared by calcination to improve its inertness and stability.

Calcination is a process of thermal decomposition of an aqueous solution of fission product nitrates, and calcine is the dry oxide product remaining after water and nitrogen oxide gases are driven off at temperatures of 400 to 600°C. At these temperatures, however, there may be residual nitrates on the order of 1 to 2 wt % and slightly less residual water. The Idaho Chemical Processing Plant has reported on the corrosivity of metal containment in storage bins of such calcine (also containing aluminum or zirconium from cladding) and on the mobility of fission products in temperature gradients. For wall temperatures of about 100°C and bulk temperatures not exceeding 700°C, wall corrosion of stainless steel type 304 is no more than 1 mil/century.[71] The only fission products (after 6 yr cooling) that undergo vapor transport are cesium and ruthenium (only when temperatures are above 600°C); these apparently redeposit at temperatures of about 500°C or lower, and appear to offer no special hazard to containment.[72] Although these data on calcine are not considered definitive for all possible forms of commercial wastes that might be encountered at a future RSSF, they indicate the present expectation that with adequate temperature control solid calcine will not be corrosive to type 304 stainless steel while the calcine remains in the unmelted condition.

The major concern with the potential of calcine for exerting a deleterious effect on the stainless steel canister is possible pressurization due to decomposition of the residual nitrate (and to a lesser extent, water) in the calcine. This problem was considered in the preceding quarterly report, ANL-75-23. As discussed previously, the potential pressure depends on the amount of nitrate and water present. Decomposition of nitrates can occur slowly due to radiation, or rapidly due to elevated temperatures (>800°C).

In canister storage, internal heat generation of the calcine results in a radial temperature gradient, with the highest temperature at the center and the lowest temperature at the wall. The volumetric average of calcine and gas temperature is the average of these temperature extremes.

2. A Method of Decreasing Residual Nitrate and Water in Calcine for Canister Storage

It appears that heat treatment of the calcine at 800°C before sealing of the canister would decompose the residuals to levels that no longer have the potential for substantial pressurization. This post-treatment of calcine could be done in a special vented vessel before the calcine is charged to the canister, but it also appears possible to provide the heat treatment within the canister before the canister is sealed.

The suitability of in-canister heat treatment of calcine can be considered in terms of standard practices for heat treatment of stainless steel 304L. The melting point of stainless steel is about 1400°C. Stress relief (e.g., of welds) is carried out by one-to-two-hour treatments at 900 to 1000°C, followed by controlled rapid cooling. In such cooling operations, the temperature range of 790°C to 430°C is critical, because if the steel is held too long in this range of temperature carbide may precipitate in the grain boundaries, leaving the stainless steel in a sensitized condition for subsequent corrosion. The low carbon content of 304L, however, reduces the susceptibility to sensitization. Precipitated carbides can be redissolved and a full anneal achieved by treatment at about 1120°C, followed by a rapid quench.[67,73]

From the above data on decomposition temperatures of calcine and allowable temperature for stainless steel, it appears that a heat treatment of the filled and vented canister at about 900°C would have the desirable effect of decomposing residual nitrate in the calcine and stress relieving the canister.

The feasibility in practice of this method would depend on the behavior of the calcine, i.e. whether effective thermal decomposition could be achieved without melting or sintering, and whether there is a suitable means of supporting the filled canister without distortion. General operations, atmosphere, and temperature would have to be carefully checked to ensure that no canister corrosion or other damage occurred.

A procedure for heat-treating the calcine-filled canister can be outlined as follows:

(1) vent decomposition gas: N_2, O_2, H_2O, and possibly some NO_x;

(2) collect volatile fission products, principally Cs and Ru;

(3) control of the temperature (considering the internal heat generated) adequate to achieve the intended decomposition of calcine and annealing of stainless steel without undesirable effects such as metal distortion, corrosion, or extensive sintering of the calcine;

(4) provide final sealing of the vent line by welding, including final stress relief of weld;

(5) adequately control radioactivity, both within the venting system and external to the canister.

Apparently, these operations could be accommodated within the basic design of the reference system. The vent gas is of small volume compared with gas volumes handled in calcination. Sealing, welding, and annealing of a small vent pipe are operations not different from those involved in any reference procedure for filling and sealing a canister.

D. Properties of Fission Product Oxides

The properties of fission product oxides were examined to elucidate factors having potential effects on canister reliability.

Typically, for LWR fuels having a burnup of 33,000 MWd/ton, fission-product element mass is 35.1 kg/tonne fuel. Of these, fission products which appear in the calcine are 28.4 kg/tonne. Thus 17.6% (wt) of the total fission products are lost as gases (Xe, Kr, etc.) in the processing steps. In Table 18, the composition of the residual calcine is given for the elements in % (wt). Also included is information on melting points, pertinent data on volatility, and free energies of formation at 1000°C. In general, oxides tend to suffer more decomposition at higher temperatures.

The fission product elements whose oxides are least stable are summarized in Table 19. Since some of these elements, in effect, do not form oxides at around 1000°C, their stability in a solid matrix depends on the properties of the elemental form. The melting points and the boiling points of the elements are given in the table.

The rare earth elements (including La and Y), alkali earth elements, and zirconium form stable oxides of high melting points and low volatility; these elements constitute about 61% of the total mass. The oxides of the noble metals Rh, Pd, and Ag decompose at temperatures approaching 1000°C, but the elemental metals are high melting and of low volatility; these elements constitute 7.55% of the total. Ruthenium (7.5%) and technetium (3%) are noble metals whose oxides are fairly stable; at sufficiently high oxygen potential, however, they form higher oxides that are volatile. Molybdenum (12.2%) is a noble metal with a fairly stable nonvolatile oxide. The alkali metals, cesium and rubidium (9.4%), have oxides of only moderate stability at temperatures approaching 1000°C; their oxides and elemental forms are significantly volatile at about 600°C. Their stability in the waste solid depends on the nature of the solid matrix and the temperature. The remaining elements (Te, Cd, Se, Sn, Sb), which constitute about 2.6% of the total, have fairly stable oxides.

Mobility under temperature gradients has been observed for cesium, rubidium, and ruthenium at temperatures of about 600°C, and this would be expected from the above properties. The stabilization of these oxides at high temperatures depends on the oxygen potential and the stability of complexes in the matrix. The addition of high melting oxides, especially those known to form compounds with alkali metals, $e.g.$, ZrO_2 TiO_2, and Al_2O_3, would tend to increase the general stability. Of course, to be effective, such

Table 18. Oxides in High-Level Waste Calcine

FP Element	g Element[74] kg Fuel (U)	wt % of Elements in Calcine	Oxide[75]	g Oxide[75] kg Fuel(U)	wt % Oxide in Calcine	Oxide[76] Melting Point, °C	Oxide[77] ΔF° 1000°C (kcal/g atom O)	Comments on Oxide
Nd	4.15	14.6	Nd_2O_3	4.52	12.8	∿1900	−116	
Zr	3.77	13.3	ZrO_2	4.94	14.0	2750	−103	
Mo	3.47	12.2	MoO_3	5.18	14.6	795(MoO_2)	−36	
Ce	2.64	9.30	CeO_2	3.32	9.38	1692(Ce_2O_3)	−103	
Cs	2.32	8.17	Cs_2O	2.88	8.13	762	−20	decomp 460°C
Ru	2.14	7.54	RuO_2	2.97	8.39	1130	0	decomp 1000°C
Ba	1.79	6.32	BaO	1.57	4.42	1923	−105	
Pd	1.41	5.96	PdO	1.48	4.19	870	+	
La	1.27	4.47	La_2O_3	1.48	4.18	2315	−116	
Pr	1.20	4.22	Pr_6O_{11}	1.48	4.18	∿2000(Pr_2O_3)	−116	
Sm	0.904	3.18	Sm_2O_3	0.924	2.61	2300	−116	
Tc	0.835	2.94	Tc_2O_7	1.29	3.64	−	−25 (TcO_2)[a]	subl 1000°C
Sr	0.778	2.74	SrO	1.06	2.99	2430	−110	
Te	0.572	2.01	TeO_2	0.725	2.05	733	−10	volat ∿800°C
Y	0.465	1.63	Y_2O_3	0.598	1.69	2417	−113	
Rh	0.392	1.38	Rh_2O_3	0.48	1.33	1100	+	decomp 1100°C
Rb	0.346	1.22	Rb_2O	0.354	1.00	∿500	−26	decomp 477°C
Eu	0.164	0.58	Eu_2O_3	0.200	0.56	2050	−113	
Gd	0.123	0.43	Gd_2O_3	0.137	0.39	2330	−113	
Pm	0.085	0.30	Pm_2O_3	0.123	0.35	∿2000	−116	
Cd	0.084	0.29	CdO	0.097	0.27	830	−26	decomp 900°C
Ag	0.060	0.21	Ag_2O	0.088	0.25	∿200	+	decomp 300°C
Se	0.052	0.18	SeO_2			340	−10	
Sn	0.052	0.18	SnO			1080	−38	decomp 1080°C
Sb	0.011	0.04	Sb_2O_3			656	−30	subl 1500°C
Dy	0.001		Dy_2O_3			∿2000	−110	
Ho	0.00008		Ho_2O_3			∿2000	−110	
Er	0.00003		Er_2O_3			∿2000	−110	

Mass Total 28.4 g/kg fuel (U) (kg/tonne)   Mass Total 35.9 g/kg fuel (U) (kg/tonne)

[a] Higher oxides that are much more volatile can form; see text.

Table 19. Properties of Selected Elements[a] as Metals

Element	Melting Point, °C	Boiling Point, °C	Free Energy of Formation of Oxide at 1000°C kcal/g atom oxygen	
Mo	2620	3700	-36	
Cs	28	620	-20	
Ru	2430	3700	0	oxide decomposes
Pd	1555	2200	>0	oxide decomposes
Tc	2200	~4700	-25	
Te	452	1390	-10	
Rh	1955	>2500	>0	oxide decomposes
Rb	38	700	-26	
Cd	321	767	-26	
Ag	960	1950	>0	oxide decomposes
Se	220	688	-10	
Sn	232	2260	-38	
Sb	630	1380	-30	

[a] These elements are fission products whose oxides are least stable and most subject to decomposition at 1000°C.

additives would have to be distributed homogeneously on an atomic or micro-crystalline scale. This distribution is certainly achieved in fusion to glass and may be achieved by prior addition to aqueous solutions or by extensive sintering of powders. A list of potential additives is given in Table 20.

Table 20. Properties of Some Selected Oxides for Stabilizing Ceramics

Oxide	Metal Valence	Melting Point, °C
B_2O_3	3	723
Al_2O_3	3	2318
SiO_2	4	1993
MgO	2	2913
CaO	2	2773
TiO_2	4	2123
V_2O_5	5	943
Fe_2O_3	3	1838
NiO	2	2263
ZnO	2	1800
ZrO_2	4	2983
Nb_2O_5	5	943
BaO	2	2193
UO_2	4	2773

The above oxides have very low vapor pressures at their melting points.

Cesium and rubidium form complex oxide compounds with other metals having valences of 4 to 6. For example, Rb_2MoO_4 has a melting point of 929°C and Cs_2MoO_4, a melting point of 925°C. The oxide-formers with Rb_2O and Cs_2O include MoO_3, SiO_2, and Nb_2O_5.[78] Some phase diagrams are shown in Fig. 26.[79] Note the eutectics at 748°C in the Nb_2O_5-containing binary and at 460°C in the MoO_3 binary. The more refractory oxides such as TiO_2 and ZrO_2 would be expected to have the least tendency for liquid formation. These assumptions do not seem to be established.

Other oxides, for example, TeO_2, are known to form low melting mixtures with oxides of pentavalent and hexavalent metals. TeO_2 is also volatile at 790-940°C. Such behavior tends to mobility and possible corrosion of steel.

The ideal of a stable and inert form for fission product waste is a solid of very low vapor pressure and low chemical reactivity under storage conditions. A high melting point and high thermal conductivity are also ideal properties of the waste solid because of internal heat generation. For the chemical elements of a fission product mixture, it appears likely that oxides of fission product metals incorporated into certain ceramic matrices are a practical approximation to these ideal properties.

E.   Canister Design Parameters for Temperature Control

1.   Heat Conduction in a Cylindrical Canister

The basic model for temperatures within a cylindrical canister of solid high-level waste considers heat conduction within a solid for which there is uniform heat generation, and for which heat is transferred to the surface of the cylinder where it is dissipated to the environment; *i.e.*, there is a specific heat generation rate [a, Btu/(hr)(ft³)] within the solid, which has a thermal conductivity of k, Btu/hr ft °F. Neglecting end effects, the heat conduction follows radial paths for the circular cross section of the cylindrical container.

The differential equation describing the heat transfer across any circumference of the waste form at a radius r and of unit length is:

$$q = a\pi r^2 = 2\pi r\left(-k\frac{dT}{dr}\right) \tag{1}$$
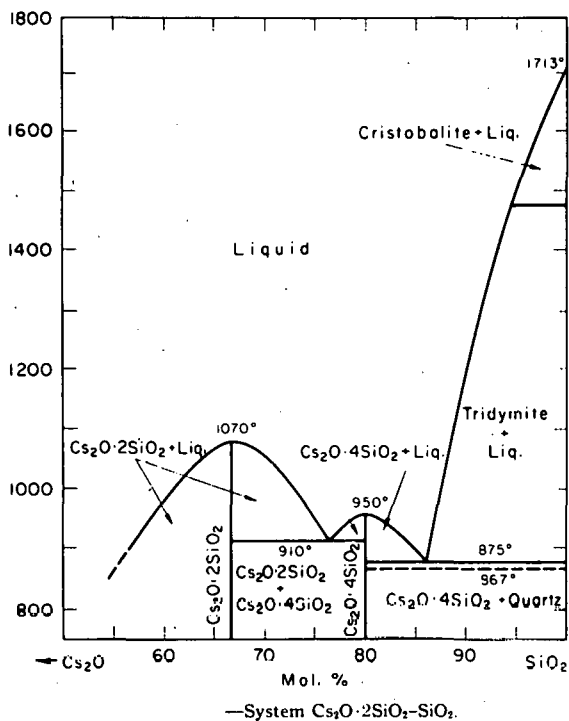
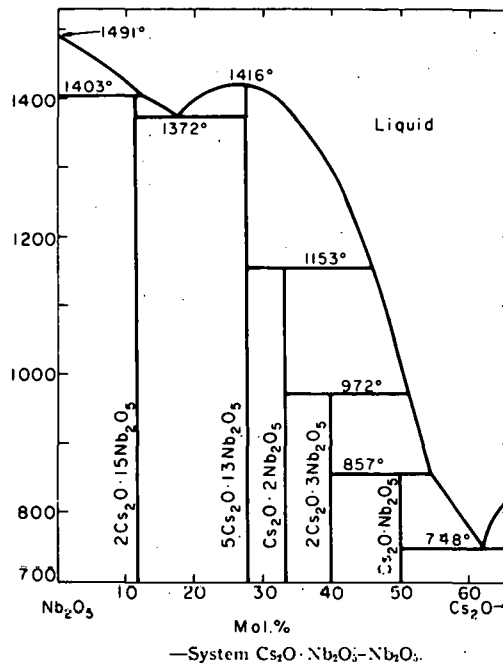or

$$\frac{dT}{dr} = \frac{ar}{2k} \tag{2}$$

Solution of Equation 2 for a solid waste form with no central cavity is:

$$T_c - T_s = \frac{ar_s^2}{4k} = \Delta T \tag{3}$$

where: T_c = Center line temperature

T_s = Surface temperature

r_s = Radius of the waste solid

—System Cs₂O·2SiO₂–SiO₂.

Z. D. Alekseeva, *Zh. Neorgan. Khim.*, 11 [5] 1171 (1966); *Russ. J. Inorg. Chem. (English Transl.)*, 627 (1966).

—System Cs₂O·Nb₂O₅–Nb₂O₅.

Arnold Reisman and Joan Mineo, *J. Phys. Chem.*, 65, 997 (1961).

—System Rb₂MoO₄·MoO₃.
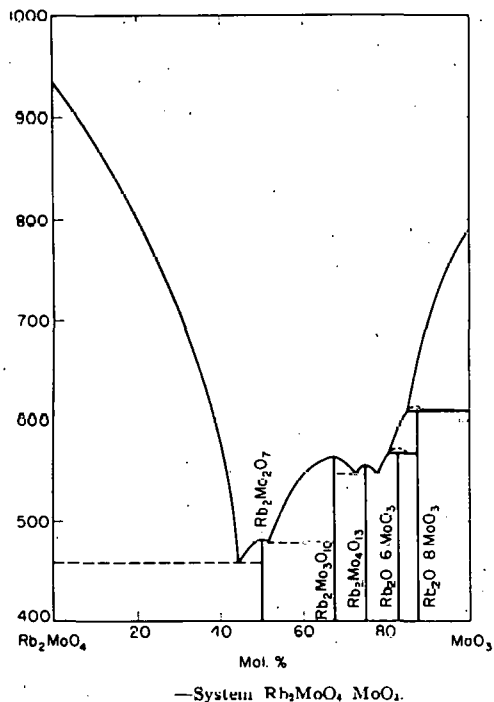
Viktor Spitzyn and I. M. Kuleshov, *Zhur. Obshchei Khim.*, 21, 1370 (1951).

—System Rb₂MoO₄–MoO₃.
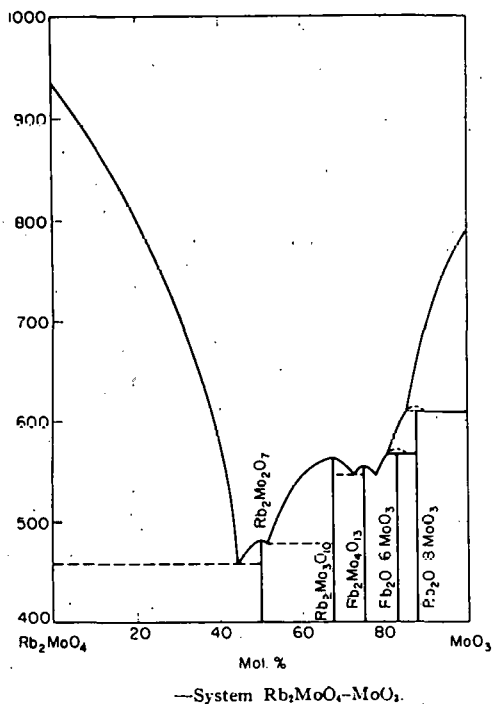
Viktor Spitzyn and I. M. Kuleshov, *Zhur. Obshchei Khim.*, 21, 1370 (1051).

Fig. 26. Phase Diagrams of Selected Complex Oxides of Cesium and Rubidium[79]

If Q is the total heat generation rate per unit length ($= \pi r_s^2 a$), Equation 3 becomes:

$$T_c - T_s = \frac{Q}{4\pi k} = \Delta T \qquad (4)$$

which indicates that ΔT is dependent on Q and k but not on r_s.

The volume average of the temperature T_v, is obtained from:

$$\overline{T}_v = \frac{\int TdV}{V_T} = \frac{\int_o^{r_s} (T_c - \frac{ar^2}{4k}) \, d(\pi r^2)}{\pi r_s^2} = \frac{T_c + T_s}{2} \qquad (5)$$

where: $V = \pi r^2$
$V_T = \pi r_s^2$

This relation is useful for calculating internal pressures.

2. Use of Internal Fins

The design objective for internal fins in a waste canister is to provide inner metal "walls" (*i.e.*, fins) to conduct heat directly to the outer canister wall. The thermal conductivity of steel is about 120 times that of calcine, so that a thin cross section of steel can provide a heat-conducting path equivalent to a 100-fold larger cross section of calcine. A simplified view is to assume that all internal heat generation occurs at the center line. The heat is transferred through N fins having a thickness d and a thermal conductivity of k_F for a distance of r_s, the radius of the canister. Thus,

$$Q = \frac{k_F (N \cdot d) \Delta T_F}{r_s} \qquad (6)$$

where ΔT_F is the resulting temperature difference between the center line and surface. Equating this expression to that of Equation 4 with suitable subscripts, and eliminating Q,

$$\frac{\Delta T_F}{\Delta T_{NF}} = 4\pi \frac{k_F}{k_s} \frac{r_s}{N \cdot d} \qquad (7)$$

where: ΔT_F = temperature difference with fins

ΔT_{NF} = temperature difference without fins

k_F = thermal conductivity of fins

k_s = thermal conductivity of waste form

r_s = canister radius

N = number of fins

d = thickness of fins

3. Comparative Design Parameters for Waste Canisters

    a. Comparison of Glass and Calcine

A modification of Equation 3 utilizes the factor A, the mass specific rate of heat generation, Btu/(hr) (lb fission product oxide), and ρ, the density of oxides:

$$\Delta T = \frac{A \rho r_s^2}{4k} \tag{8}$$

The use of fins with calcine introduces a fin factor f that reduces ΔT_C by the factor f. This is the inverse of Equation 7. Thus,

$$\Delta T_C = \frac{A \rho_C r_C^2}{4f k_C} \tag{9}$$

where subscript C refers to calcine

For the glass case, a dilution factor n is introduced:

$$n = \frac{\text{mass of glass form}}{\text{mass of contained fission product oxide}}$$

Thus,

$$\Delta T_G = \frac{\left(\frac{A}{n}\right)\rho_G r_G^2}{4 k_G} \tag{10}$$

where subscript G refers to glass

The weight of contained fission products per unit length is:

$$\text{For calcine, } W_C = \pi r_C^2 \rho_C \tag{11}$$

$$\text{For glass, } W_G = \frac{\pi r_G^2 \rho_G}{n} \tag{12}$$

Eliminating r^2 from Equations 9 and 11, and 10 and 12, one obtains the maximum weight of fission product oxides (per foot) for a given ΔT:

$$\text{For calcine, } W_{C,\ Max} = \frac{4\pi f k_C \Delta T_C}{A} \tag{13}$$

$$\text{For glass, } W_{G,\ Max} = \frac{4\pi k_G \Delta T_G}{A} \tag{14}$$

The ratio of maximum weight of fission product oxides per canister in the glass form to that in the calcine form is obtained by dividing Equation 14 by 13:

$$\frac{W_{G,\,Max}}{W_{C,\,Max}} = \frac{1}{f} \cdot \frac{k_G}{k_C} \cdot \frac{\Delta T_G}{\Delta T_C} \tag{15}$$

The corresponding volume ratio is:

$$\frac{V_{G,\,Max}}{V_{C,\,Max}} \doteq \frac{W_{G,\,Max}}{W_{C,\,Max}} \cdot \frac{\rho_C}{\rho_G} \tag{16}$$

Note that the ratios shown in Equations 15 and 16 are not dependent on A, the mass-specific rate of heat generation per pound of fission product oxide.

The evaluation of the ratios for air and water cooling was made for the following values of the parameters:

	Calcine	Glass
Density, g/cc	$\rho_C = 2.0$	$\rho_G = 4.0$
Thermal conductivity, Btu/(hr)(°F)(ft)	$k_C = 0.2$	$k_G = 0.6$
Fin factor	f = 1 (no fins) f = 4 (fins)	
Dilution factor		n = 3
Temperatures, Center Line Maximum, °F	1112	1472
Canister Wall Maximum, °F		
Water Cooling	140	140
Air Cooling	470	470
ΔT Maximum, °F		
Water Cooling	972	1332
Air Cooling	642	1002

The results are as follows:

	Water Cooling	Air Cooling
Ratio, $\dfrac{\text{Maximum weight of fp oxides in glass}}{\text{Maximum weight of fp oxides in calcine}}$	$\dfrac{4.11}{f}$	$\dfrac{4.68}{f}$
Ratio, $\dfrac{\text{Volume of fp oxides in glass}}{\text{Volume of fp oxides in calcine}}$	$\dfrac{2.06}{f}$	$\dfrac{2.34}{f}$

The above ratios can be summarized [for the case of no fins (f-1)] as indicating that at any heating rate and at the specific reference properties, about four times the number of canisters are required for calcine as are required as for glass, and that each canister for glass has twice the

volume of that for calcine. If fins are added to the calcine such that the ΔT is reduced by a factor of four (f=4) compared to the case without fins, the number of canisters for calcine will be reduced to about the same number as that for glass.

b. Comparison of Air and Water Cooling

The ratio of maximum contained masses of fission products for water cooling to that for air cooling is the ratio of the allowable ΔTs (see Equations 13 and 14).

For calcine:

$$\frac{W_{C, \text{ Max, water}}}{W_{C, \text{ Max, air}}} = \frac{972}{642} = 1.51.$$

For glass:

$$\frac{W_{G, \text{ Max, water}}}{W_{G, \text{ Max, air}}} = \frac{1332}{1002} = 1.33$$

The number of canisters required for air cooling is thus 50% larger than for water cooling in the case of calcine, and 33% more in the case of glass.

c. Effect of Decay Time

For cooling times between 1 and 100 years, the value of A, the heat generation rate per pound of fission product oxide, can be expressed as B/t, where B is an appropriate constant and t is cooling time. Thus, according to Equations 13 and 14, the maximum weights of oxide in canisters, for both calcine and glass, increase proportionately with cooling time. The absolute effect on maximum weights of the increase in cooling time from 1 year to 10 years is thus more significant than the calcine/glass effect.

F. Principal Design Factors Controlling the Time-to-Failure for the Stress Corrosion Cracking of Stainless Steel

In the preceding quarterly report, Fig. 2-7 illustrate quantitative relationships for the principal determinants of stress corrosion cracking in austenitic 18-8 stainless steel, specifically types 304 and 304L. These relationships have the general hyperbolic form: Constant = (time-to-cracking)(intensity or amount of variable), where the variables are chloride and oxygen concentrations and temperature of the coolant and stress.

It is possible (a) to interpret these results as indicating a factorial combination of the four variables into a single hyperbolic form and (b) to calculate from this mathematical model appropriate constants and exponents to fit the data in a single correlation. Such a correlation would then allow extrapolation to a very long time-to-cracking (*i.e.*, $>10^3$ years) for sufficiently small values of the variables. Such a curve-fitting exercise would not be inconsistent with the present data, but it would be a gross extrapolation and would not constitute positive evidence as a basis for defining

2

with confidence the design conditions for immunity to stress corrosion cracking. On the other hand, by use of that same modeling concept, an experimental program sufficiently systematic to establish principles of experimental prediction could be defined with sufficient confidence to be useful in engineering design. The necessary experimental measurements for a purely empirical correlation would probably be difficult, costly, and time-consuming since conditions of very low rates of attack are of prime interest here.

A more efficient approach would be to make use of general theory. Unfortunately, no workable theory (*i.e.*, body of quantitative mechanistic principles) exists; nevertheless, a considerable body of information exists that can function as approximate working principles and strategy for design.[70,80-85]

The three general factors affecting stress corrosion cracking are: (1) the alloy composition and structure, (2) the corrosive environment (including temperature and oxygen), and (3) the manifestation of stress. The two phases in the interaction of these three conditions to produce failure by stress corrosion cracking are (1) the initiation and (2) the propagation of cracks. Cracks are by definition nonhomogeneous local structural defects, closely associated with micro residual stresses and crystal-lattice dislocations involved in deformation.[80] Stress corrosion cracking shows transgranular cracks associated with deformation rather than intergranular cracks from purely chemical effects.[85]

Welding, used to effect closure of the canister, produces sharp gradients of stress and deformation that may initiate cracks; propagation depends on the balance of crack-healing and crack-propagation conditions.

The safest strategy is very restrictive: fully annealed alloys subjected to minimal deformation and minimal load stress, and minimally aggressive environments, including low temperatures, minimal chlorides, and minimal oxygen.

Metal composition is a factor. Pure metals[78] and alloys that are not highly passive but that corrode uniformly at rates of greater than 5 mils per year[79] are less susceptible to stress cracking. Also, temperatures of 200°C are more aggressive than lower or higher temperatures,[70,83] presumably because certain healing effects appear at higher temperatures and balance the general increase of chemical corrosive attack. Thus, it would appear that austenitic stainless steels, highly immune to common aggressive environments because of special protective surface films, are likely to have rivals from among less passive alloys for water service.

The optimization of reliability and the validation of design requirements appear to call for systematic study and are likely to result in stringent controls via quality-control and quality-assurance programs.

REFERENCES

1. M. J. Steindler *et al.*, "Waste Management Programs Quarterly Report, July–September 1974," Argonne National Laboratory, Chemical Engineering Division, ANL-8152, p. 5 (February 1975).

2. M. J. Steindler *et al.*, "Waste Management Programs Quarterly Report, October–December 1974," Argonne National Laboratory, Chemical Engineering Division, ANL-75-23 (March 1975).

3. N. M. Levitz, B. J. Kullen, and M. J. Steindler, "Management of Waste Cladding Hulls, Part I. Pyrophoricity and Compaction," ANL-8139 (February 1975).

4. L. J. Howell, R. C. Sommer, and H. H. Kellogg, "Phase Diagram and Vapor Pressure in the Systems NaCl-ZrCl$_4$, KCl-ZrCl$_4$, and NaCl-KCl (1:1 molar) -ZrCl$_4$," Trans. AIME, Journal of Metals, 193–200 (January 1957).

5. M. J. Steindler *et al.*, "Waste Management Programs Quarterly Report, January–March 1974," Argonne National Laboratory Chemical Engineering Division, ANL-8106, p. 7 (May 1974).

6. M. J. Steindler *et al.*, "Waste Management Programs Quarterly Report, April–June 1974," ANL-8134 (November 1974).

7. H. T. Fullam, "High Temperature Methods for Disposal of Contaminated Metal Equipment," BNWL-B-277 (July 1973).

8. W. E. Shaw, "Study for Disposal of Uranium Contaminated Ferrous Scrap," NLCO-1110 (April 25, 1974).

9. T. C. Buschbach, "Cambrian and Ordovician Strata of Northeastern Illinois," Illinois Geol. Survey Report of Investigations 218 (1964).

10. Ohio River Valley Water Sanitation Commission, "Underground Injection of Wastewater in the Ohio Valley Region," ORSANCO, Cincinnati, Ohio (1973).

11. A. Janssens, "Stratigraphy of the Cambrian and Lower Ordovician Rocks in Ohio," Ohio Division of Geological Survey Bulletin 64 (1973).

12. D. C. Bond, "Hydrodynamics in Deep Aquifers of the Illinois Basin," Illinois State Geological Survey Circular 470 (1972).

13. Private Communication to D. L. Warner, University of Missouri-Rolla.

14. U.S. Public Health Service, "Public Health Service Drinking Water Standards," U.S. Public Health Service Pub. No. 956 (1962).

15. U.S. Public Health Service, 1946, "Drinking Water Standards," Public Health Reports 61(11), 371–384.

16. S. J. Pirson, "Handbook of Well Log Analysis," Prentice-Hall, Inc., Englewood Cliffs, N.J. (1963).

17. D. L. Katz and D. L. Coates, "Underground Storage of Fluids," Ulrich's Books, Inc., Ann Arbor, Michigan (1968).

18. George Dickinson, "Geological Aspects of Abnormal Reservoir Pressures in the Gulf Coast Louisiana," Am. Assoc. Petroleum Geologists Bull. 37(2), 410-432 (1953).

19. F. A. F. Berry, "High Fluid Potentials in California Coast Ranges and their Tectonic Significance," Bull. Am. Assoc. Petroleum Geologists 57(7), 1219-1249 (1973).

20. B. B. Hanshaw, "Natural Membrane Phenomena and Subsurface Waste Emplacement," in Underground Waste Management and Environmental Implications," T. D. Cook (ed.), Am. Assoc. of Petroleum Geologists Memoir 18, Tulsa, Oklahoma, pp. 308-315 (1972).

21. S. H. Davis and R. J. M. De Weist, Hydrogeology, Wiley and Sons, Inc., New York, N. Y. (1966).

22. Illinois Water Survey, "Feasibility Study on Desalting Brackish Water from the Mt. Simon Aquifer in Northeastern Illinois," Illinois Water Survey, Urbana, Illinois (1973).

23. Geothermal Survey of North America, American Association of Petroleum Geologists, Tulsa, Oklahoma.

24. R. O. Kehle, "The Determination of Tectonic Stresses Through Analysis of Hydraulic Well Fracturing," J. Geop. Research 69(2), 259-273 (1964).

25. M. L. Sbar and M. L. Sykes, "Contemporary Compressive Stress and Seismicity in Eastern North America: An Example of Intra-Plate Tectonics," Geol. Soc. of Am. Bull. 84(6), 1861-1882 (1973).

26. M. J. Clifford, "Hydrodynamics of the Mt. Simon Sandstone, Ohio and Adjoining Areas," in Underground Waste Management and Artificial Recharge, Jules Braunstein (ed.), Am. Assoc. of Petroleum Geologists, Tulsa, Oklahoma, pp. 349-356 (1973).

27. D. C. Bond, "Deduction of Flow Patterns in Variable-Density Aquifers from Pressure and Water-Level Observations," in Underground Waste Management and Artificial Recharge, Jules Braunstein (ed), Am. Assoc. Petroleum Geologists, Tulsa, Oklahoma, pp. 357-378 (1973).

28. J. D. Haun and L. W. Le Roy (eds.), "Subsurface Geology in Petroleum Exploration," Colorado School of Mines, Golden, Colorado (1958).

29. H. Y. Jennings and A. Timur, "Significant Contributions in Formation Evaluation and Well Testing," J. Petroleum Technology, 25, 1432-1446 (December 1973).

30. W. S. Keys and R. F. Brown, "Role of Borehole Geophysics in Underground Waste Storage and Artificial Recharge," in Underground Waste Management and Artificial Recharge, Jules Braunstein (ed). Am. Assoc. of Petroleum Geologists, Tulsa, Oklahoma, pp. 147-191 (1973).

31. Carl Gatlin, <u>Petroleum Engineering Drilling and Well Completions</u>, Prentice-Hall, Inc., Englewood Cliffs, N. J. (1960).

32. E. J. Lynch, <u>Formation Evaluation</u>, Harper and Row, New York, N.Y. (1962).

33. C. S. Matthews and D. G.Russell, "Pressure Buildup and Flow Tests in Wells," Am. Inst. of Mining, Met., and Petr. Engrs., Soc. of Petroleum Engrs. Monograph, Vol. 1 (1967).

34. W. E. Wilson, *et al.*, "Hydrologic Evaluation of Industrial-Waste Injection at Mulberry, Florida," in <u>Underground Waste Management and Artificial Recharge</u>, Jules Braunstein (ed.), Am. Assoc. Petroleum Geologists, Tulsa, Oklahoma, pp. 552-564 (1973).

35. P. A. Witherspoon and S. P. Neuman, "Hydrodynamics of Fluid Injection," in <u>Underground Waste Management and Environmental Implications</u>, T. D. Cook (ed.), Am. Assoc. Petroleum Geologists Memoir 18, Tulsa, Oklahoma (1972).

36. S. H. Lohman, "Ground-Water Hydraulics," U.S. Geol. Survey Prof. Paper 708 (1972).

37. G. P. Kruseman and N. A. De Ridder, "Analysis and Evaluation of Pumping Test Data," International Institute for Land Reclamation and Improvement, Bulletin 11, Wageningen, The Netherlands (1970).

38. P. A. Witherspoon *et al.*, "Interpretation of Aquifer Gas Storage Conditions from Water Pumping Tests," Am. Gas Assoc., Inc., New York, N.Y. (1967).

39. D. A. Goolsby, "Geochemical Effects and Movement of Injected Industrial Waste in a Limestone Aquifer," in <u>Underground Waste Management and Environmental Implications</u>, Am. Assoc. of Petroleum Geologists Memoir 18, Tulsa, Oklahoma, pp. 355-367 (1972).

40. D. A. Goolsby, "Hydrogeochemical Effects of Injecting Wastes into a Limestone Aquifer Near Pensacola, Florida," Ground Water, $\underline{9}$(1) 13-19 (1971).

41. J. Bear, <u>Dynamics of Fluids in Porous Media</u>, Elsevier Pub. Co., New York (1972).

42. <u>U.S. Environmental Protection Agency, 1974</u>, "Compilation of Industrial and Municipal Injection Wells in the United States," 2 Vols., EPA-520/9-74-020, U.S. Environmental Protection Agency, Washington, D.C.

43. J. Bear and M. Jacobs, "The Movement of Injected Water Bodies in Confined Aquifers," Underground Water Storage Study Rpt. No. 13, Technion, Haifa, Israel (1964).

44. L. W. Gelhar *et al.*, "Density Induced Mixing in Confined Aquifers," U.S. Environmental Protection Agency, Water Pollution Control Research Series, Publication 16060 ELJ 03/72 (1972).

45. J. D. Bredehoeft and G. F. Pinder, "Application of Transport Equations to Groundwater Systems," in Underground Waste Management and Environmental Implications, T. D. Cook (ed.), Am. Assoc. Petroleum Geologists Memoir 18, pp. 191-199 (1972).

46. J. B. Robertson and J. T. Barraclough, "Radioactive- and Chemical-Waste Transport in Groundwater at National Reactor Testing Station, Idaho: 20-year Case History and Digital Model," in Underground Waste Management and Artificial Recharge, Jules Braunstein (ed.), Am. Assoc. Petroleum Geologists, Tulsa, Oklahoma, pp. 291-322 (1973).

47. D. L. Brown and W. D. Silvey, "Underground Storage and Retrieval of Fresh Water from a Brackish-Water Aquifer," in Underground Waste Management and Artificial Recharge, Jules Braunstein (ed.), Am. Assoc. of Petroleum Geologists, Tulsa, Oklahoma, pp. 379-419 (1973).

48. M. K. Hubbert and D. G. Willis, "Mechanics of Hydraulic Fracturing," in Underground Waste Management and Environmental Implications, T. D. Cook (ed.), Am. Assoc. of Petroleum Geologists Memoir 18, Tulsa, Oklahoma (1972).

49. C. B. Raleigh, "Earthquakes and Fluid Injection," in Underground Waste Management and Environmental Implications, T. D. Cook (ed.), Am. Assoc. of Petroleum Geologists Memoir 18, pp. 273-279 (1972).

50. D. L. Warner, "Subsurface Disposal of Liquid Industrial Wastes by Deep-Well Injection," in Subsurface Disposal in Geologic Basins - A Study of Reservoir Strata, J. E. Galley (ed.), Am. Assoc. Petroleum Geologists Memoir 10, pp. 11-20 (1968).

51. J. E. Galley (ed.), "Subsurface Disposal in Geologic Basins - A Study of Reservoir Strata," Am. Assoc. of Petroleum Geologists Memoir 10, A.A.P.G., Tulsa, Oklahoma (1968).

52. C. A. Repenning, "Geologic Summary of the Central Valley of California, with Reference to Disposal of Liquid Radioactive Waste," U.S. Geol. Survey Trace Elements Inv. Rpt. 769 (open file) (1961).

53. C. A. Sandberg, "Geology of the Williston Basin, North Dakota, Montana, and South Dakota, with Reference to Subsurface Disposal of Radioactive Wastes," U.S. Geological Survey Rpt. TEI-809, 14 (1962).

54. H. M. Beikman, "Geology of the Powder River Basin, Wyoming and Montana, with reference to subsurface disposal of radioactive wastes," U.S. Geol. Survey Trace Elements Inv. Rpt. 823 (open file) (1962).

55. M. E. MacLachlan, "The Anadarko Basin (of parts of Oklahoma, Texas, Kansas, and Colorado)," U.S. Geol. Survey Trace Elements Inv. Rpt. 831 (1964).

56. H. E. Le Grand, "Geology and Ground-Water Hydrology of the Atlantic and Gulf Coastal Plain as Related to Disposal of Radioactive Wastes," U.S. Geol. Survey Trace Elements Inv. Rpt. 805 (1962).

57. J. D. Love and Linn Hoover, "A Summary of the Geology of Sedimentary Basins of the United States, with Reference to the Disposal of Radioactive Wastes," U.S. Geol. Survey Trace Elements Inv. Rpt. 768 (open file) (1960).

58. R. E. Bergstrom, "Feasibility of Subsurface Disposal of Industrial Wastes in Illinois," Illinois State Geological Survey Circular 426 (1968).

59. W. L. Kreidler, "Preliminary Study of Underground Disposal of Industrial Liquid Waste in New York State," in Subsurface Disposal of Industrial Wastes, Published and distributed by the Interstate Oil Compact Commission, P. O. Box 53127, Oklahoma City, Oklahoma (1968).

60. V. C. Newton, Jr., "Geologic Consideration in the Disposal of Chemical and Radioactive Wastes," Oregon Dept. of Geology and Mineral Industries, Portland, Oregon (1970).

61. Neilson Rudd, "Subsurface Liquid Waste Disposal and its Feasibility in Pennsylvania," Pennsylvania Geological Survey, Fourth Series, Environmental Geology Report 3, Harrisburg (1972).

62. M. J. Clifford, "Feasibility of Deep-Well Injection of Industrial Wastes in Ohio," Ohio State University, unpublished M.S. thesis (1972).

63. W. E. Tucker and R. E. Kidd, "Deep-Well Disposal in Alabama," Geological Survey of Alabama (1973).

64. R. V. Hidalgo and L. D. Woodfork, "EDP as an Aid for Decision Making in Subsurface Injection of Liquid Wastes," in Underground Waste Management and Artificial Recharge, Jules Braunstein (ed.), Am. Assoc. of Petroleum Geologists, Tulsa, Oklahoma, pp. 133-146 (1973).

65. Battelle Pacific Northwest Laboratories, "Quarterly Progress Report Research and Development Activities, Waste Fixation Program, April through June 1974," BNWL-1841 (July 1974).

66. J. R. Hutchins and R. V. Harrigton, "Glass" in Kirk-Othmer, Encyclopedia of Chemical Technology, 2nd Ed. Vol. 10, pp. 533-604 (1966).

67. J. L. Everhart, Engineering Properties of Nickel and Nickel Alloys, Plenum Press (1971).

68. Metals Handbook, 8th Ed., Vol 1, T. Lyman (ed.), American Society for Metals, Novelty, Ohio (1961).

69. F. A. McClintock and A. S. Argon (ed.), Mechanical Behavior of Materials Chap. 12, "Residual Stress," Addison-Wesley Publishing Co., Inc. (1966).

70. R. M. Latanisian and R. W. Staehle, "Stress-Corrosion-Cracking of Iron-Nickel-Chromium Alloys," in Proceedings of the Conference on the Fundamental Aspects of Stress Corrosion Cracking at The Ohio State University, Columbus, Ohio, Sept. 11-15, 1967.

71. T. L. Hoffman, "Corrosion Monitoring of Storage Bins for Radioactive Calcine," presented at 1975 Conference of NACE, April 14-18, 1975. To be published (same author & title) as ICP-7071 (May 1975).

72. M. W. Wilding and D. W. Rhodes, "Stability Studies of Highly Radioactive Alumina Calcine During High Temperature Storage," 1DO-14670 (January 1966).

73. Metals Handbook, 8th Ed., Vol 2 (1964).

74. Oak Ridge National Laboratory, "Siting of Fuel Reprocessing Plants and Waste Management Facilities," ORNL-4451 (July 1970).

75. W. F. Bonner (PNL), private communication to W. B. Seefeldt (ANL), January 24, 1975, Attachment, "Radioactive Wastes After Conversion to Calcine."

76. Lange's Handbook of Chemistry.

77. A. Glassner, "The Thermochemical Properties of the Oxides, Fluorides, Chlorides to 2500°K," ANL-5750 (October 1965).

78. F. M. Perelman, Rubidium and Cesium, Pergaman Press (1965).

79. J. P. Coughlin, "Phase Diagrams for Ceramicists," Bulletin of Mines, 542.

80. D. Birchon and G. C. Booth, "Stress Corrosion Cracking of Some Austenitic Steels," 2nd International Congress on Metallic Corrosion, New York, New York (1963).

81. J. E. Truman and H. W. Kirkby, "The Possibility of Service Failure of Stainless Steels by Stress Corrosion Cracking," Metallurgia 72(430), 67-71 (August 1965).

82. R. W. Staehle, "Comments on the History, Engineering, and Science of Stress Corrosion Cracking," in Proceedings of a Conference on the Fundamental Aspects of Stress Corrosion Cracking, The Ohio State University, September 11-15, 1967.

83. J. W. Frey and R. W. Staehle, "Effect of Temperature, Stress, and Alloy Composition on the Role of Stress Corrosion Cracking in Fe-Ni-Cr Alloys," presented at the 23rd NACE Conference, March 16, 1967, pp. 35-41.

84. G. E. Moeller, "Understanding Stress Corrosion Cracking," in Proceedings 3rd Western States Corrosion Seminar, NACE, May 6-8, 1969, San Dimas, California. (Reprinted by International Nickel Co.).

85. P. R. Swann, "Stress-Corrosion Failure," Scientific American 214(2) 73-81 (February 1966).